AMERICAN UNIVERSITY OF BEIRUT

THYMOQUINONE INDUCES APOPTOSIS AND DNA DAMAGE IN 5-FLUOROURACIL-RESISTANT COLORECTAL CANCER STEM /PROGENITOR CELLS AND SENSITIZES THEM TO RADIATION

by
FARAH RABIH BALLOUT

A Dissertation
submitted in partial fulfillment of the requirements
for the degree of Doctor of Philosophy
to the Department of Biology
of the Faculty of Arts and Sciences
at the American University of Beirut

Beirut, Lebanon
June 2020

AMERICAN UNIVERSITY OF BEIRUT

THYMOQUINONE INDUCES APOPTOSIS AND DNA DAMAGE IN 5-FLUOROURACIL-RESISTANT COLORECTAL CANCER STEM /PROGENITOR CELLS AND SENSITIZES THEM TO RADIATION

by
FARAH RABIH BALLOUT

Approved by:

Nadine Darwiche — 11/6/2020
Dr. Nadine Darwiche, Professor — Chair
Department of Biochemistry, AUB-FM

Hala Muhtasib
Dr. Hala Muhtasib, Professor — Advisor
Department of Biology, AUB-FAS

11/6/2020
Dr. Wassim Abou-Kheir, Associate Professor — Co-advisor
Department of Anatomy, Cell Biology & Physiological Sciences
AUB-FM

June 6, 2020
Dr. Rabih Talhouk, Professor — Member
Department of Biology, AUB-FAS

Tamara Boulos — 11/6/2020
Dr. Tamara Abou Antoun, Associate Professor — External Member
School of Pharmacy, LAU

George Hilal — 11/6/2020
Dr. George Hilal, Associate Professor — External Member
Department of Medicine, USJ

Date of thesis defense: June 11, 2020

AMERICAN UNIVERSITY OF BEIRUT

THESIS, DISSERTATION, PROJECT RELEASE FORM

Student Name:

Ballout	Farah	Rabih
Last	First	Middle

○ Master's Thesis ○ Master's Project ⊗ Doctoral Dissertation

☐ I authorize the American University of Beirut to: (a) reproduce hard or electronic copies of my thesis, dissertation, or project; (b) include such copies in the archives and digital repositories of the University; and (c) make freely available such copies to third parties for research or educational purposes.

☒ I authorize the American University of Beirut, to: (a) reproduce hard or electronic copies of it; (b) include such copies in the archives and digital repositories of the University; and (c) make freely available such copies to third parties for research or educational purposes after:

One ✓ year from the date of submission of my thesis, dissertation, or project.
Two ---- years from the date of submission of my thesis, dissertation, or project.
Three ---- years from the date of submission of my thesis, dissertation, or project.

Farah Ballout	June 19 - 2020
Signature	Date

ACKNOWLEDGMENTS

I would like to express my sincere gratitude to the following individuals who have helped me complete this dissertation and without whom this project may not have been possible.

At the forefront, I would like to thank my advisors, Drs. Hala Muhtasib and Wassim Abou-Kheir for their continuous support and guidance throughout the dissertation stages. Dr. Hala Muhtasib, thank you for your patience, immense knowledge and the effort you have always put in for the benefit of this dissertation. Dr. Wassim Abou Kheir, I can't explain how grateful I am to have an advisor that is incredibly dedicated and supportive. I am heartily thankful for your encouragement, enthusiasm and inspiration. Thank you for believing in me, pushing me to do my best, always boosting my confidence and always being ready to help.

I would like to thank the committee members: Dr. Nadine Darwiche, Dr. Rabih Talhouk, Dr. Tamar Abou Antoun and Dr. George Hilal, for reviewing this dissertation and for their insightful comments and questions.

I had the privilege to belong to two labs: the HM lab and the WAK lab. I have made a new family in both and I am thankful for each one of them. Thank you Dr. Maamoun for being ready to help at times of need. Thank you Hala El Ouweini for contributing to this project. Thank you, Samar, Maya, Jolie, Joyce and all lab members for the beautiful friendship that I will always cherish. A special thank you goes to my partner in crime, Alissar Monzer, for the stimulating discussions, for the late nights we were working together, for all the fun we have had in the last four years and for always being there.

Last but not the least, I would like to acknowledge the immense impact and support that my family has given me, including my father and mother whose encouragement was beyond description. I would like to thank my two brothers, Jad and Shadi, and my one and only sister Sylvana for all the love and support and for always believing in me and being there for me. I dedicate this work to you, and I hope I have made you proud.

AN ABSTRACT OF THE THESIS OF

Farah Rabih Ballout for Doctor of Philosophy
Major: Cell and Molecular Biology

Title: Thymoquinone induces apoptosis and DNA damage in 5-Fluorouracil-resistant colorectal cancer stem/progenitor cells and sensitizes them to radiation

Background: Colorectal cancer (CRC) is one of the most prevalent cancers among men and women. It is a heterogenous disease that arises from a combination of genetic and epigenetic alterations. Despite the advances in treatment options, CRC is associated with high mortality and recurrence rates. High recurrence rates have been recently attributed to a population of cancer stem cells (CSCs) characterized by self-renewal capacity and resistance to chemo and radiation therapy. Isolation of colorectal CSCs remains to be a challenge due to the lack of universally characterized markers. Therefore, it is essential to adopt new approaches for the treatment of this disease by identifying and effectively targeting colorectal CSCs. The black seed extract Thymoquinone (TQ) has shown promising antitumor properties on numerous cancer systems both *in vitro* and *in vivo*; however, its effect on colorectal CSCs is poorly established. In addition, studies on the effect of TQ as a radiosensitizer against CSCs are limited.

Objective: The overall aim of this thesis was to investigate the effect of TQ on targeting colorectal cancer stem/progenitor cells either alone or in combination with radiation. Our first aim was to demonstrate the inhibitory effect of TQ on 5FU-sensitive and resistant human colorectal cancer HCT116 cells cultured in 2D. Considering that three-dimensional (3D) sphere cultures are rapidly emerging as an *in vitro* model to study CSC properties, our second aim was to employ 3D sphere formation assay to isolate and enrich for colorectal CSCs from both cell lines and study the effect/mechanism of action of TQ on proliferation and self-renewal capacity of colonospheres. The third aim was to establish the effect of TQ on sensitizing 2D and 3D cultured cells to radiation. Our last aim was to characterize the *in vivo* tumor initiation capacity of colonospheres and determine cellular/molecular effects of TQ on resistant colonospheres *in vivo*.

Methods: We first assessed the response of TQ on 2D cultures, and then tested its efficacy in a 3D sphere-formation assay against an enriched population of colorectal

cancer stem/progenitor cells in which single cell suspensions were plated in a 3D environment using Matrigel as an extracellular matrix. Immunofluorescent analysis, immunohistochemistry and western blot were used to determine TQ's mechanism of action. The effect of TQ and radiation combination in 2D and 3D cultures was established using immunofluorescence staining for γ-H2AX and xenotransplantation mouse model of colorectal cancer along with molecular assays were used to characterize TQ's effect *in vivo*. Statistical analysis was performed using Graphpad prism 7.

Results: Our results showed that TQ significantly decreased self-renewal potential of CSC populations enriched from 5FU-sensitive and resistant HCT116 cells at 10-fold lower concentrations when compared to 2D monolayers. TQ decreased the expression levels of colorectal stem cell markers CD44 and EpCAM and proliferation marker Ki67 in colonospheres derived from both cell lines and reduced cellular migration and invasion. Further investigation revealed that TQ treatment led to increased TUNEL positivity and a dramatic increase in the amount of the DNA damage marker γ-H2AX particularly in 5FU-resistant colonospheres, suggesting that the diminished sphere forming ability in TQ-treated colonospheres is due to induction of DNA damage and apoptotic cell death. Interestingly, combination of TQ and radiation induced a dramatic increase in γ-H2AX 24 hours after radiation, suggesting that TQ sensitizes 5FU-sensitive and resistant cells to radiation. TQ and radiation treatment also significantly reduced the number of 5FU-sensitive and resistant colonospheres when compared to radiation alone. The intraperitoneal injection of TQ in mice inhibited subcutaneous tumor growth of spheres derived from 5FU-sensitive and 5FU-resistant HCT116 cells. Also, TQ treatment induced apoptosis and inhibited NF-κB and MEK signaling in these tumors.

Conclusion: This study underscores the importance of 3D sphere culture assay for studying colorectal CSC properties. Moreover, this study demonstrates TQ's potential as an effective treatment strategy against colorectal cancer stem/progenitor cells either alone or in combination with radiation.

CONTENTS

ILLUSTRATIONS

TABLES

ABBREVIATIONS

2D: Two-dimension

3D: Three-dimension

5FU: 5-Fluorouracil

5FU-R: 5-Fluorouracil resistant cells

5FU-S: 5-Fluorouracil sensitive cells

ABC: ATP-binding cassette

ALDH1: Aldehyde dehydrogenase 1

APC: Adenomatous polyposis coli

Bcl-2: B-cell lymphoma 2

Bcl-xL: B-cell lymphoma-extra large

BMP: Bone Morphogenetic Protein

BSA: Bovine Serum Albumin

CDK2: Cyclin dependent kinase 2

CHEK1: Checkpoint kinase 1

CIMP: CpG island methylator phenotype

CIN: Chromosomal instability

CK19: Cytokeratin 19

CK8: Cytokeratin 8

COX2: Cyclo-oxygenase 2

CRC: Colorectal cancer

CSCs: Cancer Stem Cells

DAB: Diaminobenzidine

DMSO: Dimethyl Sulfoxid

ECM: Extracellular Matrix

EGFR: Epidermal Growth Factor Receptor

EMT: Epithelial-Mesenchymal Transition

EpCAM: Epithelial cell adhesion molecule

FAK: Focal Adhesion Kinase

FBS: Fetal Bovine Serum

G: Generation

GSH: Gluthathione

GSK-3β: Glycogen synthase kinase 3β

H&E: Hematoxylin and Eosin

HCT116: Human colorectal cell line

IF: Immunofluorescence

IHC: Immunohistochemistry

IL-4: Interleukin 4

IR: Ionizing Radiation

Lgr5: Leucine-Rich Repeat-Containing G-Protein-Coupled Receptor

MAPK: Mitogen-Activated Protein Kinase

MLH1: Mult homolog 1

MMP: Matrix metalloproteinase

MSI: Microsatellite instability

MTT: 3-(4, 5-dimethylthiazol-2-yl)-2, 5-diphenyltetrazolium bromide

MUC: Mucin

NF-κB: Nuclear factor kappa

NGS: Normal Goat Serum

NOD-SCID: Non-obese Diabetic Severe Combined Immunodeficiency

NOG: Non-obese Diabetic/Shi-scid IL2rgamma^{null}

PBS: Phosphate Buffered Saline

PFA: Paraformaldehyde

PPAR: Peroxisome proliferator-activated receptor

ROS: Reactive oxygen species

SCs: Stem cells

SD: Standard deviation

SEM: Standard error mean

SFU: Sphere formation unit

Shh: Sonic hedgehog

TGF-β: Transforming Growth Factor-Beta

TNF-α: Tumor Necrosis Factor α

TQ: Thymoquinone

VEGF: Vascular Endothelial Cell Growth Factor

XIAP: X-Linked Inhibitor of Apoptosis Protein

CHAPTER I

INTRODUTION

A. Colorectal cancer

1. Colon structure and function

The first part of the large intestine, the colon, is a muscular tube about 1.5 meters long and 5 centimeters in diameter. It is made up of four sections: ascending, transverse, descending and sigmoid colon. The ascending and transverse colon are referred to as the proximal colon, while the descending and sigmoid are referred to as the distal colon. Histologically, the colon is made up of mucosa, submucosa, muscularis and serosa/adventitia. The mucosa is lined by simple columnar epithelium and contains crypts of Lieberkuhn, the basic functional unit of the intestine, and numerous goblet cells [1]. The key functions of the colon include absorption of water, nutrients and vitamins, feces compaction, moving waste material towards rectum and secretion of potassium and chloride [2].

Intestinal epithelial cells display the highest turnover rate, and the entire intestinal epithelial lining in humans is replaced every 5 to 7 days. This rapid regeneration is fueled by the proliferation of stem cells (SCs) [3, 4]. Intestinal SCs are undifferentiated, multipotent, and self-renewable/maintained cells involved in tissue homeostasis and repair, located at the crypt base [5]. These cells divide mostly asymmetrically and give rise to two different daughter cells, with one being identical to the original cell, while the other has the potential to differentiate (progenitor). An

intestinal crypt contains approximately 16 SCs and harbors two distinct pools of putative SCs. One pool is located at the crypt base and is characterized by the expression of leucine-rich repeat containing G protein-coupled receptor 5 (Lgr-5). The other pool resides at +4 position and consists of B lymphoma Moloney murine leukemia virus (Mo-MLV) insertion region 1 homolog (Bmi-1) and telomerase reverse transcriptase (Tert) expressing cells [6, 7]. Intestinal SCs niche consists of cellular and extracellular components that ensure the optimal conditions for SCs maintenance through the secretion of various cytokines, growth factors, and direct interactions [5, 8]. Intestinal SCs may also be affected by components in the crypt lumen, derived from epithelial cells or from bacteria. Intestinal subepithelial myofibroblasts mediate the crosstalk between epithelial and mesenchymal cells and secrete a wide range of morphogenetic factors [9]. Epithelial–mesenchymal interactions regulate the normal intestinal architecture and additionally define the balance between proliferation and differentiation. Wingless/Int (Wnt), Hedgehog, bone morphogenetic protein (BMP), Notch, and platelet derived growth factor pathways are involved in these interactions [9]. Identification and isolation of SCs remains a challenge due to the lack of specific molecular markers. Some of the molecules involved in critical stages of proliferation and differentiation and which are used for the identification of SCs include Musashi-1 (Msi-1), CD29, Bmi-1, Lgr-5, aldehyde dehydrogenase 1 (ALDH-1), Tert, and achaete scute-like 2 [10, 11]. For a more detailed presentation of the used markers, refer to Table 1.

2. Colorectal cancer epidemiology and mechanism of carcinogenesis

Colorectal cancer (CRC) is the third most common cancer in men and women. The incidence rates have been reduced in the past few years in older aged groups mainly due to the increased screening and uptake of colonoscopy; however, incidence rates are rising in individuals younger than 50 [12]. Many factors influence the risk of developing CRC including age, sex, race and ethnicity, diet, smoking and sedentary lifestyle [13].

The progression of CRC starts with uncontrolled epithelial cell replication, followed by formation of adenomas, which eventually evolve into adenocarcinomas with metastatic potential [14]. CRC can arise from one or a combination of three different mechanisms, namely chromosomal instability (CIN), CpG island methylator phenotype (CIMP), and microsatellite instability (MSI) (Figure 1) [15]. CIN is associated with 65%-70% of sporadic CRCs. It begins with the acquisition of mutations in the adenomatous polyposis coli (APC), followed by the mutational activation of the oncogene KRAS and the inactivation of the tumor suppressor gene, TP53. Aneuploidy and loss of heterozygosity (LOH) are the major players in CIN tumors [16]. MSI is found in 15% of CRCs. It involves inactivating mutations in the DNA mismatch repair genes responsible for correcting DNA replication errors and these include ATPases hMSH2, hMSH6, hMSH3, hMLH1, hPMS2, hPMS1, and hMLH3. MSI tumors are often associated with proximal colon and poor differentiation but better prognosis [17]. The CIMP pathway is characterized by promoter hypermethylation that results in transcriptional inactivation of various tumor suppressor genes, most importantly MGMT and MLH1. This hypermethylation is often associated with BRAF mutation and

MSI [18]. The three mechanisms often overlap in molecular CRC subtypes and classifying tumors according to the particular mutations present is necessary in determining the treatment regimen to be offered.

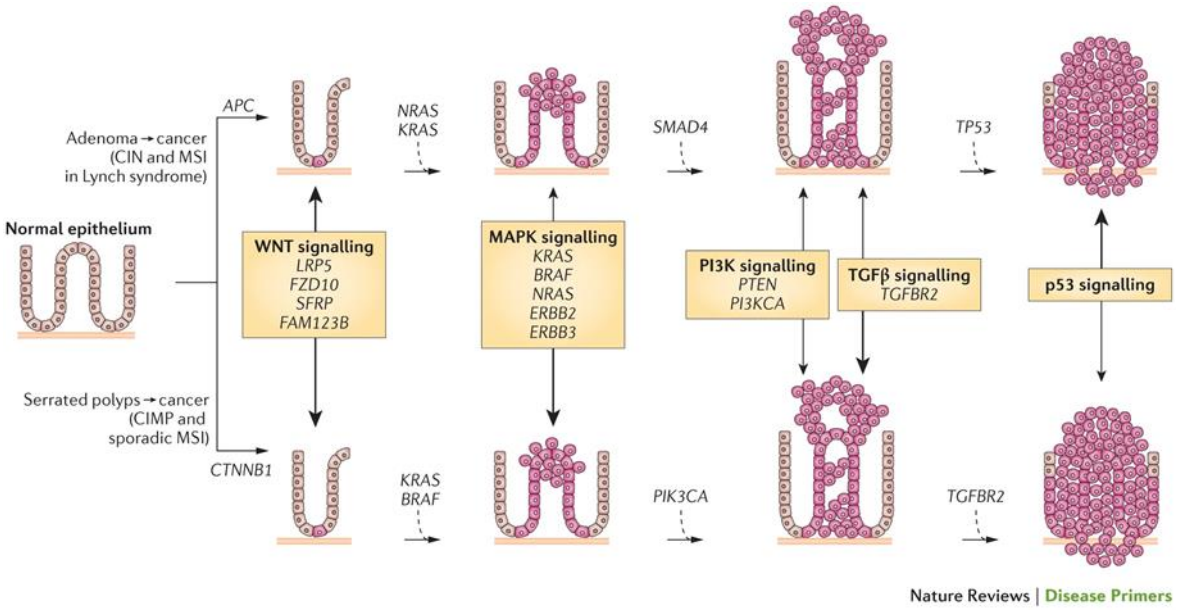

Figure 1. Mechanism of colorectal cancer progression. Two pathways have been described: the classic pathway (top) involves progression of tubular adenomas to adenocarcinomas and the alternate pathway (bottom) involves serrated polyps, and their progression to serrated colorectal cancer. Important molecular, genetic and epigenetic changes and deregulated signaling pathways with respect to colorectal cancer progression are shown. *CTNNB1*, catenin-β1; *FAM123B*, family with sequence similarity 123B (also known as *AMER1*); *FZD10*, frizzled class receptor 10; *LRP5*, low-density lipoprotein receptor-related protein 5; MAPK, mitogen-activated protein kinase; MSI, microsatellite instability; PI3K, phosphatidylinositol 3-kinase; *PI3KCA*, phosphatidylinositol-4,5-bisphosphate 3-kinase catalytic subunit-α; *PTEN*, phosphatase and tensin homologue; *SFRP*, secreted frizzled-related protein; *SMAD4*, SMAD family member 4; TGFβ, transforming growth factor-β; *TGFBR2*, TGFβ receptor 2. [Adapted from [19]].

3. Diagnosis and management of colorectal cancer

Diagnosis of CRC is based on screening and on patient assessment when symptoms are present. Various methods can be used for diagnosis including colonoscopy, rectoscopy, occult blood test [19]. CRC is categorized into four stages (Figure 2) and treatment is driven by the tumor stage at the time of diagnosis. Surgery is the main treatment when cancer has not spread to distant sites. In stage 0 CRC in which colon growths have not developed past the internal covering of the colon, surgery is all that is required by evacuating the polyp or expelling part of the colon if necessary. Stage I is defined by the appearance of small tumorigenic nodules that have developed into the layers of the colon but have not spread outside. Surgery is the standard treatment for stage I CRC patients. Stage II is characterized by numerous tumorigenic nodules through the mass of the colon and potentially into neighboring tissues with no spread to the lymph nodes. Surgery is the first line of treatment in stage II CRC and is sometimes used in combination with adjuvant chemotherapy, which incorporates various blends including 5-fluorouracil (5FU) and leucovorin, or capecitabine if there is a high chance of recurrence due to specific variables including proximity to blood or lymph vessels and puncturing of the colon. Stage III CRC has spread outside the colon to one or more lymph nodes. Surgery combined with adjuvant chemotherapy is usually utilized for the treatment of this stage. Chemotherapy regimens that are frequently used include either FOLFOX (5FU, leucovorin, and oxaliplatin) or CapeOx (capecitabine and oxaliplatin). Radiation may sometimes be exhorted when in doubt that some malignant cells are spared after surgery. In stage IV CRC, the tumor has spread to other organs mainly liver and lungs. Surgery alone is not enough at this stage and is combined

with various chemotherapy regimens and is focused on treatments to control the disease. Radiation may be also employed in some cases [20]. Postsurgical survival depends on the stage of the tumor, around 90% in early stages and 50% in late stages.

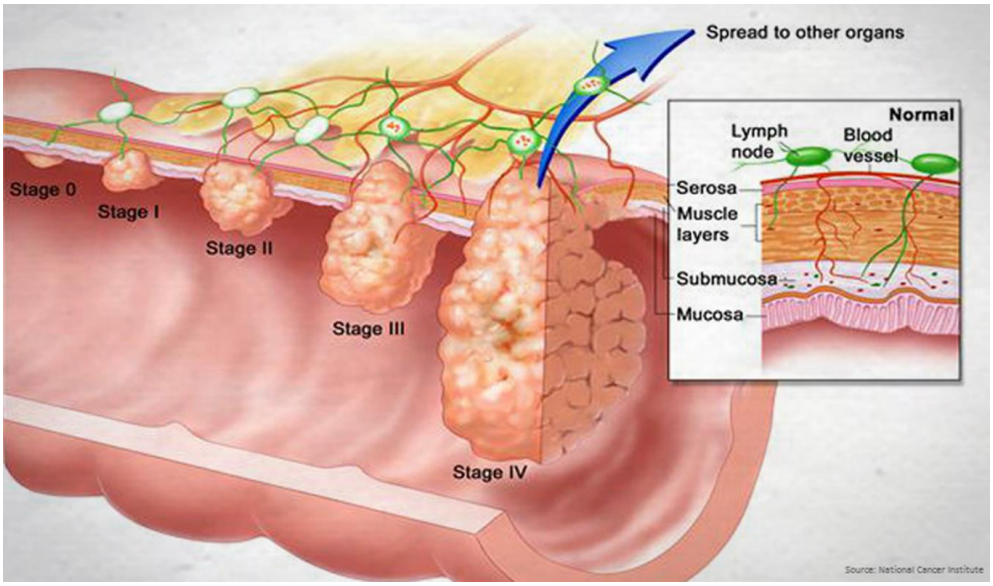

Figure 2: Colorectal cancer stages. Stage 0-II are characterized by progressive growth of small tumorigenic nodules at the lining of the colon. Stage III tumors attain neighboring lymph nodes. Stage IV tumors spread to distant organs. Treatment is applied based on the tumor stage at the time of diagnosis [Adapted from [20]].

Despite the advances in treatment options, CRC is associated with high mortality and recurrence rates. 5FU is the standard chemotherapy for metastatic CRC. It is a heterocyclic aromatic organic compound with a structure similar to that of the pyrimidine molecules of DNA and RNA; it is an analogue of uracil with a fluorine atom at the C-5 position in place of hydrogen (Figure 3) [21]. Due to its structure, 5FU interferes with nucleoside metabolism and can be incorporated into RNA and DNA, leading to cytotoxicity and cell death [22]. 5FU effectiveness has been greatly limited due to drug resistance that has been associated with multiple factors including:

- High-level expression of thymidylate synthase (TS) [23]
- Increased activity of deoxyuridine triphosphatase and the corresponding catabolism of 5FU may lead to 5FU resistance [24].
- Methylation of the MLH1 gene [25], a DNA mismatch repair gene, which silences the expression of this gene. This can lead to MSI in cells, which have been found to be more resistant to 5FU.
- Overexpression of Bcl-2 and Bcl-xL proteins [26], which play an important role in the anti-apoptotic function.
- Cell cycle perturbation including cell cycle delays in G1 and G1/S boundary and prolonged DNA synthesis time that prevent incorporation of 5FU metabolites into DNA and provide cancer cells with enough time to correct the misincorporated nucleotides. In addition to reduction in CDK2 protein, Thr-160 phosphorylated CDK2, cyclin D3 and cyclin A are reduced [27].

- Down-regulation of mitochondrial ATP synthase that has been shown to antagonize 5FU-induced suppression of cell proliferation and may lead to cellular events responsible for 5FU resistance [28].
- Aberrant expression of genes such as midkine gene expression and increased expression of metabotropic glutamate receptor 4 (mGluR4) [29]. In addition, ATP-binding cassette (ABC) proteins play an important role in drug resistance of 5FU [30]. Microarray technology has enabled the identification of several genes related to anticancer 5FU resistance and data suggest that altered regulation of nucleotide metabolism, amino acid metabolism, cytoskeleton organization, transport, and oxygen metabolism may underlie the differential resistance to 5FU seen in cell lines [21].

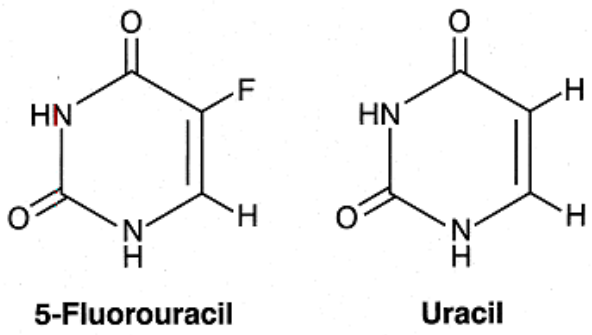

Figure 3: 5-Fluorouracil and Uracil structure

B. Cancer Stem Cells

The fraction of cells that are capable of tumor initiation are referred to as cancer stem cells (CSCs). These cells are characterized by self-renewal, multipotency, limitless proliferation potential, angiogenic, and immune evasion features [31]. Intriguingly, CSCs are relatively highly resistant to traditional tumor therapeutic measures and are thus responsible for tumor relapse due to the expression of DNA repair mechanisms, detoxifying enzymes, anti-apoptosis proteins and multiple drug resistance transporters [32, 33] (Figure 4) .

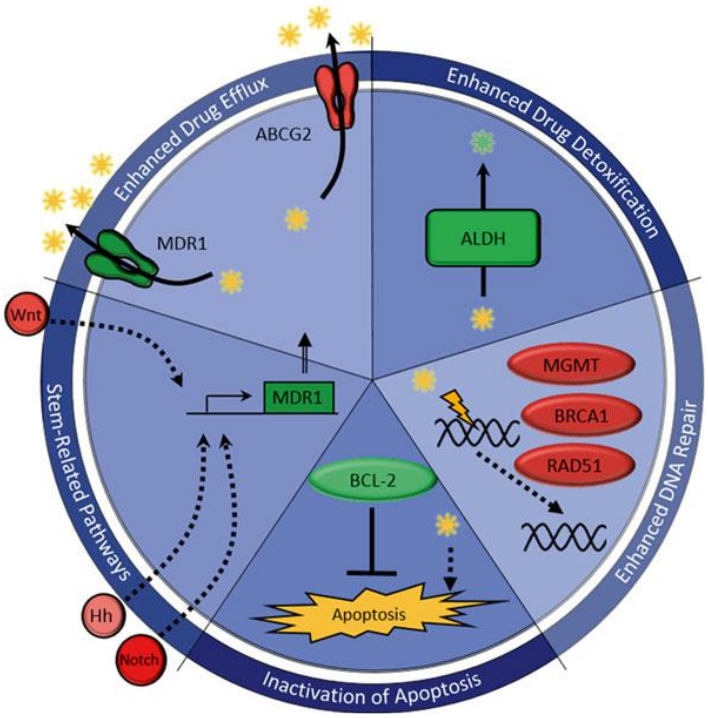

Figure 4. Mechanisms of CSC-associated chemotherapy resistance. Multiple mechanisms of CSC-associated chemotherapy resistance mechanisms have been identified and are shown here in clockwise order: (1) Increased expression of ABC transporters including MDR1/ABCB1 and BCRP/ABCG2 leads to increased efflux of many subclasses of chemotherapeutic and multidrug resistance. (2) Increased expression of ALDH enzymes leads to detoxification and inactivation of chemotherapeutics. (3) Enhanced DNA repair due to increased expression of DNA repair proteins such as MGMT, BRCA1, and RAD51. (4) Reduced apoptosis due to increased levels of the anti-apoptotic protein Bcl-2. (5) Increased activation of

embryonic signaling pathways Wnt, Notch and Hedgehog leads to chemoresistance via altered signaling (e.g. increase expression of drug efflux proteins such as MDR1). [Adapted from [33]].

Lapidot and colleagues provided the first solid evidence to support the CSC hypothesis in acute myeloid leukemia (AML) where they identified a rare population of stem-like cells that could initiate human AML when transplanted into immunodeficient mice [34]. The identification of leukemia stem cells has fostered an intense effort to isolate and characterize CSCs in solid tumors including breast [35], colon [36], brain [37], pancreas [38, 39], and prostate [40, 41].

Tumors can originate from both stem cells and non-stem cells. The rapid turnover of the intestinal epithelium led to the assumption that the long-lived intestinal stem cells (ISCs) are the most likely cell of origin for tumorigenesis; however, studies have shown that tumors can also be derived from progenitor cells [42]. These tumor-forming cells could hypothetically originate from a stem cell that undergoes a mutation, or a progenitor cell that acquires two or more mutations, or a fully differentiated cell that undergoes several mutations driving it back to a stem-like state (Figure 5). In all three scenarios, the resultant CSC has lost the ability to regulate its own cell division. Hence, CSCs share similarities with normal stem cells, but they do not necessarily originate from them. Self-renewal ability, proliferation and quiescence state are some of these shared characteristics. Several stem cell surface markers are also common, but the difference resides in tumor-specific CSC surface markers, the degree of dependence on

the microenvironment where stem cells reside and deregulated signaling pathways involved in survival and differentiation of progeny [43].

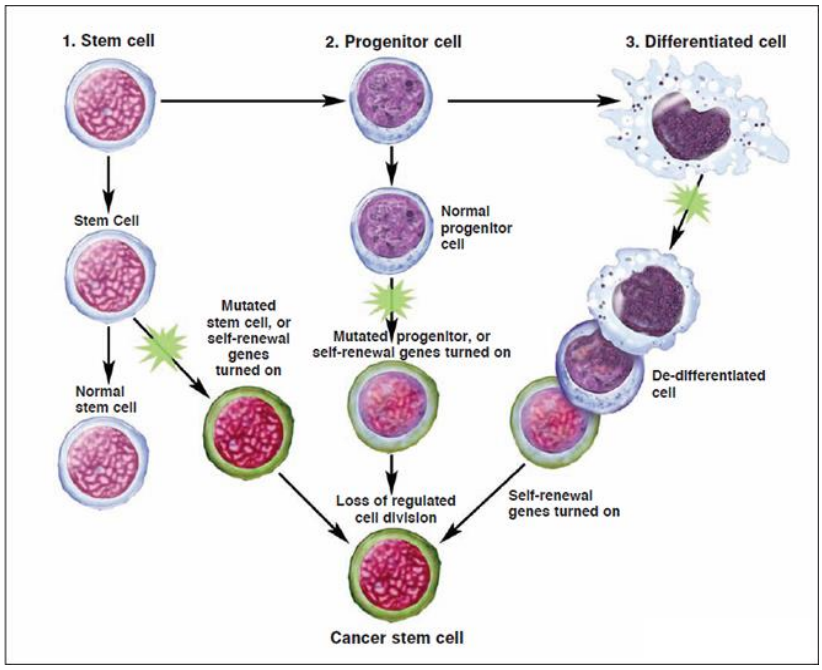

Figure 5: Origin of Cancer Stem Cells. A cancer stem cell may arise from mutations in (1) stem cell, (2) progenitor cell or (3) differentiated cell that result in loss of regulated cell division. [Adapted from NIH Stem Cell Information Home Page. In Stem Cell Information. Bethesda, MD: National Institutes of Health, U.S. Department of Health and Human Services, 2016. Available at < //stemcells.nih.gov/info/Regenerative_Medicine/2006chapter9.htm>]

Like the normal SCs, CSCs reside in a qualified microenvironment that has gained tumor-promoting traits [44]. Genetic or epigenetic aberrations in the SCs compartment may lead to alterations of the niche [45, 46]. This tumorigenic niche is composed of transformed myofibroblasts, recruited myeloid cells, other cell types, and extracellular components, which produce various growth factors and cytokines,

including hepatocyte growth factor (HGF), tumor necrosis factor α (TNF-α), and interleukin (IL)-6, which promote dedifferentiation, carcinogenesis, and invasiveness [9, 46].

Evidence suggests that it is the fine tuning between pathways involved in self-renewal that switch a normal stem cell into a malignant stem cell [47]. Three major signaling pathways contribute to stem cell development and oncogenesis: Notch, Sonic hedgehog (Shh) and Wnt signaling [47-49], with Wnt being the most relevant for CRC development. These pathways control the balance between proliferation, differentiation, migration, and renewal. The Wnt pathway is responsible for endoderm formation and exerts fundamental role in crypt development, maintenance, and proliferation, as it is depicted by the failure of Wnt knockout mice to develop colonic crypts [50-52]. A Wnt gradient loss of expression from the base to the top is closely related with differentiation and expression of the ephrin family proteins, which regulate positioning [53]. Mutations in the APC gene, beta-catenin, or the regulatory proteins in the Wnt pathway result in constant activation [51]. This may lead to uncontrolled proliferation, a shift from asymmetrical to symmetrical divisions, and augmented survival. Wnt signaling is also involved in the process of epithelial to mesenchymal transition (EMT) and invasion [9, 50]. Understanding stem cell biology and its relationship with oncogenesis hold insight for development of efficient targeted cancer therapies.

C. Colorectal Cancer Stem Cells

1. Overview

Human colorectal CSCs were first isolated based on CD133 expression and were found to induce tumors that resembled the original malignancy when injected in mice [36, 53]. The use of CD133 as an effective marker of colorectal CSCs has been challenged by data that support its use. CD133+ cells in HT29 colorectal cancer cells were found to be more tumorigenic than CD133- cells both *in vitro* and *in vivo* [54]. Some data argue against the use of CD133 as an effective marker since it was shown to be ubiquitously expressed in differentiated epithelial cells and its expression was not restricted to the CSC fraction in metastatic colon cancers [55]. Moreover, CD133+ HCT116 colorectal cancer cells were found not to be radio-resistant [56]. The search for other surface markers of colorectal CSCs continued with the hope of finding specific markers that can be used as therapeutic targets. Markers that have been described to characterize colorectal CSCs include CD133, CD44, CD24, CD166, Lgr-5, and ALDH-1 [11, 57]. For a more detailed presentation of the used markers, refer to Table 1.

Table 1. Normal and colorectal cancer stem cell markers
[Adapted and modified from [58]]

	Markers	Cellular Function
Normal Stem Cell	Musahi-1	RNA binding protein
	Hes-1	Transcriptional repressor
	Bmi-1	Policomb-repressor protein
	Lgr-5	Wnt target gene
	ALDH1A1	Enzyme
	DCAMKL1	Kinase
Colorectal Cancer Stem Cell	CD24	Heat-stable antigen; membrane glycoprotein, adhesion molecule
	CD29	β1 integrin, adhesion molecule
	CD44	Hyaluronic acid receptor
	CD58	Cell adhesion molecule
	CD133	Associated with poor prognosis, low survival, and distant metastasis in colorectal adenocarcinoma
	CD166	Cell adhesion molecule
	DCLK1	Kinase
	EpCAM	Cell adhesion molecule
	Lgr-5	Wnt target gene
	ALDH1A1	Aldehyde dehydrogenase, detoxification enzyme
	ATP binding cassette protein	Drug transporter, effluxes drugs.
	OCT 4	POU-domain transcription factor, highly expressed in embryonic stem (ES) cells
	SOX2	Group B of the Sox family of transcription factor, involved in development
	c-Myc	Transcription factor, high c-Myc levels blocks cell differentiation and enhance self-renewal of committed and differentiated cells

Cancer stem cell markers are expressed in a complex pattern; neither single marker expression nor simple combinations can be universally used for isolation and enrichment of colorectal CSC [59]. Many questions remain to be answered when it comes to colorectal CSCs identification including 1) the consistency of CSC-associated markers because the CSC phenotype itself has been shown to be unstable and may vary depending on tumor stage, 2) the type and timing of therapy, and 3) a series of microenvironmental and individual factors that are predictably difficult to define [60].

Therefore, colorectal CSCs are not universally characterized by their CSC markers but need to be further supported through molecular and/or functional features. A major molecular feature of colorectal CSCs has been shown to be a hyperactivated β-catenin pathway, which translates into the ability to generate serial tumors *in vivo* [46]. Self-renewal is a functional trait that in colorectal CSCs has been shown to depend on transcriptional regulators namely ID1, ID3 [61] and BMI1 [62]. Another insight on functionality of colorectal CSCs is obtained by molecular tracking studies, which can monitor CSC behavior in an *in vivo* setting [63].

2. Enrichment of Colorectal Cancer Stem Cells

Most techniques used for the isolation of CSCs are cumbersome and expensive making them unideal for screening and testing of drugs for development of CSC-based therapy. In addition, no simple combination of markers can be used for the identification of CSCs from different sources of tumor cells [59]. Three-dimensional (3D) *in vitro* models have been used in cancer research as an intermediate model between *in vitro* cancer cell line cultures and *in vivo* tumors [64, 65]. Sphere cultures, also known as tumorospheres, represent a major 3D *in vitro* model in cancer stem cell research [66]. It provides a means to evaluate the self-renewal capacity and the differentiation potential of CSCs [67]. Sphere cultures can be used to grow spheres in 3D in two different ways: in a suspension or on a reconstituted basement membrane (BD Matrigel matrix) [68].

As opposed to 2D monolayer cultures composed mainly of proliferating cells, 3D spheroids are comprised of cells in various stages, usually including proliferating,

quiescent, apoptotic, hypoxic, and necrotic cells [69, 70]. The outer layers of a spheroid, which is highly exposed to the medium, are mainly comprised of viable, proliferating cells. The core cells receive less oxygen, growth factors, and nutrients from the medium, and tend to be in a quiescent or hypoxic state [71]. Such cellular heterogeneity is very similar to *in vivo* tissues, particularly in tumors. Studies have found that drug sensitivity also differs between cells cultured in 2D versus 3D models. Cells cultured in 3D models are more resistant to anticancer drugs than 2D cultures. This difference can be attributed to dynamic cellular interactions between neighboring cells and extracellular matrix (ECM) [72], limited diffusion through the spheroid that depends on the depth to the surface where the cells are located, hypoxia, and differences in morphology, gene/protein expression and cell stages. Such chemoresistance developed in 3D spheroids is observed *in vivo* as well.

Unlike other 3D cultures, tumorospheres do not fully replicate the 3D structure and environment of an *in vivo* tumor [73] and their main purpose is to study CSC properties rather than mimic cancer tissues. Sphere cultures have been used to isolate CSCs from various cancer cell lines including breast [74, 75], renal [76], liver [77], prostate [78-80], pancreatic [81], and brain [82-84] cancers. Tumorosphere cultures in serum-free medium were also used to isolate and propagate colorectal CSCs from primary tumors but have been rarely used to enrich CSCs from colorectal cancer cell lines [85-87].

Tumorospheres are heterogenous structures containing a range of morphologically distinct entities displaying inter- and intra-sphere molecular heterogeneity, including stem cells, progenitors, and differentiated cells [88]. Three

different types of undifferentiated CSCs were resolved from patient tumors using tumorosphere cultures and these are: 1) a rare subset of CSCs that maintained tumor growth on serial transplantations; 2) a subset of tumor-initiating cells with limited self-renewal capacity that contributed to tumor formation only in primary mice and are therefore not consistently defined as CSCs; and 3) a more latent subset of CSCs apparently activated in second or tertiary transplantation assays. This confirms that the tumorosphere assay selectively enriches for the growth of CSCs [46]. Studies have also reported that the tumorosphere assay enriches CSC population in a cell line–dependent manner [89].

In our study we adopted a 3D sphere formation assay to isolate and enrich colorectal CSCs from colorectal cancer cell lines in which single cell suspension in serum-free medium is mixed with Matrigel, a semi-solid basement membrane majorly composed of laminin, collagen IV, heparin sulfate proteoglycans, entactin, nidogen and growth factors, mimicking the interaction between CSCs and the ECM *in vivo* [90].

3. Targeting Colorectal Cancer Stem Cells

Most of the CRC-associated mortality stems from the recurrence and metastatic spread of chemo-resistant cells to other vital organs, mainly the liver and lungs [91]. The presence of chemotherapy-resistant CSCs is one of the significant causes of tumor recurrence [14]. Therefore, traditional chemo-radiotherapy should be combined with new practical therapeutic approaches that target CSCs and prevent relapse [92, 93].

Direct CSC targeting can be achieved by several approaches which include inhibiting self-renewal pathways including Wnt, Notch, and Hedgehog, as well as

selectively targeting surface markers, inhibiting ABC cassette, interfering with vital antiapoptotic or metabolic pathways, activating differentiation pathways, and/or by acting on the protective microenvironment (Figure 6) [63, 94]. Monoclonal antibodies against the CD133 cell surface molecule effectively inhibited the growth of hepatocellular and gastric cancer cells [95]. Small molecule inhibitors of Wnt and γ-secretase inhibitors of Notch have been suggested as novel agents against CRC [5]. Induction of colorectal CSCs differentiation by bone morphogenetic protein 4 (BMP4) caused apoptosis and enhanced chemo-sensitization of these cells to 5-fluorouracil and oxaliplatin [96]. Manipulating the apoptotic machinery to induce apoptosis of CSCs represents a promising approach. CD133+ CSCs from colon carcinomas could produce and use IL-4 to protect them from apoptosis. Inhibition of the IL-4 pathway with an anti-IL-4 antibody or an IL-4 receptor antagonist in CD133+ colorectal CSCs augmented the antitumor effects of conventional chemotherapeutics, 5-fluorouracil and oxaliplatin [97]. Interruption of the crosstalk network between the elements of the niche and CSCs including disruption of EMT and angiogenesis can exhaust the source of nutrition and change the essential signals needed by CSCs, thus restricting growth and resulting in loss of metastatic capacity [94]. Recently, much attention has been focused on several phytochemicals showing promising anti-cancer properties due to their safety, availability, cost effectiveness and more importantly their ability to improve efficacy when combined with conventional chemo- and radiotherapy [98]. Since CSCs are more resistant to conventional therapies in comparison with the differentiated cells constituting the tumor bulk, a combination of naturally derived drugs and conventional

anti-cancer drug therapies may have the potential to overcome tumor resistance and reduce recurrence.

Figure 6: Therapies targeting cancer stem cells. Targeting CSCs can be achieved by inhibiting self-renewal pathways (green area), by inhibiting ABC cassette (purple area), selectively targeting surface markers of CSCs (red area), or by acting on the protective microenvironment (blue area). [Adapted from [99]]

D. Thymoquinone

Thymoquinone (TQ: 2-isopropyl-5-methylbenzo-1,4-quinone) is the primary active molecule of the essential oil of *Nigella sativa* L. black seed that has been extensively utilized in traditional medicine owing to its various health promoting capacities [100]. TQ has a basic quinone structure consisting of a para substituted dione conjugated to a benzene ring to which a methyl and an isopropyl side chain groups are added in positions 2 and 5, respectively [101] (Figure 7).

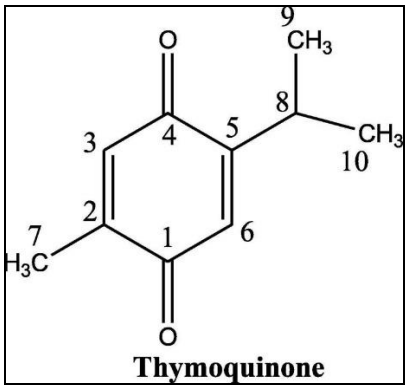

Figure 7: Chemical structure of Thymoquinone. [Adopted from [101]]

TQ has a wide range of beneficial biological and pharmacological properties. It possesses outstanding antioxidant [102], hypoglycemic [103], anti-inflammatory [104], anticancer [100], neuro- [105], cardio- [106], nephro- [107] and hepato-protective [108] activities. TQ showed promising effects on various cancer types both *in vitro* and *in vivo* [109] including breast [110], prostate [111], gastric [112], lung [113], colorectal

[114-117], osteosarcoma [118] and bladder [119] cancer. Refer to tables 2 and 3 for more detailed information.

The ability of TQ to target nine of the ten hallmarks of cancer as well as its efficacy, selectivity against colorectal cancer and lack of toxicity to normal tissues makes it potentially interesting for CRC therapy [120]. TQ's ability to inhibit colorectal cancer growth and invasion and induce cell cycle arrest and apoptosis in colorectal cancer cell culture and animal models have been documented by our group and by others [120-124]. TQ has been shown to inactivate the JAK/STAT signaling pathway by inhibiting STAT3 phosphorylation, reducing c-Src and JAK2 activity and attenuating the expression of STAT3 target gene products [125]. TQ is known to modulate Wnt signaling through GSK-3β activation, β-catenin translocation, and reduction of nuclear c-myc [126]. TQ was also found to activate p53, induce PARP cleavage, and reactive oxygen species production (reviewed in [127]). Comprehensive studies about TQ's potential effect on colorectal CSCs either alone or in combination with other clinically available drugs are lacking [128].

Naturally derived drugs are an important component of cancer combination chemotherapy and are integrated with traditional regimens to improve efficacy, safety and tolerability [98]. They establish their effects by either acting synergistically with conventional drugs or by sensitizing the cells to them [129]. TQ was shown to enhance chemotherapeutic potentiality when combined with clinically available drugs [130]. Combination of TQ with 5FU increased apoptotic activity in gastric cancer cells *in vitro* and *in vivo* [131, 132]. Kensara et al. reported that 5FU and TQ cooperate to repress the expression of pro-cancerous Wnt, β-catenin, NF-κB, COX-2, iNOS, VEGF, and

TBRAS and to up-regulate the expression of anti-tumorigenesis markers DKK-1, CDNK-1A, TGF-β1, TGF-βRII, Smad4, and GPx in colorectal carcinogenesis in rats [133]. Combination of cisplatin and TQ was shown to be highly effective in enhancing cisplatin-mediated cytotoxicity in lung and ovarian cancer cells and mouse models [134, 135]. TQ and paclitaxel combination showed synergistic effects against triple negative breast cancer [136]. Treatment with TQ and docetaxel induced cytotoxicity and apoptosis by modulating PI3K-Akt pathway in Castrate-resistant prostate cancer cells [137]. Moreover, TQ in combination with zoledronic acid showed significant synergistic cytotoxic activity and DNA fragmentation in PC-3 and DU-145 prostate cancer cells [137]. In addition to its adjuvant chemotherapeutic effect, TQ also mediates radio-sensitization [138] whereby it was found to exert supra-additive cytotoxic and apoptotic effects on MCF7 and T47D breast cancer cells when combined with a single dose of ionizing radiation (2.5 Gy). TQ was also shown to have protective effects on radiation induced small intestine injury in mice by inhibiting p53 pathway, thus reducing intestinal cell apoptosis [139]. Considering TQ's multiple molecular mechanisms of action, its potency in small concentrations, *in vivo* success, and success in combination with chemo and radiotherapy, it is important to focus on its clinical translation.

Despite the promising anticancer activity of TQ, the main limitation for its clinical translation lies in its hydrophobicity, poor bioavailability and high capacity to bind to plasma proteins [140]. Very few studies investigated the pharmacokinetic and pharmacodynamic characteristics of TQ. One study showed that TQ is reduced into hydroquinone by catalyzing liver enzymes [141] and was detected in the plasma of rats

for up to 12hrs post oral administration [142]. In rabbits, the absolute bioavailability of TQ upon oral administration was 58% with a lag time of 23 minutes, and 99% of TQ was bound to plasma proteins [143]. Using the nanomaterial platform for encapsulation of TQ and synthesizing more effective new chemical derivatives with improved pharmacokinetic characteristics might be interesting and may hold great promise for future drug development and clinical use.

Table 2: TQ's anticancer activity *in vitro*

Cancer type	Cell line	TQ's mechanism of action	Reference
Acute lymphoblastic leukemia	CEM-ss	• Generated ROS and HSP70 • Induced apoptosis by down-regulating Bcl-2, up-regulating Bax, and activating caspase 3 and 8	[144]
	HTLV-1 negative Jurkat and CEM	• Decreased glutathione and increased ROS production	[145]
Acute promyelocytic leukemia	HL-60	• Induced apoptosis by activating caspase-3 and 8	[146]
Myeloid leukemia	KBM-5	• Suppressed TNF-α-induced NF-κB activation • Downregulated the expression of NF-κB - regulated antiapoptotic gene products • Downregulated the expression of proliferative gene products like cyclin D1, cyclooxygenase-2, and c-Myc, and angiogenic gene products MMP-9 and VEGF	[147]
Bladder cancer	T24	• Attenuated mTOR activity • inhibited PI3K/Akt signaling	[148]

Lung cancer	A549	• Reduced cell viability • Altered cellular morphology	[149]
		• Reduced ERK1/2 phosphorylation • Inhibited proliferation and migration	[150]
Breast cancer	MDA-MB-468, T47D	• Interfered with PI3K/Akt signaling and promoted G1 arrest	[151]
	MCF-7	• Induced apoptosis by upregulating p53	[152]
	BT549	• Downregulated TWIST1 and EMT	[153]
Colorectal cancer	HCT116	• Induced apoptosis by upregulating Bax, inhibiting Bcl-2, activating caspases -9, -7 and -3 and induction of PARP cleavage • Blocked STAT3 signaling via inhibition of JAK2- and Src-mediated phosphorylation of EGFR tyrosine kinase	[154, 155]
		• Inhibited the stress response sensor CHEK1	[156]
	HCT116w, DLD-1, HT29	• Changed conformation and scaffold function of oncogene PAK1 by binding to it • Interfered with RAF/MEK/ERK1/2 pathway and controlled cancer cell growth	[115]
	Caco-2, HCT-116, LoVo, DLD-1 and HT-29	• Inhibited proliferation	[116]
	DLD-1	• Induced apoptosis and activated JNK and ERK signaling via generation of ROS	
Gastric cancer	HGC27,	• Inhibited STAT3	[125]

	BGC823, SGC7901	phosphorylation, associated with reduction in JAK2 and c-Src activity, as well as Bcl-2, cyclin D, survivin, and VEGF	
Glioblastoma	M059K, M059J	• Induced DNA damage, telomere attrition by inhibiting telomerase and cell death	[157]
	U-87, CCF-STTG1	• Downregulated FAK • Reduced ERK phosphorylation as well MMP-2 and MMP-9 secretion • Inhibited cell migration and invasion	[158]
Hepatic carcinoma	HepG2	• Induced expression of pro-apoptotic Bcl-xS and TRAIL death receptors • Inhibited expression of the anti-apoptotic gene Bcl-2 • Inhibited NF-κB and IL-8	[159]
Osteosarcoma	MG63	• Induce oxidative damage and apoptosis by generating ROS	[118]
	SaOS-2	• Downregulated NF-κB DNA-binding activity, XIAP, survivin and VEGF • Upregulated cleaved caspase-3 and Smac	[160]
Prostate Cancer	DU145, PC-3, LNCaP	• Inhibited DNA synthesis and proliferation	[161]
	PC-3	• Acted as an angiogenesis inhibitor by suppressing VEGF	[162]
Pancreatic cancer	FG/ COLO357, CD18/HPAF	• Downregulated MUC4 expression through the proteasomal pathway • Induced apoptosis by the activation of JNK and p38 MAPK pathways	[163]

Table 3: TQ's anticancer activity *in vivo*

Cancer type	***In vivo* model**	**TQ's mechanism of action**	**Reference**
Breast cancer	Mouse xenograft	• Inhibited NF-κB • Downregulated p38 MAPK via the generation of ROS • Inhibited TWIST1 expression and regulated EMT	[153, 164, 165]
Colorectal cancer	1,2-dimethyl hydrazine (DMH) and xenografts mouse models	• Delayed tumor growth • Reduced tumor cell invasion • Increased apoptosis	[117]
Familial adenomatous polyposis	Mouse	• Induced tumor-cell specific apoptosis • Modulated Wnt signaling through the activation of GSK-3β	[166]
Gastric cancer	Mouse xenograft	• Downregulated STAT3	[125]
Hepatic carcinoma	Rat	• Decreased the expression of antioxidant enzymes including glutathione peroxidase, glutathione-stransferase and catalase • Regulated G1/S phase cell cycle transition	[167]
Pancreatic cancer	Nude mouse	• Downregulated MMP-9 and XIAP	[168]
Squamous cell carcinoma	Mouse xenograft	• Inhibited cell proliferation • Induced apoptosis by inhibiting Akt and JNK phosphorylation	[169]
Prostate cancer	Mouse xenograft	• Inhibited human umbilical vein endothelial cell migration, invasion, and tube formation, thus preventing tumor angiogenesis	[162]

Lung cancer	Mouse xenograft	• Inhibited cell proliferation • Induced apoptosis, and reduced tumor volume and tumor weight	[134]
		• Inhibited tumor growth by activating caspase 3	[170]

E. Aim of the study

Colorectal cancer is the third leading cause of death in patients and most patients die of metastasis due to the resistance of their disease to standard therapies. Therapy failure occurs because available chemotherapeutics shrink the tumor bulk by eliminating the highly proliferating chemo-sensitive clones and sparing the quiescent chemo-resistant CSCs that retain the ability of self-renewal and differentiation into highly proliferative cells which replenish the tumor. Therefore, it is essential to adopt new approaches for the treatment of this disease. The combination of conventional chemotherapy and CSC-targeted therapy is the strategic therapeutic for tumor regression and for avoiding tumor relapse.

No effective drug treatment was launched clinically to target CSCs, but putative and promising studies developed immune therapies such as monoclonal antibodies against specific CSC markers, differentiation-induced drugs that stimulate differentiation pathways and inhibit self-renewal signaling (Wnt, Hedgehog and Notch pathways) as well as affect hypoxia, angiogenesis and other microenvironmental factors.

In the process of development and discovery of new potential anticancer agents, growing interest is heading towards ‘safe’, widely available and cost-effective molecules, prominently from plant extracts. The plant-derived molecule TQ was shown to regulate cell death mechanisms, inhibit cell growth and interfere with several stages of colorectal carcinogenesis; however, TQ’s effect on CSCs was poorly reported.

In this study, we aim to investigate the inhibitory potential of TQ on colorectal cancer stem/progenitor cells and understand the mechanisms of CSC inhibition both *in*

vitro and *in vivo*. The cell culture model we used includes two isogenic human colorectal cancer HCT116 cell lines (HCT116 $p53^{+/+}$/$p21^{+/+}$) that differ in their sensitivity to 5FU. HCT116 cells were originally isolated from a primary tumor in the colon ascendens of a 48-year-old male with stage III colorectal carcinoma [171]. These cells are characterized by mutations in KRAS and PIK3CA oncogenes, CpG island methylator phenotype (CIMP) and microsatellite instability (MSI) phenotype [172]. The HCT116 cell line is known to be a highly aggressive cell line with little or no capacity to differentiate and which does not express the differentiation marker CDX1 [173], suggesting that it contains mainly CSCs. Thus, HCT116 represent a good model for the purpose of our study. To address the issue of targeting chemo-resistant cell lines, Abdel-Samad et al. generated a 5FU chemo-resistant HCT116 cell line by continuous exposure to increasing doses of 5FU to achieve resistance at clinically relevant doses [174]. *In vitro* identification of colorectal cancer stem/progenitor cells is through the assessment of their ability to form spheroids under low-serum conditions. Sphere-formation and propagation 3D culture assays were used to assess TQ's effect on targeting the self-renewal potential of colorectal CSCs enriched from the parental and 5FU-resistant cell lines over several generations. Immunocompromised NOD-SCID and NOD/Shi-scid IL2rgamma^{null} (NOG) mouse models were used to experimentally prove that the HCT116 spheres are enriched in CSCs and to validate TQ's effect on targeting an enriched population of CSCs *in vivo*.

This work has offered an understanding of colorectal cancer stem cell biology and has documented TQ's effects on colorectal CSCs and provided insights on its underlying mechanisms of action.

CHAPTER II

MATERIALS & METHODS

A. Cell Culture Conditions

Human colorectal cancer HCT116 5FU-sensitive (5FU-S) cells were purchased from ATCC (ATCC, USA), and HCT116 5FU-resistant (5FU-R) cells were obtained from the group of Prof. Nadine Darwiche (American University of Beirut, Lebanon) [174]. Cells were cultured and maintained in RPMI 1640 (Sigma-Aldrich, Germany) with 20 mM HEPES and L-Glutamine supplemented with antibiotics [1% Penicillin-Streptomycin (100 U/ml)] and 10% heat-inactivated fetal bovine serum (FBS) (Sigma-Aldrich, Germany). Cells were incubated at 37ºC in a humidified incubator containing 5% CO_2 and 95% air. All cells were mycoplasma free.

B. Drug Preparation and Treatment

Directly before use, fresh stocks of the purified synthetic compound TQ (Sigma-Aldrich: CAS: 490-91-5; 99.5% purity) reconstituted in methanol and of 5FU (Sigma-Aldrich, Germany) reconstituted in dimethylsulfoxide (DMSO) were prepared as per manufacturer's instructions.

C. MTT Cell Proliferation Assay

The anti-proliferative effects of TQ and 5FU on the used cell lines were measured *in vitro* using MTT ([3-(4, 5-dimethylthiazol-2-yl)-2, 5-diphenyltetrazolium bromide]) (Sigma-Aldrich) assay according to the manufacturer's instructions. 5FU-sensitive and resistant HCT116 cells were plated in 100 µl complete medium in 96-well culture plates at a density of 10,000 and 12,000 cells/well, respectively. Cells were incubated overnight then treated in triplicates with various drug concentrations for 24, 48, and 72hrs. Each experiment was repeated three times and in triplicate measurements. Cell viability was then assessed by MTT that measures the ability of metabolically active cells to convert tetrazolium salt into violet formazan crystals. At specific time points, 10 µL of MTT yellow dye (5mg/mL in DMSO) was added to each well and incubated at 37°C for 4hrs. 100µl isopropanol was used as a solubilizing solution to dissolve violet crystals. Consequently, MTT optical density (OD) was measured at a wavelength of 595 nm using ELISA reader (Multiskan Ex). Cell proliferation was expressed as a percentage of the control.

D. Trypan Blue Viability Assay

5FU-sensitive and resistant HCT116 cells were plated in 1 ml complete medium in 12-well culture plates at a density of 50,000 and 100,000 cells/well, respectively. Cells were incubated overnight then treated in duplicates with various drug concentrations (TQ 20-100 µM) for 24, 48, and 72hrs. Each experiment was repeated three times and in duplicate measurements. Supernatants containing dead cells were collected, and attached live cells were harvested by trypsin EDTA and added to the

supernatant. The cell pellet was re-suspended in 100 µl media, and 50 µl of cell suspension was mixed with 50 µl of trypan blue and then live/dead cells were counted using a hemocytometer.

E. Transwell Migration and Invasion Assays

$2.5x10^5$ 5FU-sensitive and $3.5\ x10^5$ 5FU-resistant HCT116 cells were seeded in a serum-free medium with or without treatment in the top chamber of 24-well inserts (pore size, 8 µm; Falcon) coated with Matrigel™ in the case of invasion assay, and a medium supplemented with serum was used as a chemo-attractant in the lower chamber. Each well was freshly coated with 100 µl of Matrigel™ (BD Bioscience, Franklin Lakes, NJ, USA) at a dilution of 1:10 in cold PBS and was then air-dried overnight before starting the invasion assay. Cells were allowed to migrate through the membrane coated or not with Matrigel™ at 37^0C in a 5% CO_2 incubator for 24 and 48hrs. Non-migratory cells in the upper chamber were then gently scraped off with a cotton-tip applicator. Migrating and invading cells on the lower surface of the membrane were fixed and stained with Hematoxylin and Eosin (H&E). After staining, the total number of migrating and invading cells was counted using an inverted light microscope (10X objective) from six consecutive fields for each well.

F. Sphere Formation Assay

The sphere formation assay was used as previously reported by our laboratory [65]. In brief, single cell suspensions (2×10^3 cells/well) of HCT116 cell lines were seeded in cold growth factor-reduced Matrigel™/ serum-free RPMI-1640 medium (1:1) in a total volume of 50 µl. The solution was then plated gently around the rim of individual wells of 24-well culture plate (50 µL per well). Each experimental condition was performed in duplicate. The Matrigel™ (Corning Life Sciences) was allowed to solidify for 1hr at 37°C in a humidified incubator. Wells were randomly assigned to control and treatment conditions, and 1 mL/well of complete media (+5% FBS), with or without treatment, was gently added to the center of each well and changed regularly every 2 to 3 days. Sphere counts were performed at day 9 and 13 of sphere culture, respectively, for the sensitive and resistant cell lines. The sphere-forming unit (SFU) was calculated as the ratio of the number of spheres counted to the number of cells originally seeded. Bright field images of the spheres were obtained using Axiovert microscope from Zeiss at 5× magnification.

G. Propagation Assay

To enrich for the stem-like population of cells, the media was aspirated from the well and the Matrigel™ -containing spheres was digested by 500 µl dispase solution (Invitrogen, Carlsbad, CA, 1mg dissolved in 1ml RPMI-1640 incomplete medium) for 1hr at 37°C. Spheres were collected and incubated in 0.5 ml Trypsin/EDTA at 37°C for 1-3 minutes. Single cells resulting from the dissociation of spheres were counted and re-plated at the same density of 2000 cells/well in 24-well plates as previously described.

H. Irradiation

Cells were irradiated with a 225 kV Precision X-Ray (PXi) irradiator model No X-RAD 225. Irradiation was performed at 2 Gy.min−1 and a 1.5 mm Aluminum filter was used.

I. Assessing the effect of TQ and irradiation on sphere-forming and self-renewal ability

Sphere-formation assay allows for identifying CSCs and studying their properties *in vitro*. Cells' response to radiation can therefore be evaluated by counting the number of spheres after irradiation.

5FU-sensitive and resistant HCT116 cells were seeded as single cells in Matrigel™/RPMI (serum-free) (1:1) at a concentration of 2×10^3 cells/well in a total volume of 50µl in duplicates, as previously described. Cells were then plated around the rim of the wells of 24-well culture plates and allowed to solidify in the incubator for 45 minutes. RPMI media with 5% heat-inactivated fetal bovine serum was then added to the center of the wells with or without TQ treatment. Irradiation at a dose of 2 Gy was performed at day 4 of sphere culture. Spheres were counted on a Zeiss Axio Vert.A1 microscope 9 days post irradiation with the Zen 2.3 lite blue edition software.

J. Side population (SP) assay

We performed the side population (SP) assay to identify and quantify the cancer stem-like and/or drug resistant cancer cells. SP cells are defined as a sub-population of cells with high expression of ATP-binding cassette transporters (ABCG2) and the ability to exclude Hoechst 33,342 nuclear dye [175]. We used FACSAria™ technology platform to determine and compare the SP cells in 5FU-sensitive and resistant HCT116 cells. $1x10^6$ cells/mL were resuspended in complete medium containing 5 µg/mL Hoechst 33342 dye for 30 minutes at 37°C. Cells were then pelleted by centrifugation and resuspended in 1x PBS to be analyzed by flow cytometry. After identification and cell sorting, sphere formation assay was performed from 5FU-resistant sorted SP cells as mentioned above. Sphere forming ability was measured and compared between TQ treated and untreated conditions.

K. Sphere Embedding Protocol

Spheres were harvested from 24-well plates by adding 500 µl/well ice-cold media and centrifuged at 200G for 5 minutes. Sphere pellets were then washed with 1 ml ice cold media to dissolve residual Matrigel followed by centrifugation at 200G for 5 minutes at 4°C. Sphere pellets were then resuspended in 500 µl 4% Paraformaldehyde and incubated for 30 minutes at room temperature. After that sphere pellets were incubated with 500 µl 70% ethanol overnight at 4°C. Samples were centrifuged at 200G for 5 minutes and the pellet was slowly transferred by pipetting up and down to the center of a speci-wrap (Histological paper for tissue retention Ref#11WR60) which was then folded carefully around the pellet and placed in a cassette. Cassettes were placed in

90% ethanol for 45 minutes followed by 100% ethanol for 45 minutes and finally xylol for 45 minutes. Paraffin blocks were prepared by adding a small amount of paraffin to the metal piece then slowly removing the sample from the speci-wrap using fine tweezers and placing it in the center of the metal piece. The sample was fixed in place in the metal piece by putting it on ice for few seconds. The metal piece was then covered with cassette and filled with paraffin. The block was kept on ice for at least 1 hour or overnight to solidify and then sections were obtained.

L. 3D Imaging of Colonospheres

Spheres were grown then collected with cold RPMI media and centrifuged to washout all Matrigel debris. After centrifugation, spheres were fixed by 4% PFA for 20 minutes. After washing with PBS three times, spheres were permeabilized with 0.5% Triton X-100 for 30 minutes and blocked with sphere blocking buffer (0.1% BSA, 0.2% Triton X-100, 0.05% Tween-20, and 10% normal goat serum in PBS) for 2hrs at room temperature. Spheres were washed and incubated overnight at 4°C with various primary antibodies (refer to table 4 for details on antibodies used) prepared in blocking solution. Spheres were then washed with PBS and incubated with secondary antibody (listed in table 4) for 1hr at room temperature. Finally, spheres were washed and mounted using 5-7 µL anti-fade reagent Fluoro-gel II with DAPI (Abcam, Cambridge, UK). Fluorescent signals were captured using a Zeiss LSM 710 laser scanning confocal microscope (Zeiss, Germany), and images were acquired and analyzed using the Zeiss ZEN image software.

For paraffin embedded spheres and tumor mouse tissues, slides were dried, dewaxed in xylene and rehydrated using a decreasing alcohol series. Antigen retrieval was performed in 10 mM citrate buffer, pH 6. Slides were then blocked with a blocking buffer (3% BSA, 0.1% Triton X-100, and 10% normal goat serum in PBS) for 1hr at room temperature, after which slides were incubated with the primary antibody overnight at 4°C (table 4). Spheres were then washed with PBS and incubated with the respective secondary antibody (table 4) for 1hr at room temperature. Fluoro-gel II with DAPI (Abcam, Cambridge, UK) was used for mounting. Fluorescent signals were captured using a Zeiss LSM 710 confocal microscope (Germany), and images were acquired and analyzed using the Zeiss LSM image software.

M. Immunofluorescence Analysis of Cells Grown as Monolayer

5FU-sensitive and resistant HCT116 cells were grown on coverslips in 12-well culture plates at a density of 50,000 and 100,000 cells/well, respectively. Adherent cells were then fixed using 4% PFA in PBS for 20 minutes, then permeabilized with 0.5% Triton X-100 in PBS for 20 minutes. Non-specific sites were blocked by incubation in blocking buffer (0.1% BSA, 0.2% Triton X-100, 0.05% Tween-20 and 10% NGS in PBS) for 1hr. Cells were then incubated overnight with specific primary antibodies at 4°C (Vimentin, E cadherin, CK8 and CK19 listed in table 4). After washing with PBS containing 0.1% Tween-20, cells were incubated with the corresponding secondary antibodies (table 4), then washed gently and mounted with anti-fade reagent Fluoro-gel II with DAPI.

N. TUNEL Assay

Apoptosis was determined using the In-Situ Cell Death Fluorescein Detection Kit (11684795910, Sigma-Aldrich, Germany). Spheres were grown then collected with cold RPMI media and centrifuged to washout all Matrigel debris. After centrifugation, spheres were fixed by 2% formaldehyde for 20 minutes. After washing with PBS three times, spheres were fixed further in 70% ice-cold ethanol overnight. Spheres were then resuspended in 50 µL TUNEL mix and incubated in humidified chamber at 37°C for 1hr. For visualization of nuclei and mounting, Fluoroshield Mounting Medium with DAPI (ab104139; Abcam, Cambridge, UK) was used and samples were analyzed using a Zeiss LSM 710 laser scanning confocal microscope (Zeiss, Germany).

O. Western Blot Analysis

Spheres were grown with or without treatment in 24-well plates then collected with cold RPMI media and centrifuged to wash out all Matrigel debris. Cells were plated in 100-mm tissue culture dishes and treated with 40 and 60 µM TQ for 48hrs. Cellular protein extracts were prepared in RIPA lysis buffer (sc-24948, Santa Cruz, CA, USA). Protein extracts were quantified using the DC Bio-Rad Protein Assay (Bio-Rad Laboratories, Hercules, California, USA) according to the manufacturer's protocol. Protein samples were mixed with 10% β-mercaptoethanol and 2X Laemmli Sample Buffer (Bio-Rad, CA, USA) for gel electrophoresis. An equal amount of protein lysate was separated on 12% SDS–PAGE for 2hrs at 90 V then transferred onto 0.45 µm nitrocellulose membrane (Bio-Rad, CA, USA) in transfer buffer overnight at 40^0C. Membranes were blocked with 5% skim milk in tris-buffered saline with 0.1% tween 20

(TBST) for 1hr and then incubated overnight at 4°C with the primary antibody (antibodies used are listed in table 5). Membranes were then washed three times with TBST and incubated with the diluted secondary antibody (table 5) for 1hr at room temperature. Hybridization with GAPDH-HRP (6C5) (1:10,000–20,000, Abnova, #MAB5476) coupled antibody was performed for 30 minutes at room temperature as housekeeping gene. Target proteins were detected using the ECL system (Bio-Rad, CA, USA). Images were generated and quantified using ChemiDoc™ Imaging Systems (Bio-Rad, CA, USA).

P. Histology and Immunohistochemical Analysis

Serial tissue sections (4 μm) were H&E stained and analyzed by an expert who was blinded for the treatment groups. Immunohistochemical staining was performed on paraffin-embedded spheres using Epithelial Cell Adhesion Molecule (EpCAM sc-25308 Santa Cruz, CA, USA) antibody. Slides were dried, dewaxed in xylene and rehydrated using a decreasing alcohol series. After blocking of endogenous peroxidase with H_2O_2, antigen retrieval was performed in 10mM citrate buffer, pH 6. Subsequently, slides were blocked with Protein Block (Novolink Polymer Detection Kit, RE7150-K, Leica). Primary antibodies were incubated at 4°C overnight, followed by Post Primary and Novolink™ Polymer (Novolink Polymer Detection Kit, RE7150-K, Leica). Staining was visualized using 3,3-diaminobenzidine (DAB), and nuclear counterstaining was performed using hematoxylin (Novolink Polymer Detection Kit, RE7150-K, Leica Biosystems, Germany). Slides were dehydrated and embedded in Histofluid (6900002; Marienfeld, Lauda Koenigshofen, Germany). Images were recorded at 40X to 400X

magnification using an Olympus BH-2 microscope and an Olympus E330 digital camera. The staining intensity was classified into 0 (no staining), 1+ (weak), 2+ (moderate), 3+ (strong), and the average of positively stained cells was recorded.

Q. Animal Experiments

Six to eight-week-old adult male NOD-SCID (injected with 5FU-sensitive cells) and NOG (injected with 5FU-resistant cells) mice were used. NOD-SCID mouse models are characterized by an absence of functional T and B cells, hypogammaglobulinemia and a normal hematopoietic microenvironment. NOG mouse models on the other hand are a new generation of severely immunodeficient mice that lack mature T, B and natural killer cells, display reduced complement activity and dysfunctional macrophages [176]. Mice were housed under optimum conditions of temperature set at 22 ± 2^0C and light set at a 12hrs light-dark cycle. Mice were kept in plastic cages covered with sawdust and had unrestricted access to a commercial mouse diet (24% protein, 4.5% fat, 4% fiber) and water. All animal studies were conducted using a protocol approved by the Institutional Animal Care and Use Committee of the American University of Beirut.

For tumor induction in mice, cells or spheres were suspended in 50 µl of the respective media, whereby cells or spheres were mixed with an equal volume of Matrigel. The mixture was subcutaneously injected into the flank of a group of mice. Animals were treated three times per week for three weeks either with vehicle (control group) or TQ (20 mg/kg) by intraperitoneal injections when a palpable tumor was observed. Mice were daily monitored for signs of morbidity. Body weight recordings

were carried out biweekly. Tumor volume was measured every other day by direct physical measurements using Mitutoyo caliper. The following formula for volume assessment was applied: V = (3.14/6)*L*W*H; where V is the tumor volume in mm^3, L is the tumor length in mm, W is the tumor width in mm and H is the tumor height in mm.

R. Statistical Analysis

All statistical analyses were performed using GraphPad Prism 7 (version 7.0, GraphPad Software Inc., La Jolla, CA, USA). Normality of the data was confirmed using D'Agostino & Pearson and Shapiro-Wilk normality tests. The significance of the data was analyzed using one-way or Two-way ANOVA statistical test, followed by multiple comparison test using Tukey post hoc analysis. P-value less than 0.05 was considered statistically significant (* $P<0.05$; ** $P<0.01$; *** $P<0.001$).

Table 4: List of primary and secondary antibodies used in immunofluorescent /immunohistochemistry staining

Antibody name	Species	Dilution	Catalog number	Company
Primary antibodies				
CD44	Mouse	1:100	sc-7297	Santa Cruz
Ki67	Mouse	1:50	sc-23900	Santa Cruz
p-Histone H2AX	Rabbit	1:500	# 9718S	Cell signaling
EpCAM	Mouse	1:100	sc-25308	Santa Cruz
Vimentin	Rabbit	1:100	sc-7557	Santa Cruz
E cadherin	Mouse	1:50	sc-8426	Santa Cruz
CK8	Mouse	1:200	904801	Biolegend
CK19	Rabbit	1:200	ab15463	Abcam
Tubulin	Mouse	1:100	sc-8035	Santa Cruz
Secondary antibodies				
Alexa fluoro 488	Goat anti-mouse	1:400	A-28175	Invitrogen
Alexa fluoro 568	Goat anti-rabbit	1:200	A-11011	Invitrogen
Phalloidin		1:200	R415	Invitrogen

Table 5: List of primary and secondary antibodies used in western blot experiments

Antibody name	Species	Dilution	Catalog number	Company
Primary antibodies				
p53	Mouse	1:50	sc-126	Santa Cruz
p21	Mouse	1:50	sc-6246	Santa Cruz
NF-κB p65	Rabbit	1:50	sc-372	Santa Cruz
p-MEK	Rabbit	1:200	# 9154S	Cell signaling
MEK	Rabbit	1:500	# 9126S	Cell signaling
PCNA	Mouse	1:50	sc-25280	Santa Cruz
p-Histone H2AX	Rabbit	1:500	# 9718S	Cell signaling
α-tubulin	Mouse	1:100	sc-8035	Santa Cruz
IKβα	Rabbit	1:100	sc-371	Santa Cruz
GAPDH-HRP (6C5)	Mouse	1:20,000	#MAB5476	Abnova
Secondary antibodies				
Goat anti-mouse	Goat	1:1000	sc-516102	Santa Cruz
Mouse anti-rabbit	Mouse	1:1000	sc-2357	Santa Cruz

CHAPTER III

RESULTS

A. Effect of TQ on the proliferation index of 5FU-sensitive and resistant HCT116 human colorectal cancer cell lines

Our first objective was to investigate the *in vitro* effect of TQ on the growth of HCT116 5FU-sensitive and resistant colorectal cancer cell lines cultured in 2D monolayers. Cells were treated with different concentrations of TQ (20-100 μM) for 24, 48 and 72hrs. MTT results showed a time- and dose-dependent reduction in proliferation in response to TQ. In the 5FU-sensitive cell line, the IC_{50} of TQ at 48hrs and 72hrs was ~40 μM (Figure 1A). In 5FU-resistant cells, the inhibitory effect of TQ commenced at a concentration of 60μM at 48hrs, decreasing cell viability by 40% (Figure 8A). The maximum percentage of reduction in viability at 72hrs in the sensitive cell line was 80-85% compared to 70-75% in the resistant cell line. These results were consistent with Trypan blue exclusion assay (Figure 8B) and with the changes in cell morphology and confluency following drug treatment in both cell lines. TQ's effect on normal cells has been previously reported where we showed that TQ was non-toxic to FHs74Int human normal intestinal cells for doses up to 60 μM [116].

A.

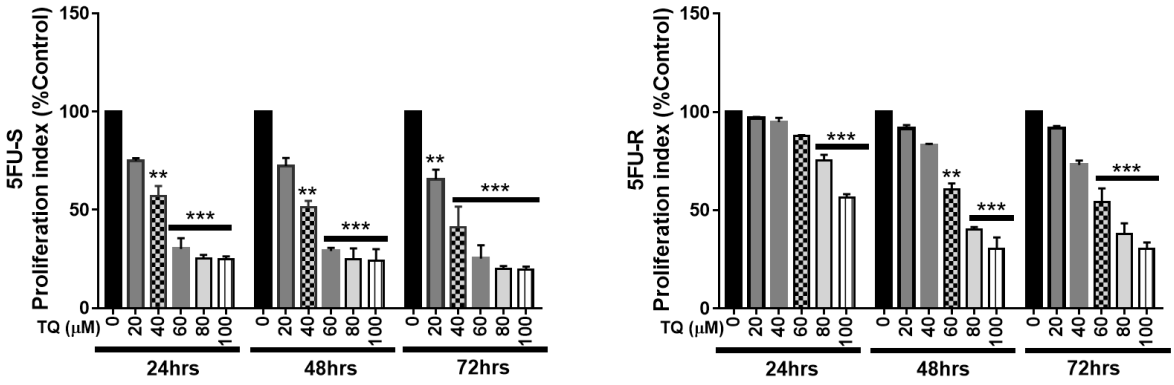

B.

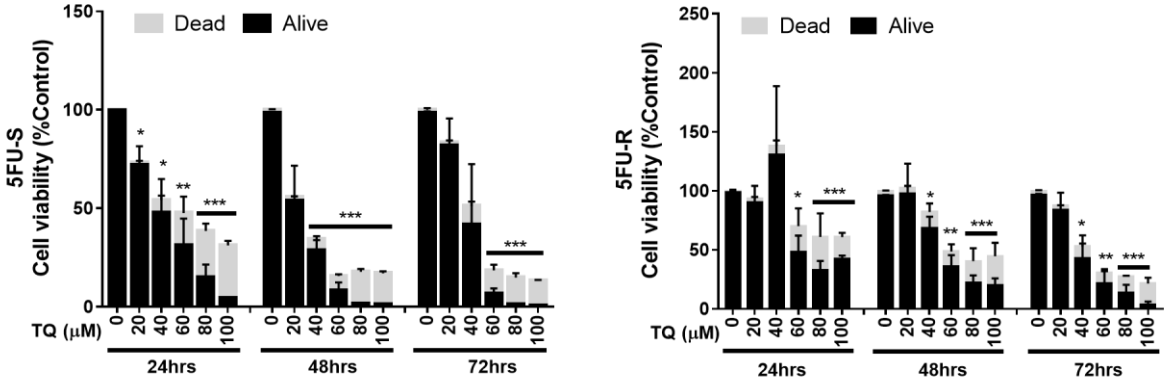

Figure 8. TQ reduces viability of 5FU-sensitive and 5FU-resistant HCT116 colorectal cancer cells. After incubation of 5FU-S and 5FU-R HCT116 colorectal cancer cells for 24, 48 and 72hrs with or without TQ, cell proliferation was determined using MTT assay (A) and cell viability was determined with trypan blue dye exclusion assay (B). Results are expressed as percentage of the studied group compared to its control. Data represent an average of three independent experiments. The data are reported as mean ± SD for MTT and mean ± SEM for Trypan blue assay (* $P<0.05$; ** $P<0.01$; *** $P<0.001$).

B. Effect of TQ on migration and invasion ability of 5FU-sensitive and resistant-HCT116 colorectal cancer cells

Next, we investigated the effect of TQ on cell migration and invasion, two hallmarks of cancer progression and metastasis. TQ significantly inhibited cell migration ability of 5FU-sensitive and resistant HCT116 cells compared to the control at 48hrs (Figure 9A). In addition, TQ treatment decreased cell invasion, whereby the invasion ability of cells in response to FBS was significantly reduced by more than 3-fold compared to the control (Figure 9B).

A.

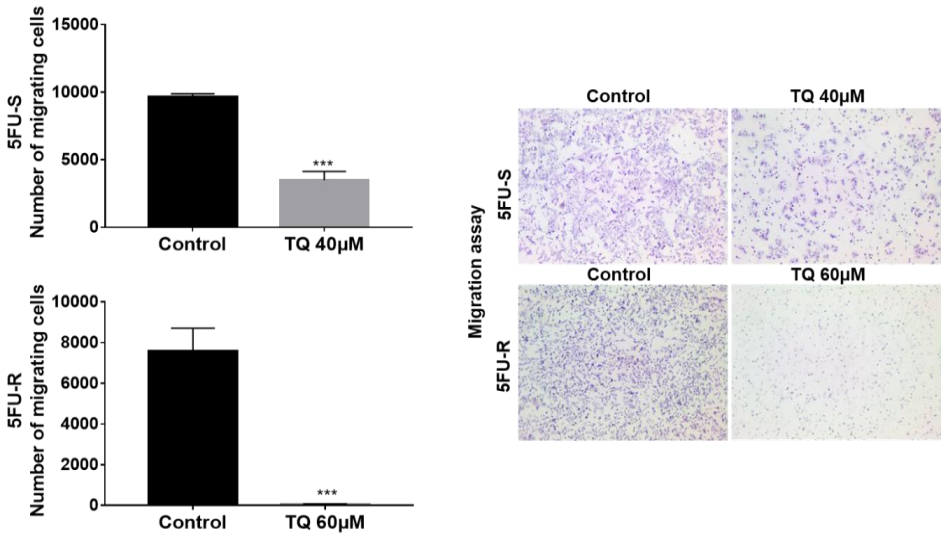

B.

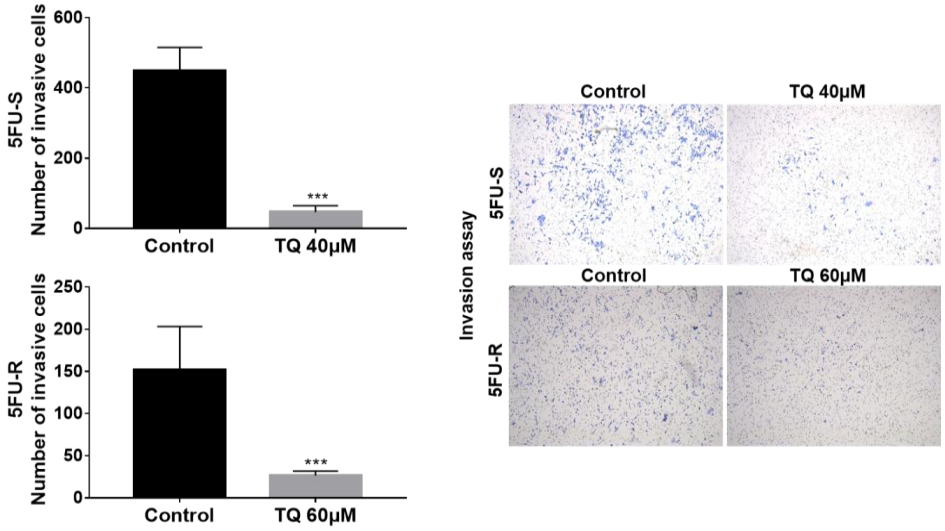

Figure 9. TQ reduces invasion and migration ability of 5FU-sensitive and 5FU-resistant HCT116 colorectal cancer cells. HCT116 cells were seeded onto the Matrigel-coated membrane (invasion assay) (A) or the uncoated membrane (migration assay) (B) in the top chamber of the transwell and were either treated or not with 40 and 60 µM TQ respectively in the presence of FBS in the lower chamber. Cells that migrated/invaded to the lower chamber after 48hrs were fixed with methanol, stained with H&E, counted and represented as number of migrating/invading cells compared to the control. Data represent an average of three independent experiments. The data are reported as mean ± SEM (* P<0.05; ** P<0.01; *** P<0.001).

Interestingly, this reduction in cell migration and invasion in response to TQ correlated with a significant downregulation in vimentin expression, an intermediate filament protein that is expressed in mesenchymal cells, and upregulation in E cadherin, an epithelial marker, in both 5FU-sensitive and resistant cells (Figure 10).

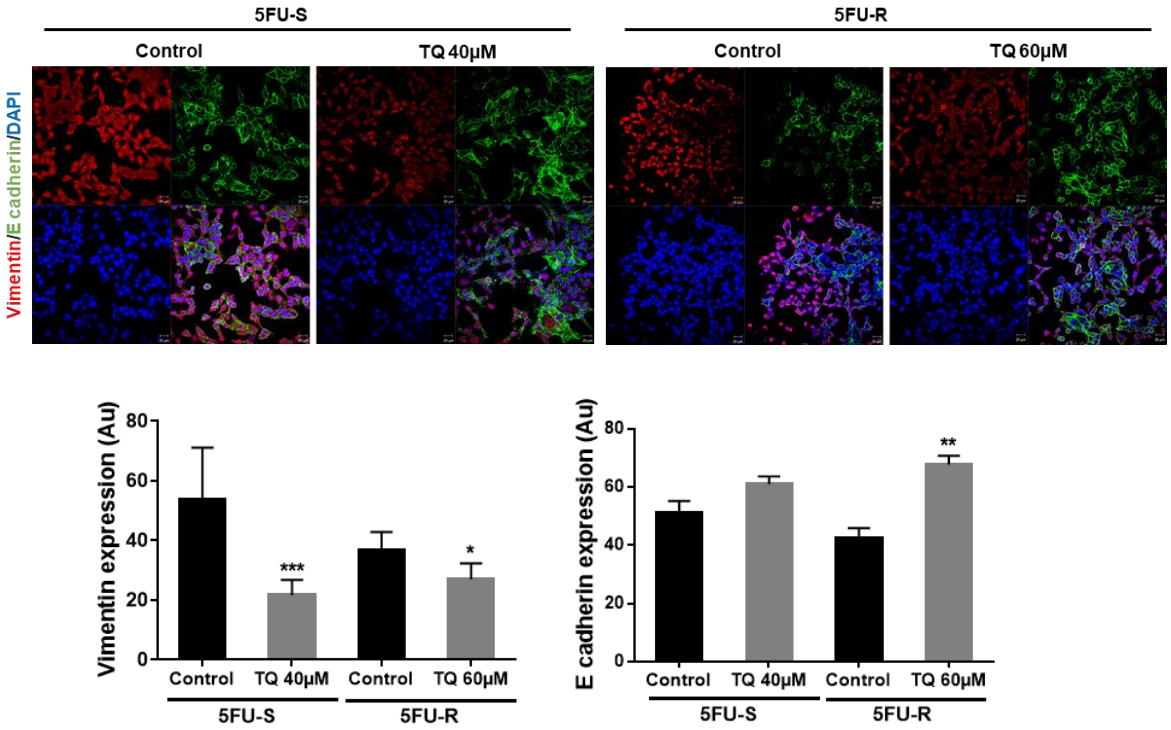

Figure 10. TQ regulates vimentin and E cadherin expression in 5FU-sensitive and 5FU-resistant HCT116 colorectal cancer cells. Representative confocal images and quantification of vimentin (red) and E cadherin (green) expression in 5FU-S and 5FU-R HCT116 colorectal cancer cells treated or not with 40 and 60 µM TQ, respectively. Data represent an average of three independent experiments and are reported as mean ± SEM (* P<0.05; ** P<0.01; *** P<0.001). Scale bar for immunofluorescent images 20 µm.

In addition, TQ up-regulated cytokeratin epithelial marker CK8 in 5FU-resistant cells when compared to control and maintained an elevated expression of both cytokeratin epithelial markers CK8 and CK19 in sensitive and resistant cells (Figure 11). Collectively, these results suggest that TQ has a high inhibitory effect on colorectal cancer cell migration and invasion.

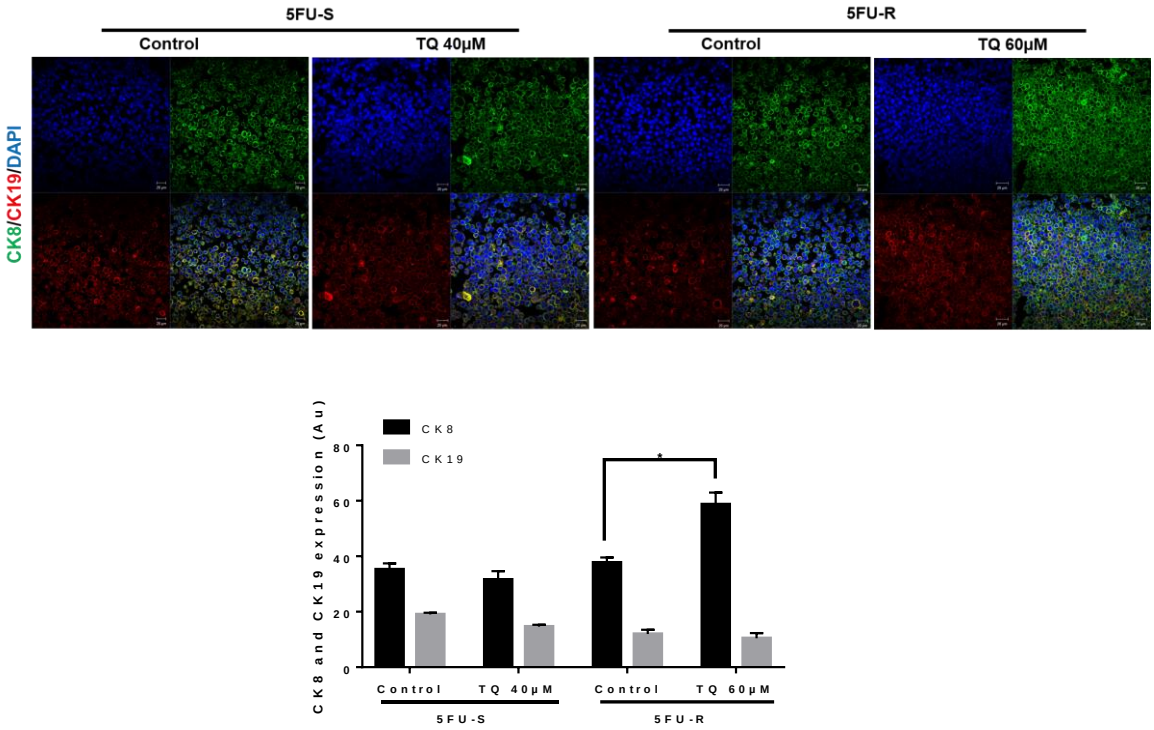

Figure 11. TQ regulates the expression of CK8 and CK19 in 5FU-sensitive and 5FU-resistant HCT116 colorectal cancer cells. 5FU-S and 5FU-R HCT116 colorectal cancer cells treated or not with 40 and 60 µM TQ respectively were immunofluorescently stained for CK8 (green) and CK19 (red). Quantification and representative images are shown. Data represent an average of three independent experiments and are reported as mean ± SEM (* P<0.05; ** P<0.01; *** P<0.001). Scale bar 20 µm.

C. Establishing TQ's effect on an enriched population of 5FU-sensitive and resistant human colorectal cancer stem cells in 3D

1. Effect of TQ on HCT116 sphere counts and size

Having established TQ's inhibitory effect on both cell lines in 2D, we next aimed at investigating its potential inhibitory effect on targeting the self-renewal capacity of colorectal CSCs enriched from 5FU-sensitive and resistant cell lines in 3D cultures using sphere formation and propagation assays. Cells that were able to form spheres in the first generation (G1) were collected and propagated by dissociating spheres into single cells and re-seeding the same number of cells (2000 cells/well). The assay was performed until the fifth generation (G5). In the 5FU-sensitive cells, treatment with 3 μM TQ significantly decreased the sphere formation ability up to G5 (Figure 12A). In the 5FU-resistant cells, on the other hand, most of the spheres treated with 3 μM 5FU remained viable up until the fifth generation, which confirms resistance to 5FU (Figure 12B). Interestingly, successive propagation and treatment of 5FU-resistant cells with 5 μM TQ significantly decreased sphere-forming unit (SFU) by a remarkable 70% after treatment (Figure 12B).

In addition to assessing the effect of TQ on self-renewal capacity, we investigated its effect on sphere size. Spheres were propagated for several generations with or without treatment, and at each generation, sphere sizes were determined (Figure 12A and B). TQ had no significant effect on the size of spheres derived from both 5FU-sensitive and resistant cells where the average diameter was around 100 μm with or without treatment.

A.

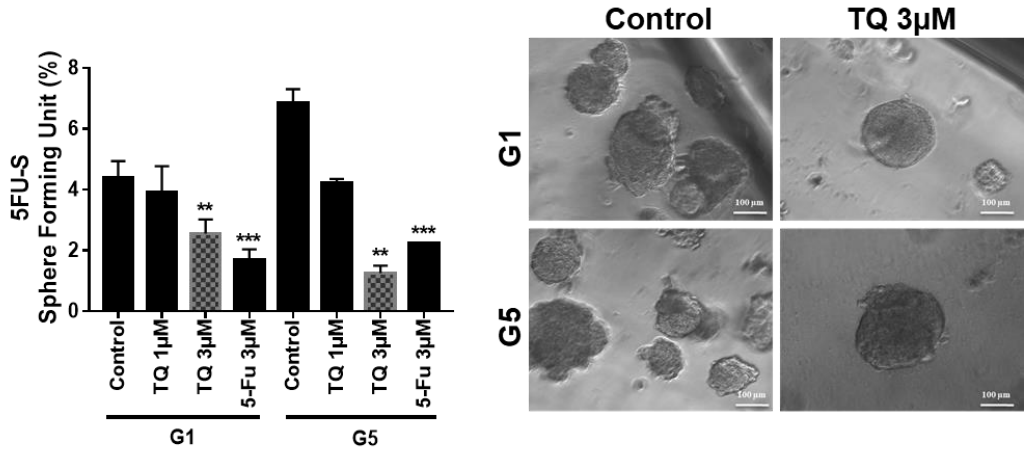

B.

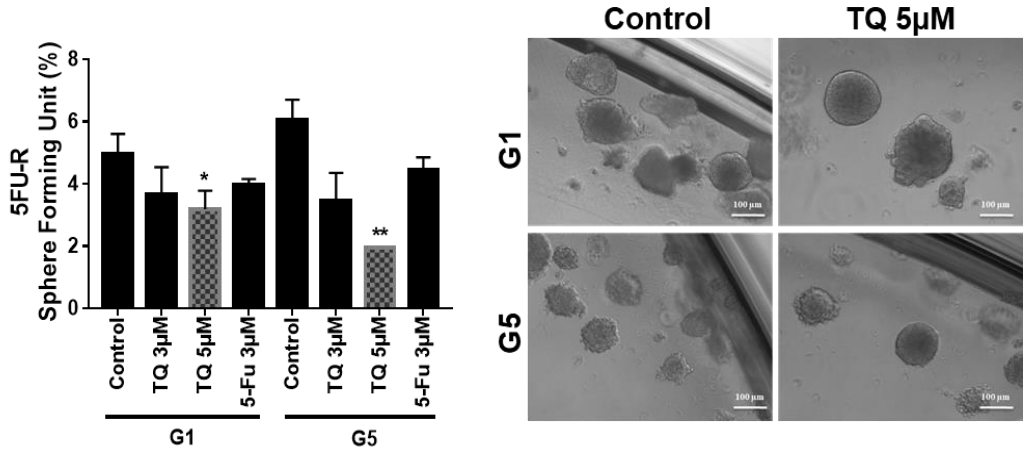

Figure 12. TQ reduces sphere-forming and self-renewal ability of colon cancer stem/progenitor cells. (A, B) Sphere forming unit (SFU) obtained from serially passaged colonopheres over five generations is shown under untreated conditions, TQ-treated (1, 3 and 5 µM) and 5FU-treated (3 µM) condition for 5FU-S (A) and 5FU-R (B) HCT116 derived spheres. SFU is calculated according to the following formula: SFU = (number of spheres counted ÷ number of input cells)*100. Colon CSCs were enriched from 5FU-S and 5FU-R HCT116 cell line and treated with either TQ (1, 3 and 5 µM) or media (control). Generated spheres are referred to as G1 (Generation 1) spheres. After each propagation, cells that were initially treated with TQ, 5FU or media (control) were seeded into separate wells. Spheres were propagated for five generations in duplicates for each condition. Data represent an average of three independent experiments and are reported as mean ± SEM (* $P<0.05$; ** $P<0.01$; *** $P<0.001$). Representative bright-field images showing the effect of TQ on SFU are shown next to the respective graphs. Images were visualized by Axiovert inverted microscope at 10X magnification and analyzed by Carl Zeiss Zen 2012 image software. Scale bar 100 µm.

To further investigate TQ's effect on colorectal CSCs, we performed the side population (SP) assay to identify and quantify the cancer stem and/or drug resistant cancer cells. SP cells are defined as a sub-population of cells with high expression of ATP-binding cassette transporters (ABCG2) which are able to exclude Hoechst 33,342 nuclear dye. Using flow cytometric analysis, we demonstrated that 5FU-resistant HCT116 cells contained a significantly increased percentage of SP cells (3.5% ± 1) when compared to 5FU-sensitive cells (0.9% ± 0.5) (Figure 13A).

We sorted the SP and the parental population from 5FU-resistant cells and cultured them in 3D sphere cultures with or without TQ treatment. Sphere forming ability was significantly decreased upon treatment of SP generated spheres with 5 and 10 μM TQ and this decrease was more pronounced in spheres generated from the parental population (Figure 13B). Resistance to 5FU was also more pronounced in the SP generated spheres when compared to the parental population (Figure 13B), which confirms the high resistance nature of SP cells. Taken together, these results suggest that TQ targets the resistant population of colorectal cancer stem/progenitor cells.

A.

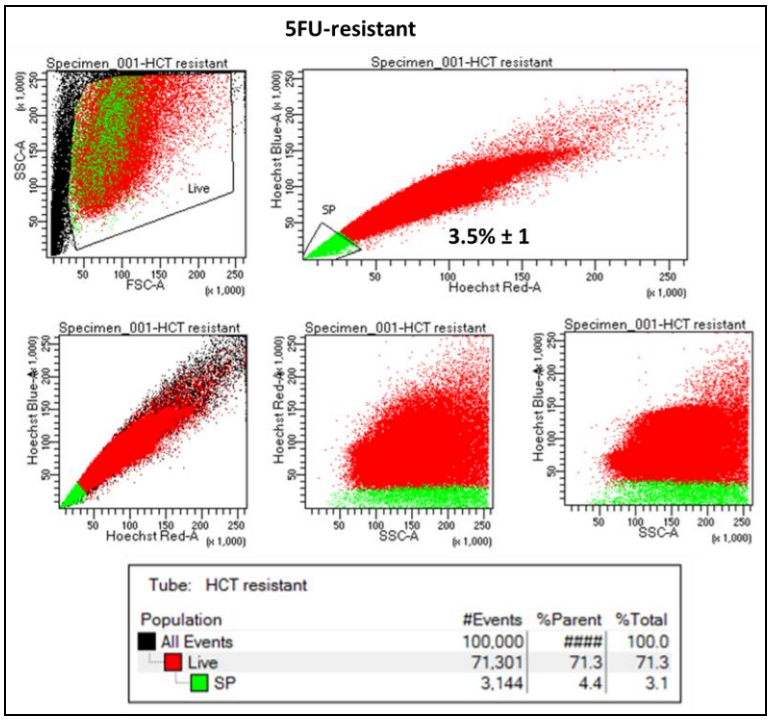
5FU-resistant
Specimen_001-HCT resistant
SSC-A
FSC-A
Live
Hoechst Blue-A
Hoechst Red-A
SP
3.5% ± 1
SSC-A
Tube: HCT resistant
Population #Events %Parent %Total
All Events 100,000 #### 100.0
Live 71,301 71.3 71.3
SP 3,144 4.4 3.1

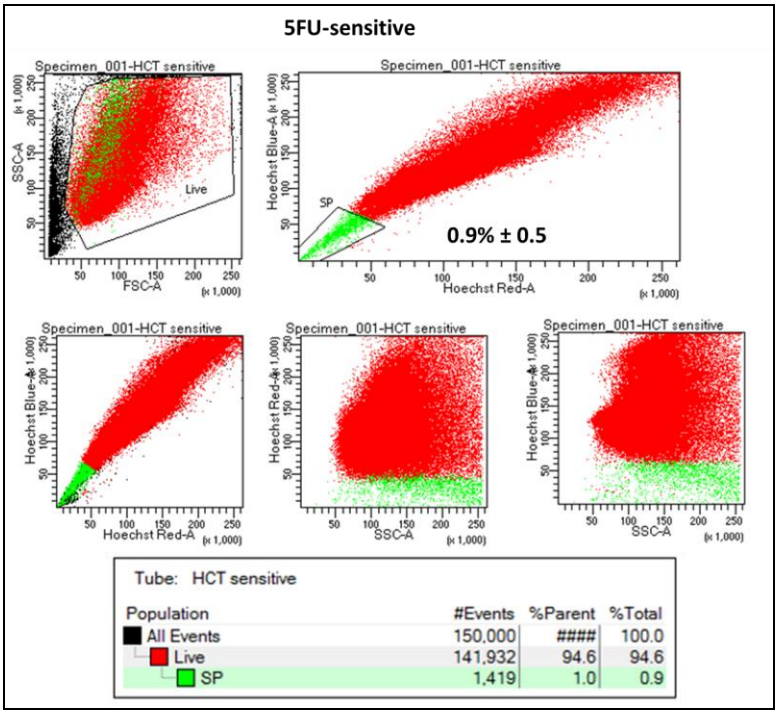
5FU-sensitive
Specimen_001-HCT sensitive
SSC-A
FSC-A
Live
Hoechst Blue-A
Hoechst Red-A
SP
0.9% ± 0.5
SSC-A
Tube: HCT sensitive
Population #Events %Parent %Total
All Events 150,000 #### 100.0
Live 141,932 94.6 94.6
SP 1,419 1.0 0.9

B.

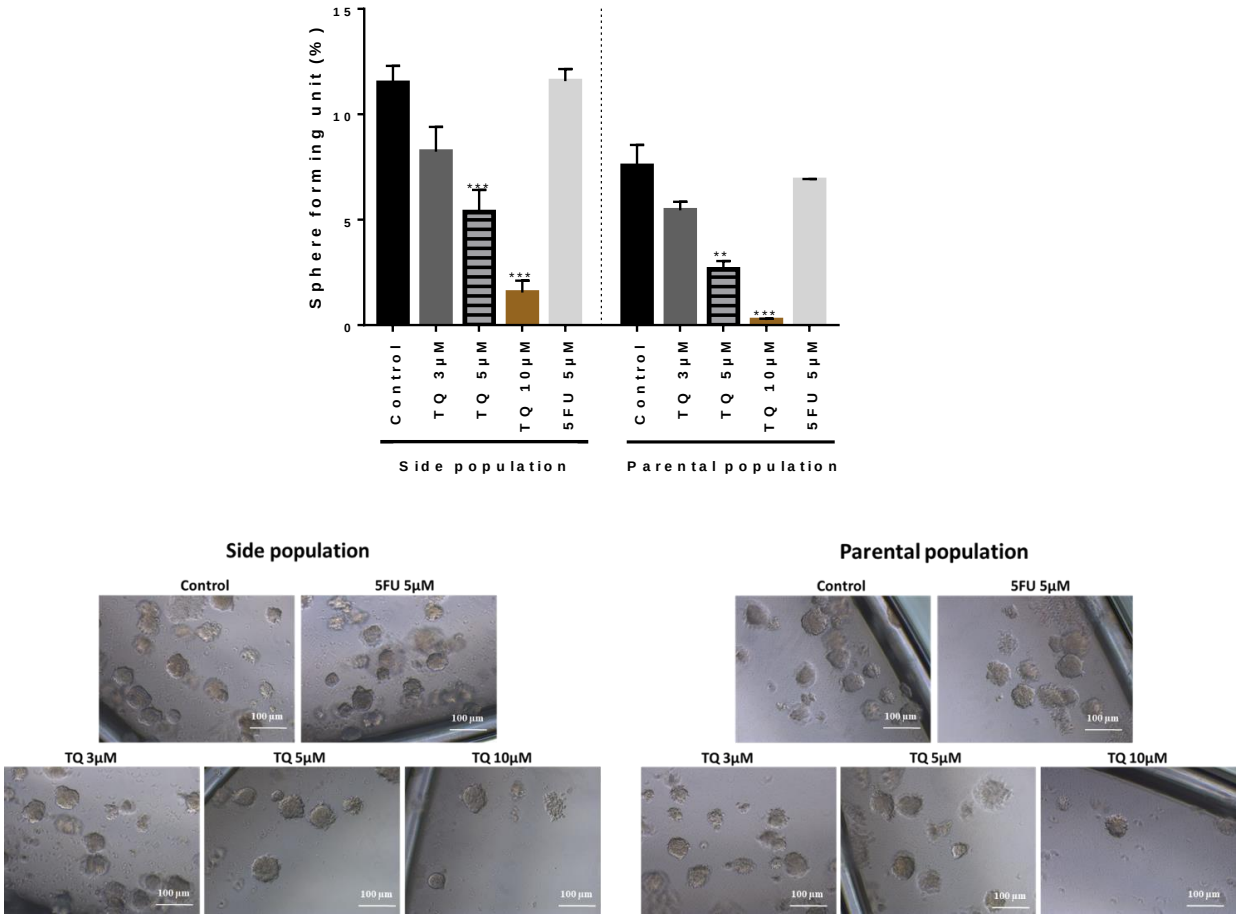

Figure 13. Inhibitory effect of TQ on sphere-forming ability of drug-resistant HCT116 cells. (A) Representative FACS analysis (n=3) demonstrating the percentage of SP cells in 5FU-sensitive compared to 5FU-resistant HCT116 cells. (B) Colonospheres generated from sorted 5FU-resistant SP and parental population cells were treated for nine days with 3, 5 and 10 µM TQ or 5 µM 5FU. Sphere forming unit (SFU) and representative bright-field images are shown. Images were visualized by Axiovert inverted microscope at 10X magnification and analyzed by Carl Zeiss Zen 2012 image software. Scale bar 100 µm. Data represent an average of two independent experiments and are reported as mean ± SEM (* P<0.05; ** P<0.01; *** P<0.001).

2. TQ effect on proliferation, epithelial and stem cell markers expression in 3D colonospheres

To further study TQ's effect on the enriched CSCs population, we analyzed the expression of the proliferation marker Ki67 and the stem cell markers CD44 and EpCAM. Immunohistochemical staining of spheres derived from both cell lines showed a significant reduction of EpCAM expression upon TQ treatment (Figure 14).

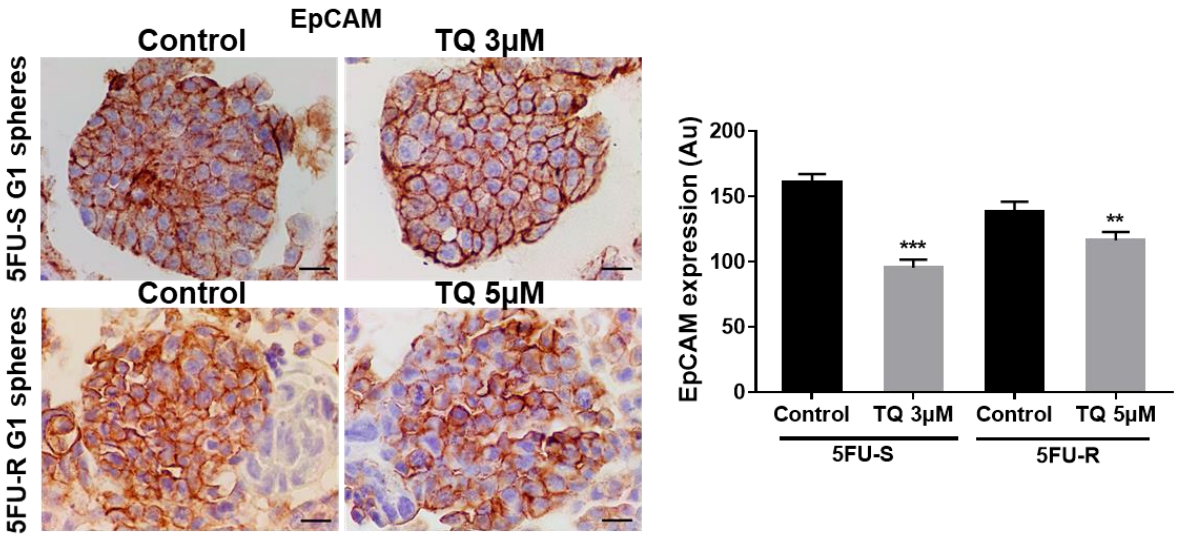

Figure 14. TQ downregulates EpCAM in 3D colonospheres. Spheres were collected, fixed and stained for EpCAM. Representative images were obtained using light microscopy and quantification of the intensity of EpCAM stain in control and TQ treated 5FU-S and 5FU-R HCT116 G1 and G5 spheres was performed using ImageJ software. Stain intensity was normalized to size. Data represent an average of three independent experiments and are reported as mean ± SEM (* $P<0.05$; ** $P<0.01$; *** $P<0.001$). Scale bar 20 µm.

Immunofluorescent analysis showed that TQ treatment significantly decreased CD44 and Ki67 expression in 5FU-sensitive and 5FU-resistant HCT116 spheres (Figure 15 and 16). This suggests that the reduction in sphere-forming ability is associated with decreased cellular proliferation and inhibition of key stem cell markers.

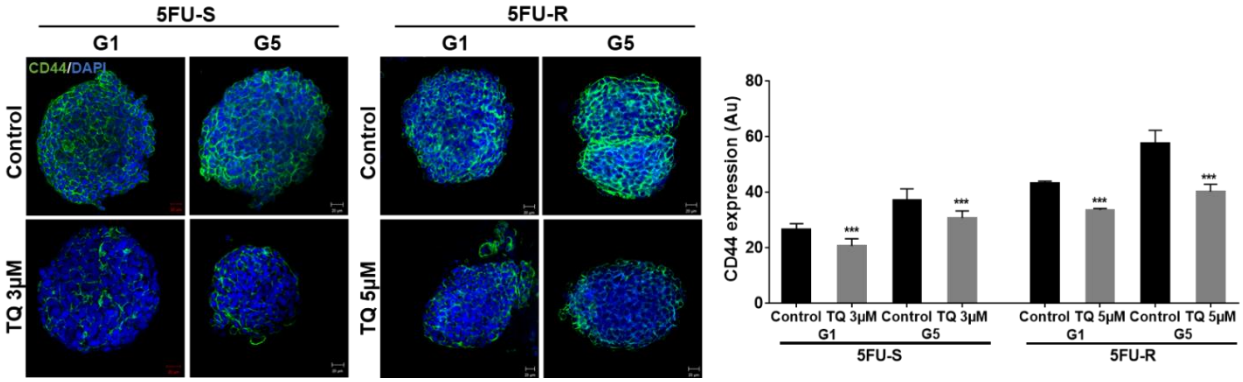

Figure 15. TQ reduces the expression of CD44 stem cell marker in 3D colonospheres. Spheres were collected, fixed and stained for CD44. Representative images were obtained using confocal and quantification of the intensity of CD44 stain in control and TQ treated 5FU-S and 5FU-R HCT116 G1 and G5 spheres was performed using Carl Zeiss Zen 2012 image software. Stain intensity was normalized to size. Data represent an average of three independent experiments and are reported as mean ± SEM (* P<0.05; ** P<0.01; *** P<0.001). Scale bar 20 μm.

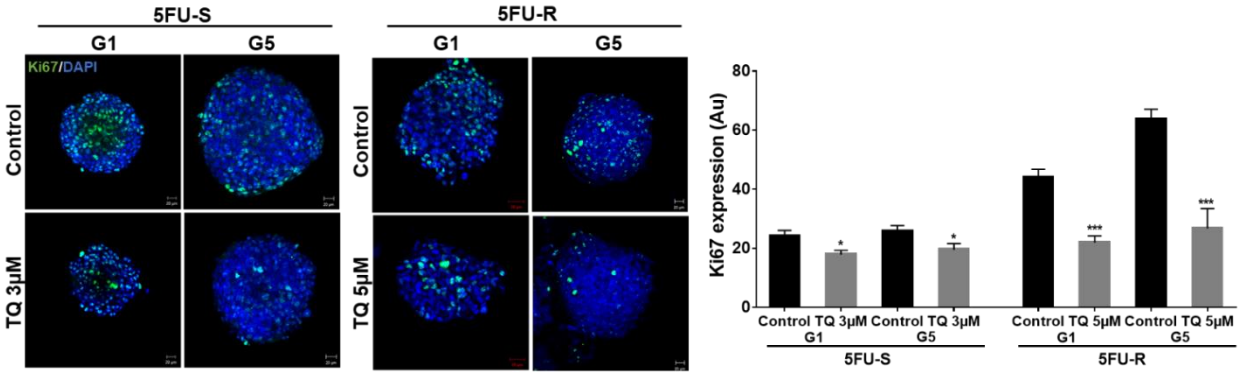

Figure 16. TQ reduces the expression of Ki67 in 3D colonospheres. Spheres were collected, fixed and stained for Ki67. Representative images were obtained using confocal and quantification of the intensity of Ki67 stain in control and TQ treated 5FU-S and 5FU-R HCT116 G1 and G5 spheres was performed using Carl Zeiss Zen 2012 image software. Stain intensity was normalized to size. Data represent an average of three independent experiments and are reported as mean ± SEM (* P<0.05; ** P<0.01; *** P<0.001). Scale bar 20 µm.

Interestingly, TQ up-regulated cytokeratin epithelial markers, CK8 and CK19, in 5FU-resistant spheres and maintained an elevated expression of both in 5FU-sensitive spheres (Figure 17), which could be indicative of reduced potential of epithelial-to-mesenchymal transition.

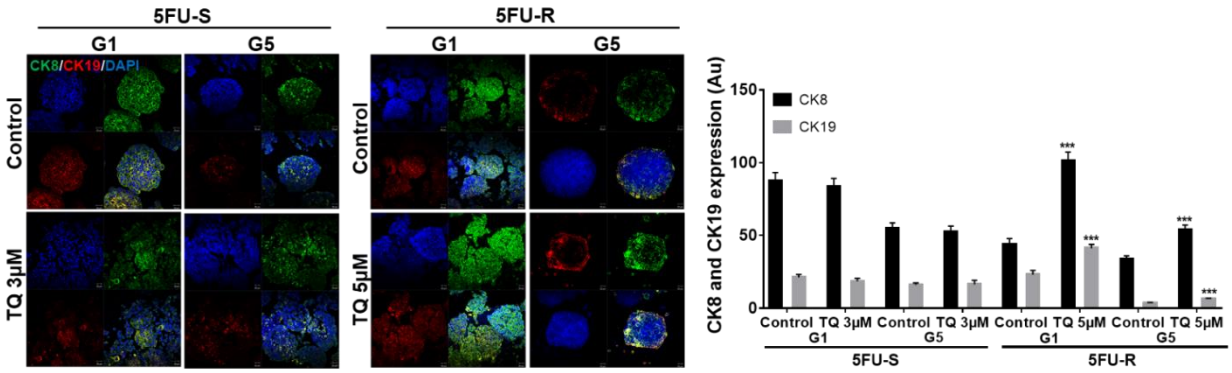

Figure 17. TQ regulates the expression of CK8 and CK19 in 3D colonospheres. Spheres were collected, fixed and stained for CK8 and CK19. Representative images were obtained using confocal and quantification of the intensity of CK8 and CK19 stain in control and TQ treated 5FU-S and 5FU-R HCT116 G1 and G5 spheres was performed using Carl Zeiss Zen 2012 image software. Stain intensity was normalized to size. Data represent an average of three independent experiments and are reported as mean ± SEM (* P<0.05; ** P<0.01; *** P<0.001). Scale bar 20 μm.

D. TQ's mechanism of action on colorectal cancer stem/progenitor cells

As mentioned previously, TQ caused a significant reduction in spheres number but not size, suggesting the involvement of a cell death mechanism. To investigate TQ's mechanism of action, we performed TUNEL staining on 5FU-sensitive and resistant HCT116 G1 and G5 spheres (Figure 18). TQ treatment led to increased TUNEL positivity, indicating that the diminished sphere forming ability in TQ-treated colonospheres was in part due to the induction of apoptosis. In the TQ-treated spheres, mean apoptotic index estimated by TUNEL was 11.3% and 11.8% as compared to 8% and 5.5% in control G1 and G5 5FU-sensitive spheres, respectively. In 5FU-resistant spheres, mean apoptotic index estimated by TUNEL was 8% and 14% in TQ-treated spheres as compared to 0.5% and 5.6% in control G1 and G5 spheres, respectively.

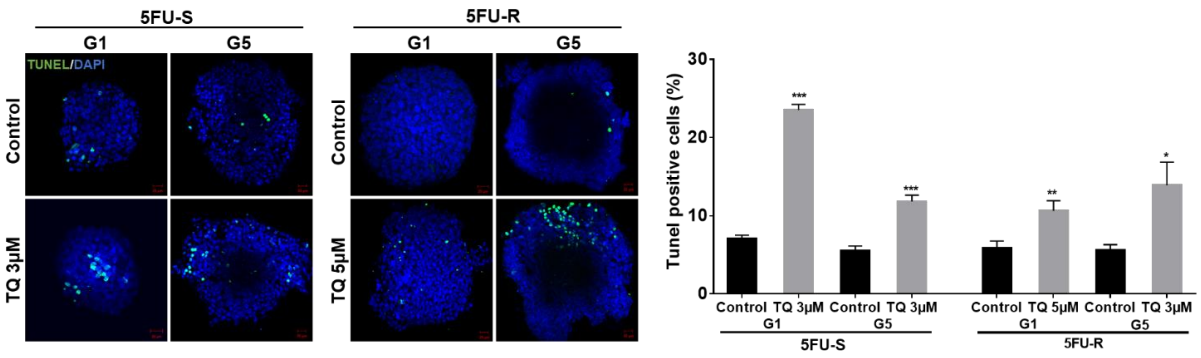

Figure 18. TQ induces apoptosis in colon cancer stem/progenitor cells. Representative images of control and TQ treated 5FU-S and 5FU-R HCT116 G1 and G5 spheres after TUNEL staining. Data represent an average of three independent experiments. TUNEL positive cells were counted and represented as mean percentage ± SD (* P<0.05; ** P<0.01; *** P<0.001 significantly different from control). Scale bar 20 μm.

Analysis of p53 protein expression in 5FU-sensitive and 5FU-resistant 2D cells and 3D spheres during TQ treatment showed up-regulation of this protein further confirming apoptosis induction (Figure 19A and B). This was also associated with an upregulation in p21 expression (Figure 19A and B). Western blot analysis also showed a decrease in NF-κB, PCNA and p-MEK expression especially in 3D colonospheres further confirming TQ's inhibitory effects on proliferation (Figure 19B).

A.

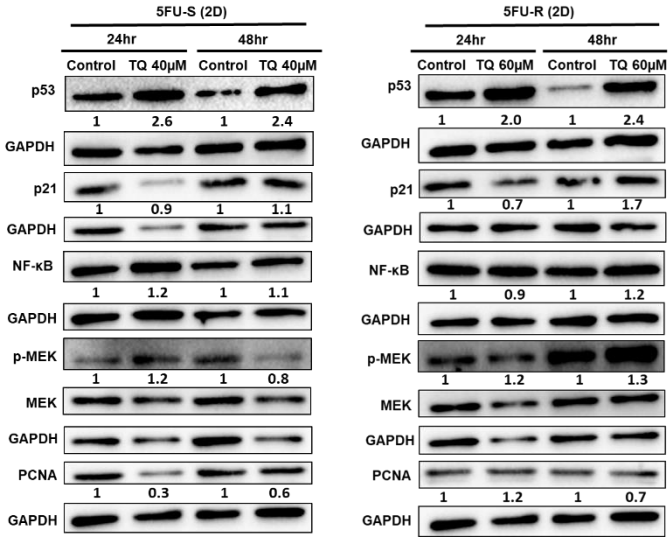

B.

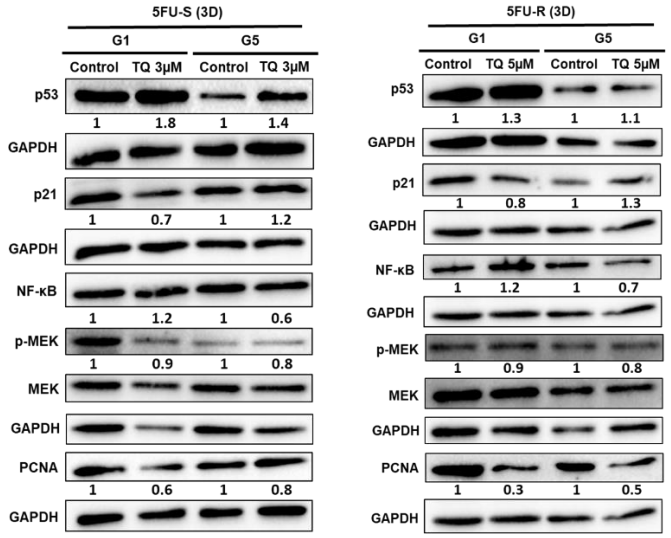

Figure 19. TQ induces apoptosis and inhibits proliferation in colon cancer stem/progenitor cells. Analysis of p53, p21, NF-κB (p65), p-MEK and PCNA protein expression in 5FU-S and 5FU-R HCT116 cells (A) and spheres (B) during TQ treatment is shown. Fold expression changes normalized to GAPDH and total MEK in case of p-MEK expression are given below the blots. Data represent an average of three independent experiments.

An early cellular response to double-strand breaks is the phosphorylation at Ser139 of a subclass of eukaryotic histones, H2AX. To study TQ's effect on inducing DNA damage, we studied the expression of H2AX. Interestingly, TQ caused a dramatic increase in the amount of H2AX protein mainly in 5FU-resistant cells and spheres (Figure 20A and B) indicating a role of DNA damage pathway in these cells in response to TQ.

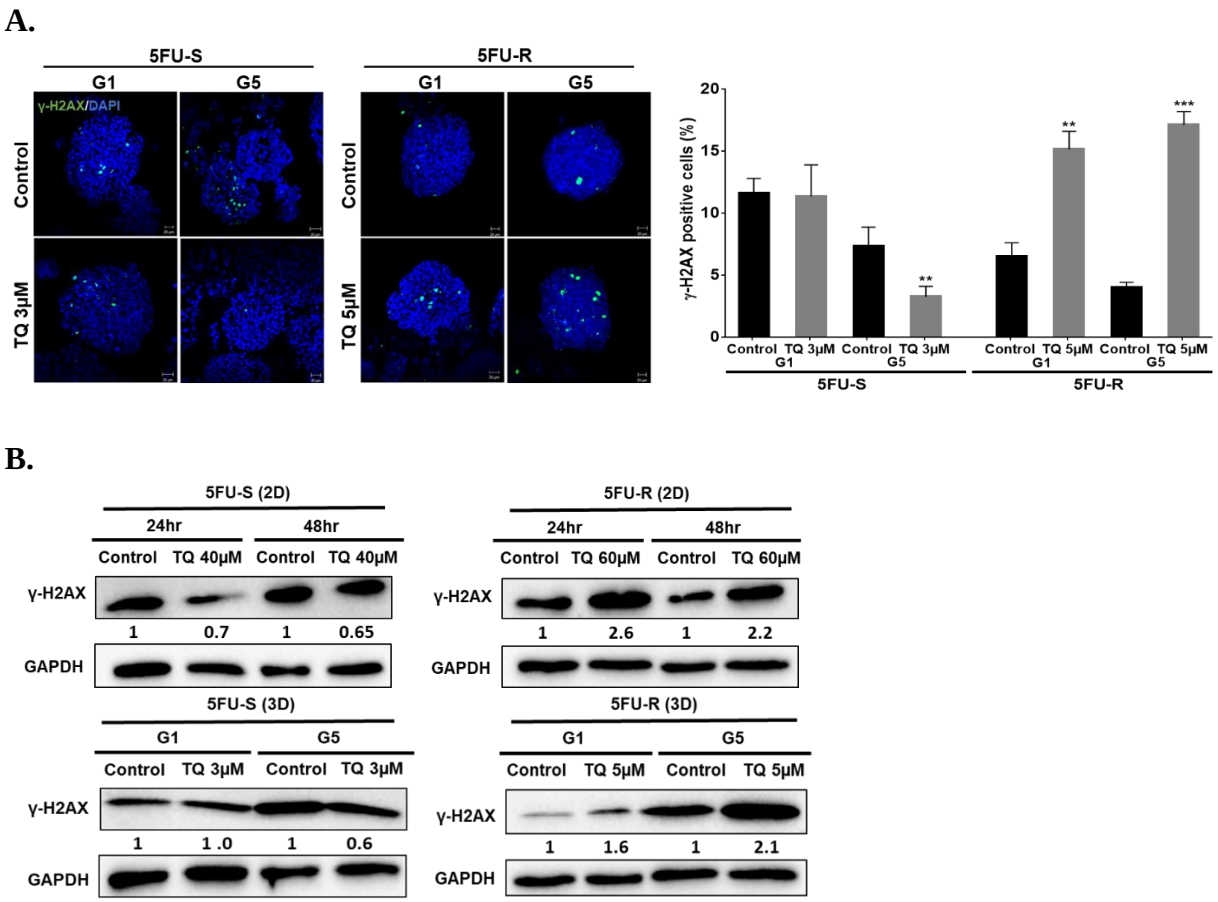

Figure 20. TQ induces DNA damage in colon cancer stem/progenitor cells. (A) Representative images of γ-H2AX staining in control and TQ-treated 5FU-S and 5FU-R HCT116 G1 and G5 spheres. Scale bar 20 μm. γ-H2AX positive cells were counted and are represented as mean percentage ± SEM (* P<0.05; ** P<0.01; *** P<0.001 significantly different from control). (B) Analysis of γ-H2AX in 5FU-S and 5FU-R HCT116 cells and spheres during TQ treatment is shown. Fold expression changes normalized to GAPDH are given below the blots. Data represent an average of three independent experiments.

E. Effect of TQ and radiation combination on colorectal cancer cells in 2D and 3D cultures

After showing that TQ induces DNA damage by upregulating H2AX, we decided to investigate its effect on colorectal cancer cells and spheres when combined with radiation. For this purpose, 5FU-sensitive and 5FU-resistant cells were treated with TQ for 24hrs followed by irradiation at a dose of 2 Gy. Cells were then fixed at 0 minutes, 10 minutes and 24hrs post irradiation and γ-H2AX expression was analyzed. We saw an upregulation in γ-H2AX expression with the highest peak in TQ and radiation combination at 10 minutes when compared to TQ or radiation alone. Interestingly, γ-H2AX expression remained significantly high after 24hrs in the combination group; whereas, it went back to control levels in cells treated with TQ or radiation alone (Figure 21A and B). Taken together, these results suggest that TQ is acting as a radiosensitizer in 5FU-sesnitive and resistant cells.

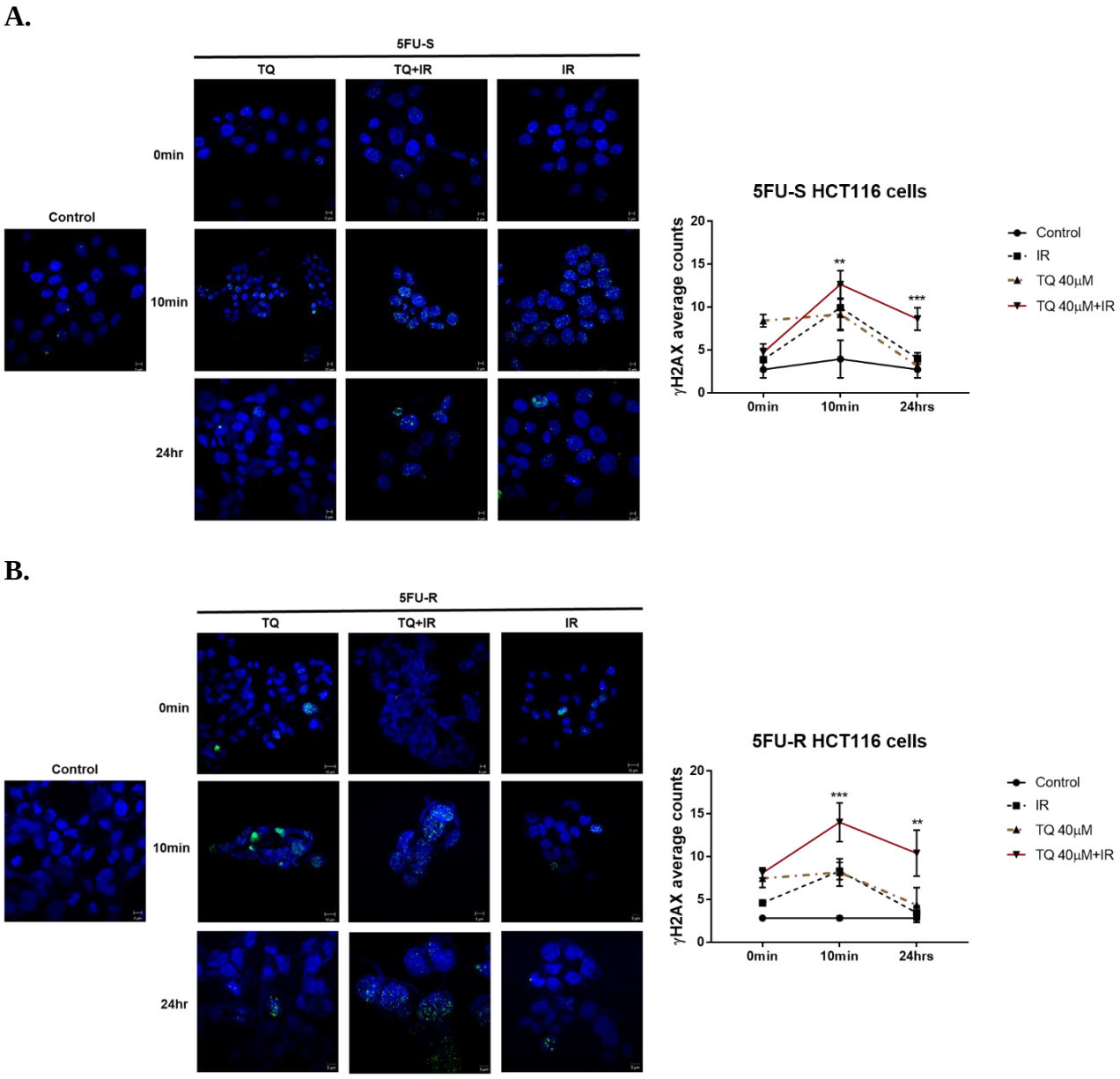

Figure 21. TQ combination with radiation increases γ-H2AX expression in 2D cultures of 5FU-sensitive and resistant cells. Representative images of γ-H2AX staining in 5FU-S (A) and 5FU-R (B) HCT116 cells untreated and treated with TQ, irradiation (IR) and combination of TQ and irradiation (TQ+IR). γ-H2AX positive cells were counted and are represented as average count ± SEM (* P<0.05; ** P<0.01; *** P<0.001 significantly different from TQ 40 μM and TQ 40μM+IR). Data represent an average of three independent experiments. Scale bar 20 μm.

Based on the 2D results, we sought to determine the effect of TQ and radiation in 3D. To assess the effect of TQ and radiation on sphere-forming and self-renewal ability, 5FU-sensitive and resistant cells were seeded with Matrigel in 3D culture sphere formation assay. Cells were treated with TQ from day zero and then irradiated at day 4. Interestingly, TQ and radiation combination resulted in a significant decrease in the number of spheres when compared to either treatment alone, suggesting that TQ is capable of sensitizing the colonospheres to radiation (Figure 22A and B).

A.

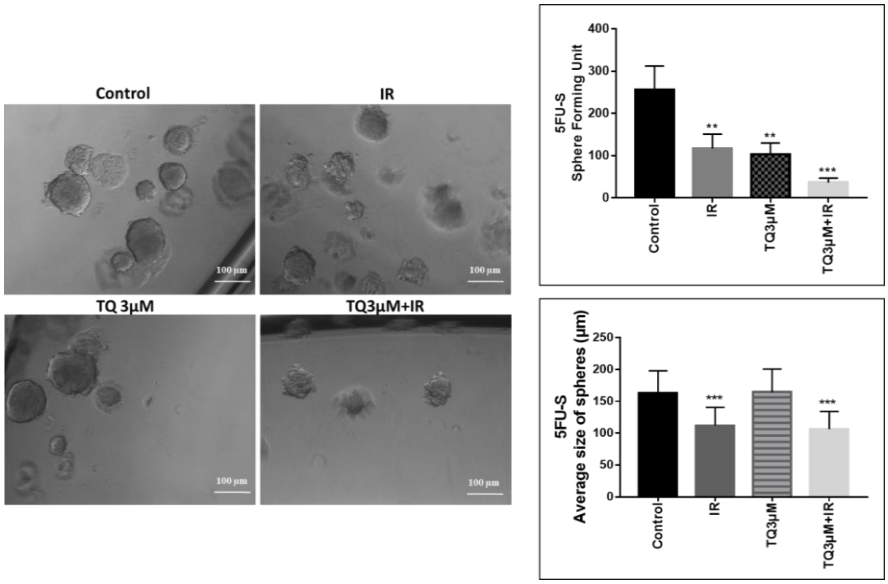

B.

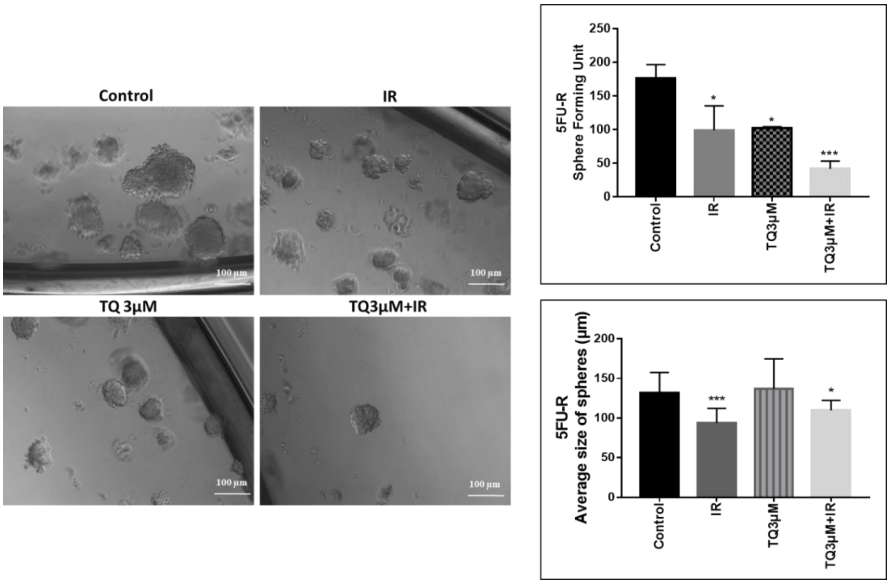

Figure 22. TQ sensitizes 5FU-sensitive and resistant colonospheres to radiation. 5FU-sensitive and 5FU-resistant spheres were treated with TQ at day 0 of sphere culture and irradiated at day 4. Representative images and sphere count 9 days post irradiation of 5FU-sensitive (A) and 5FU-resistant (B) G1 spheres untreated and treated with TQ, irradiation (IR) and combination of TQ and irradiation (TQ+IR) are shown. Data represent an average of two independent experiments. Spheres were counted and are represented as average count ± SEM (* $P<0.05$; ** $P<0.01$; *** $P<0.001$ significantly different from control). Scale bar 100 µm.

We further analyzed the effect of TQ and radiation combination on the expression of CD44 and γ-H2AX expression. CD44 expression was decreased; however, this decrease in expression was comparable to TQ or radiation treatment alone (Figure 23A). On the other hand, γ-H2AX was significantly upregulated in TQ and radiation combination (Figure 23B) suggesting enhanced DNA damage and increased sensitivity to radiation.

A.

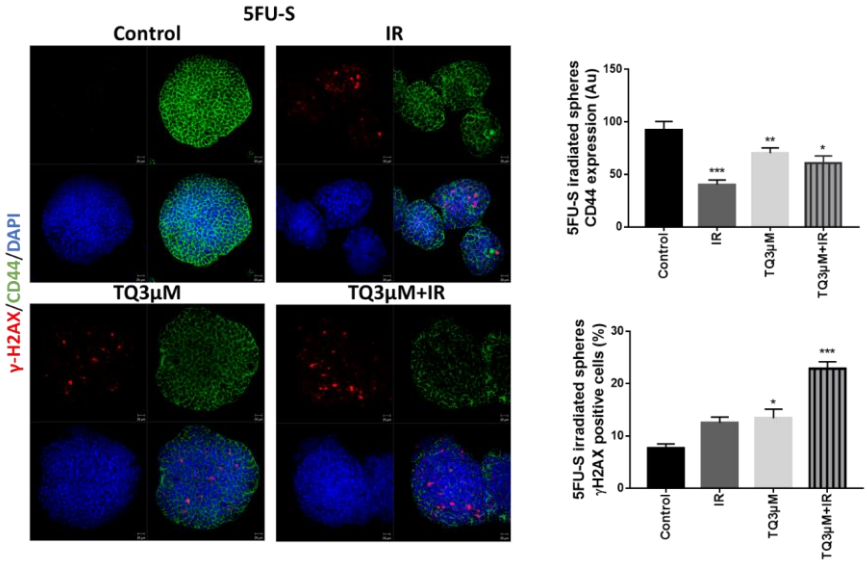

B.

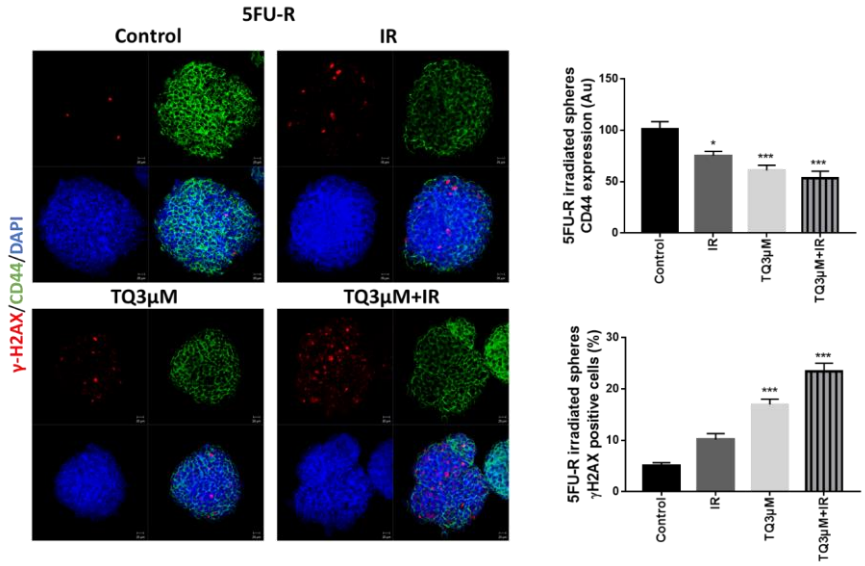

Figure 23. TQ and radiation combination regulates the expression of CD44 and γ-H2AX in 5FU-sensitive and resistant colonospheres. 5FU-sensitive and 5FU-resistant spheres were treated with TQ at day 0 of sphere culture and irradiated at day 4. Spheres were collected, fixed and stained for CD44 and γ-H2AX. Representative images were obtained using confocal microscopy and quantification of the intensity of CD44 (A) and γ-H2AX (B) stain in 5FU-S and 5FU-R G1 spheres untreated and treated with TQ, irradiation (IR) and combination of TQ and irradiation (TQ+IR) was performed using Carl Zeiss Zen 2012 image software. Stain intensity was normalized to size. Data represent an average of two independent experiments and are reported as mean ± SEM (* P<0.05; ** P<0.01; *** P<0.001). Scale bar 20 μm.

Remarkably, western blot analysis showed that radiation significantly decreased the expression of the structural protein F-actin when compared to untreated and TQ treated conditions (Figure 24A). This reduction was confirmed by immunostaining analysis of the expression of F-actin and tubulin (Figure 24B).

A.

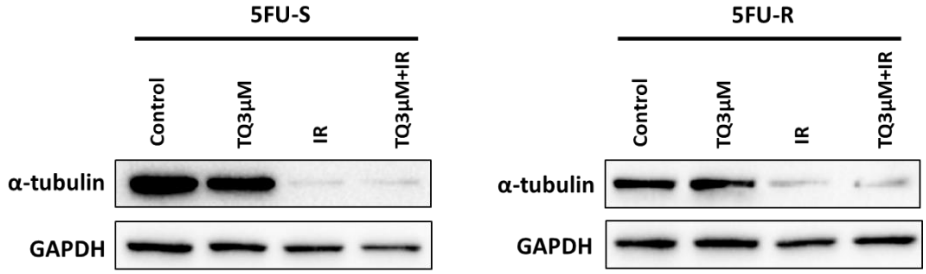

B.

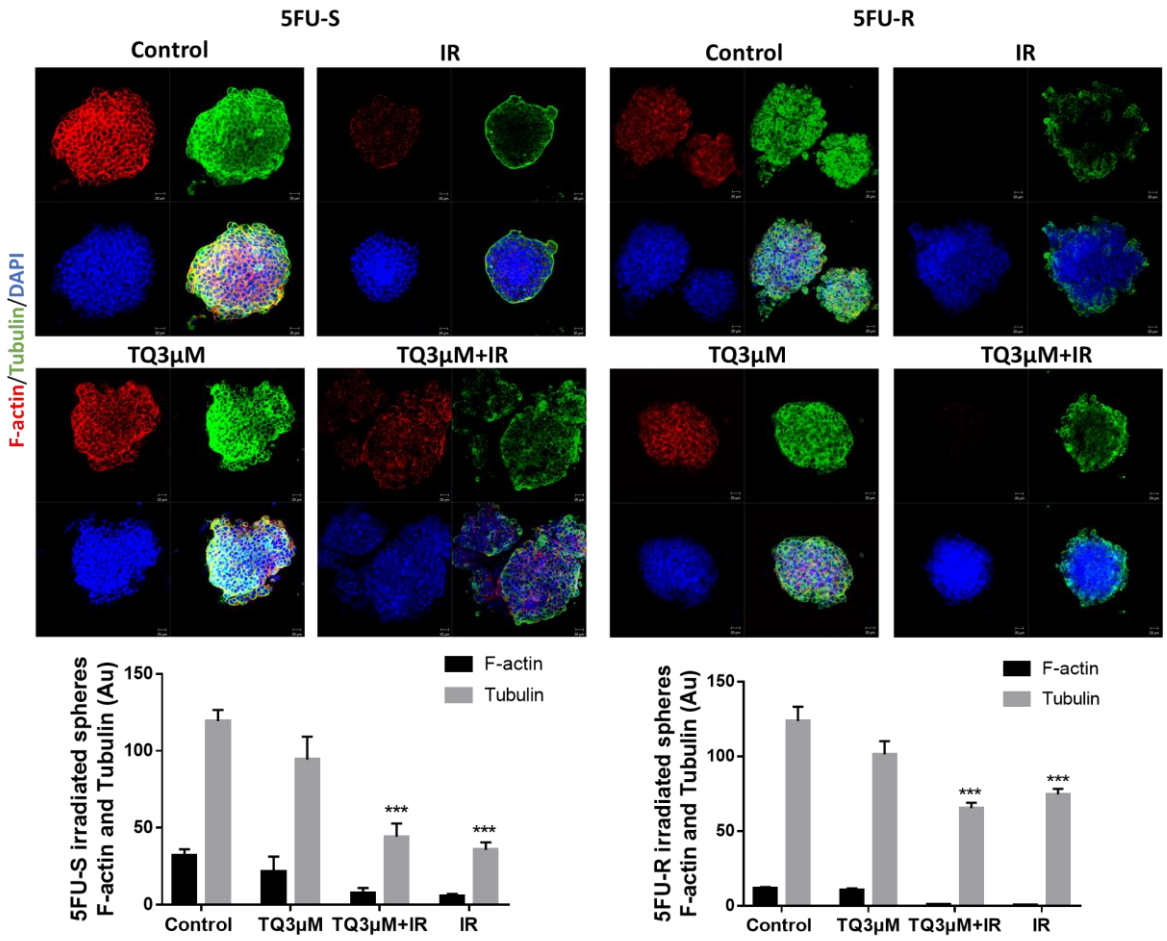

Figure 24. Radiation downregulates F-actin and tubulin expression in 5FU-sensitive and resistant colonospheres. 5FU-sensitive and 5FU-resistant spheres were treated with TQ at day 0 of sphere culture and irradiated at day 4. (A) Western blot analysis of tubulin protein expression in 5FU-S and 5FU-R HCT116 G1 spheres untreated and treated with TQ, irradiation (IR) and combination of TQ and irradiation (TQ+IR) is shown. (B) Spheres were collected, fixed and stained for F-actin and Tubulin. Representative images were obtained using confocal microscopy and quantification of the intensity of F-actin and Tubulin in 5FU-S and 5FU-R G1 spheres untreated and treated with TQ, irradiation (IR) and combination of TQ and irradiation (TQ+IR) was performed using Carl Zeiss Zen 2012 image software. Stain intensity was normalized to size. Data represent an average of two independent experiments and are reported as mean ± SEM (* P<0.05; ** P<0.01; *** P<0.001). Scale bar 20 µm.

F. TQ's effect on targeting an enriched population of colon cancer stem/progenitor cells *in vivo*

To experimentally prove that the HCT116 population derived from spheres is enriched with cells having stem-like properties, we assessed their tumorigenic potential in mice. NOD-SCID mice were used for the 5FU-sensitive cell line as they easily showed tumor development. 5FU-resistant cells failed to develop tumors in NOD-SCID mice, so NOD/Shi-scid IL2rgamma^{null} (NOG) mice were used. The number of spheres needed for tumor development was optimized by serial dilution. 100 5FU-sensitive and 250 5FU-resistant spheres induced tumor development in 4 and 8 weeks in NOD-SCID and NOG mice, respectively. We have previously reported that intraperitoneal injections of TQ at doses up to 20 mg/kg are not toxic to mice and significantly delay tumor growth in a xenograft model of 5FU-sensitive HCT116 colorectal cancer [117].

To test the effect of TQ on targeting an enriched population of cells with stem-like properties *in vivo*, we injected two groups of NOD-SCID mice with 100 spheres derived from HCT116 sensitive cell line and two groups of NOG mice with 250 spheres derived from HCT116- resistant cell line. One group acted as a control, and the other group was treated with TQ at a dose of 20 mg/kg body weight [117] three times per week for 21 days by intraperitoneal injections when a palpable tumor was observed. TQ significantly inhibited tumor growth in these mice when compared to control group (Figure 25A and B). At the end of the treatment period, the average tumor volume was 1182 mm^3 and 485 mm^3 in the control group, while it was 79 mm^3 ($P<0.01$) and 14 mm^3 ($P<0.001$) in TQ treated mice injected with 5FU-sensitive and 5FU-resistant spheres,

respectively (Figure 25A and B). A dose of 20 mg/kg TQ did not affect the body weight or resulted in animal death (data not shown), indicating that this dose is not toxic.

A.

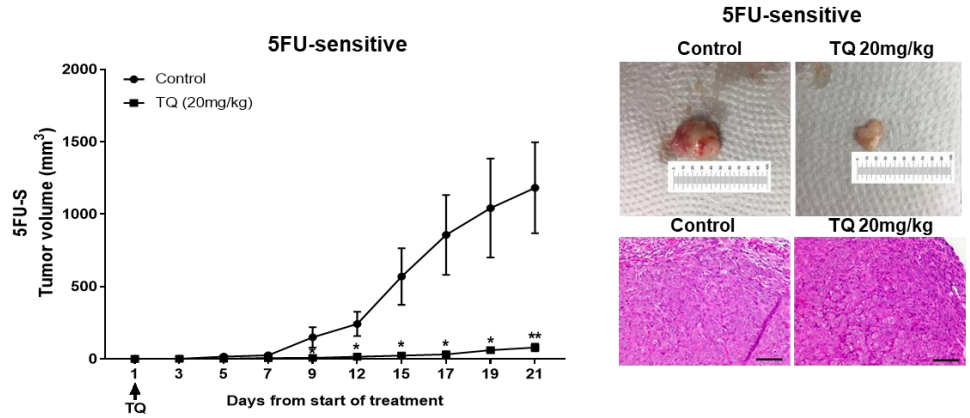

B.

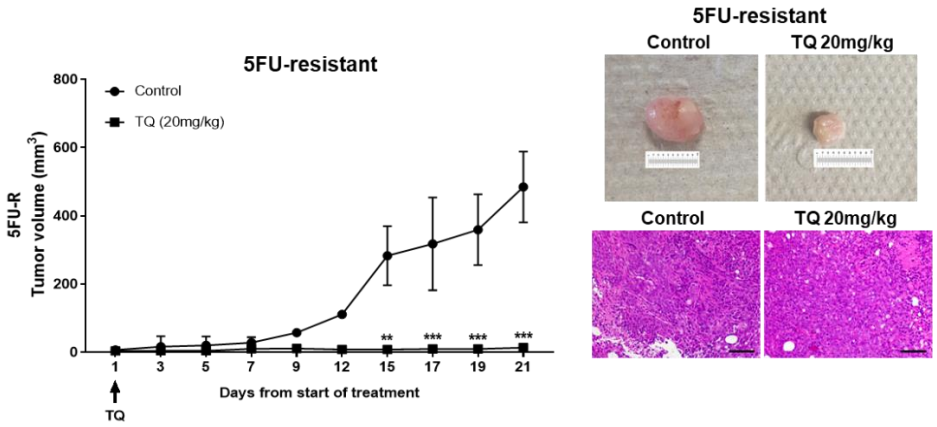

Figure 25. TQ reduces tumor growth in NOD-SCID and NOG mice. (A, B) NOD-SCID mice (8 mice/group) (A) were injected with 100 5FU-sensitive HCT116 G1 spheres and NOG mice (5 mice/group) (B) were injected with 250 5FU-resistant HCT116 G1 spheres and tumor progression was monitored. Tumor volume during 21 days of i.p. treatment (3x/week) with either 20 mg/kg TQ or 10% methanol in physiologic saline was reported. $P<0.05$ between TQ and vehicle (control) treated animals. Representative images of control and TQ-treated mice at day 21 and H&E stain of tumor tissues are shown.

Interestingly, two weeks after stopping TQ treatment, the average tumor volume in the TQ treated group (558 mm^3 in 5FU-sensitive and 37.5 mm^3 in 5FU-resistant) was still significantly lower than that of the control group (1451 mm^3 in 5FU-sensitive and 459 mm^3 in 5FU-resistant) (Figure 26A and B).

A.

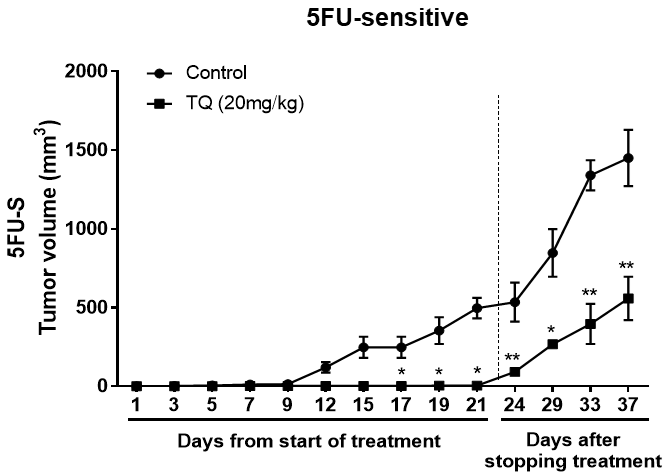

B.

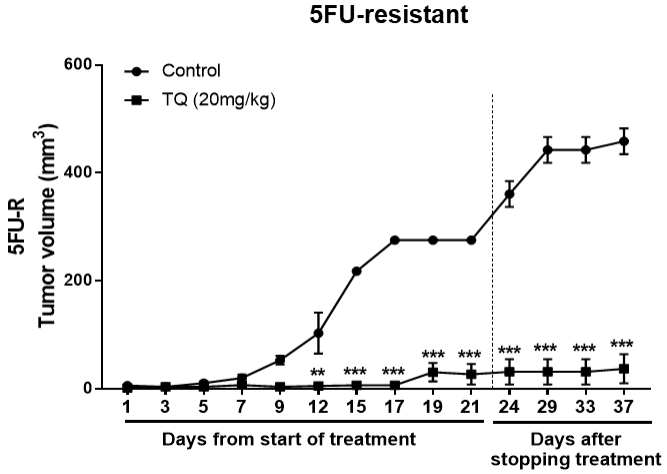

Figure 26. TQ treated mice showed minimal tumor growth after stopping treatment. (A, B) Average tumor volume of control and TQ treated mice (n=3) during and after stopping treatment for 2 weeks was reported in NOD-SCID and NOG mice. P<0.05 between TQ and vehicle (control) treated animals.

The diminished tumor size in TQ-treated xenografts was in part due to the induction of cell death, as shown by increased TUNEL positivity (Figure 27A). In the TQ-treated group, average apoptotic index estimated by TUNEL was 51.6% and 20% as compared to 4.2% and 2% in vehicle controls in mice injected with 5FU-sensitive and 5FU-resistant spheres, respectively. Similar to *in vitro* results, the stem cell marker CD44 was also decreased in mouse tumor tissues upon TQ treatment (Figure 27B). Western blot analysis showed upregulation of p53, p21, γ-H2AX and the NF-κB inhibitor Iκβα, and downregulation of the proliferation markers PCNA, NF-κB (p65), and p-MEK in tumor tissues of TQ-treated mice (Figure 27C), similar to *in vitro* 3D results.

A.

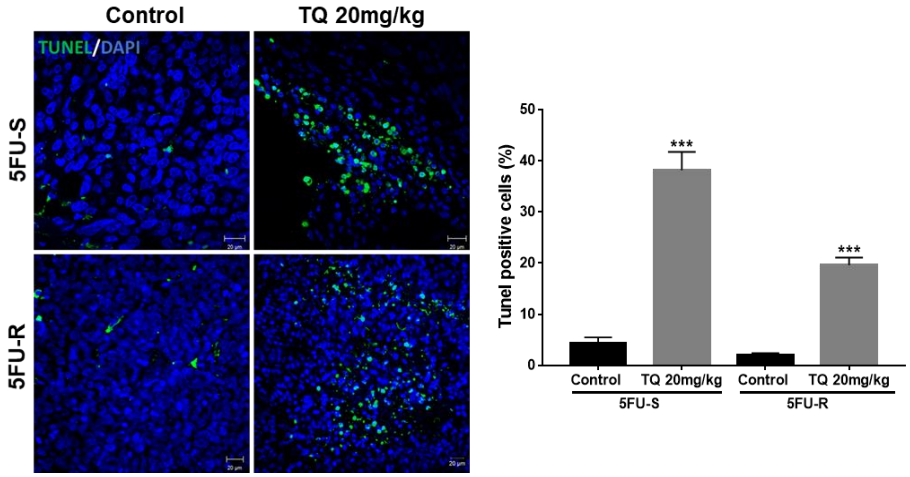
Control
TQ 20mg/kg
TUNEL/DAPI
5FU-S
5FU-R
Tunel positive cells (%)
50
40
30
20
10
0
***
***
Control
TQ 20mg/kg
Control
TQ 20mg/kg
5FU-S
5FU-R

B.

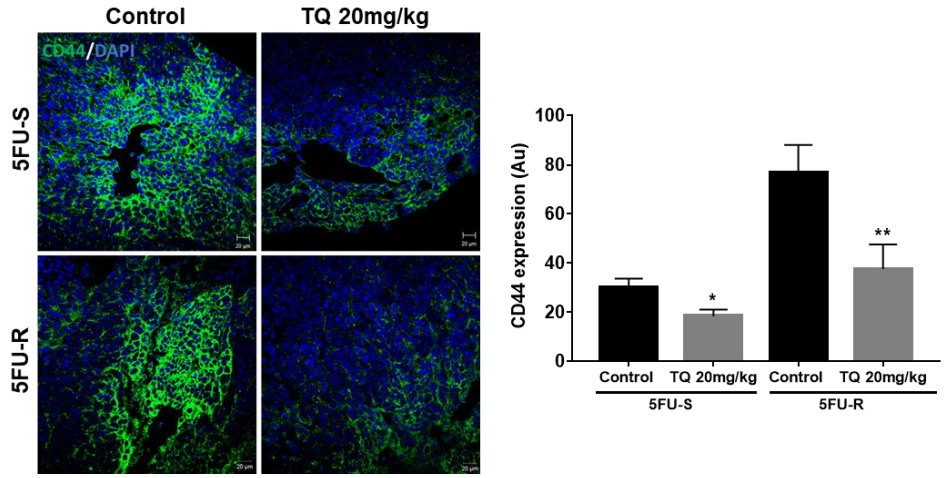
Control
TQ 20mg/kg
CD44/DAPI
5FU-S
5FU-R
CD44 expression (Au)
100
80
60
40
20
0
*
**
Control
TQ 20mg/kg
Control
TQ 20mg/kg
5FU-S
5FU-R

C.

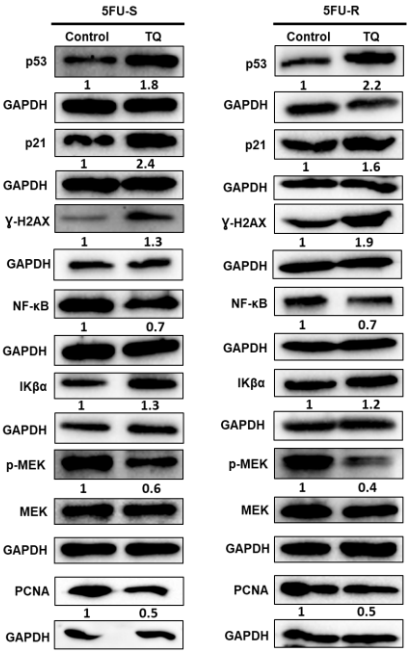

Figure 27. TQ induces apoptosis and reduces proliferation in NOD-SCID and NOG mice. (A) Representative images of control and TQ treated tissues from NOD-SCID mice injected with 100 5FU-S and 250 5FU-R HCT116 G1 spheres after TUNEL staining. TUNEL positive cells were counted and are represented as mean percentage ± SEM (* P<0.05; ** P<0.01; *** P<0.001 significantly different from control). (B) Representative confocal images of CD44 expression in control and treated tissues from NOD-SCID mice injected with 100 5FU-S and 250 5FU-R HCT116 G1 spheres. Images were analyzed and quantified by Carl Zeiss Zen 2012 image software. Scale bar 20 µm. (C) Analysis of p53, p21, γ-H2AX, NF-κB (p65), Iκβα, p-MEK and PCNA protein expression in control and TQ-treated tissues from NOD-SCID and NOG mice injected with 100 5FU-S and 250 5FU-R HCT116 G1 spheres. Fold expression changes normalized to GAPDH and total MEK in case of p-MEK expression are given below the blots. Data represent an average of three independent experiments.

CHAPTER IV

DISCUSSION

CRC is a heterogenous disease arising from one or a combination of chromosomal instability, CpG island methylator phenotype, and microsatellite instability [15]. CRC persists as one of the most prevalent and deadly tumor types in both men and women worldwide. This is in spite of widespread, effective measures of preventive screening, and also major advances in treatment options. Despite advances in cytotoxic and targeted therapy, resistance to chemotherapy remains one of the greatest challenges in long-term management of incurable metastatic disease and eventually contributes to death as tumors accumulate means of evading treatment. Malignant tumors can have intrinsic resistance and/or acquired resistance. The primary reason for treatment failure is believed to be acquired resistance to therapy which occurs in 90% of patients with metastatic CRC [177]. In general, resistance to traditional cytotoxic therapy is accomplished by a) genetic and epigenetic modifications within the cell itself that can alter drug sensitivity, b) cell cycle and signaling pathway perturbations, c) or decreased drug delivery to cancer cells either by increased efflux out of the cell, decreased uptake or change in enzymes involved in metabolism [177]. It has been recently suggested that CSCs are the tumor initiating cells in a primary tumor and that they constitute a reservoir of self-renewing cells and are at the origin of chemoresistance, minimal residual disease, and cancer recurrence [178, 179]. Although conventional cytotoxic chemotherapies inhibit the highly proliferative cells, these

quiescent or slowly cycling CSCs survive successive treatments and lead to local and distant tumor initiation [180]. Therefore, identifying new therapeutic approaches is of high importance to overcome resistance and prevent relapse.

In the process of development and discovery of new potential anticancer agents, growing interest is heading towards ‘safe’, cost-effective and widely available molecules, prominently from plant extracts. The natural compound TQ has shown promising effects against colon cancer both *in vitro* and *in vivo* [127]. However, studies tackling TQ’s effect on CSCs are limited. The current study was designed to investigate the effect of TQ on targeting the self-renewal capacity of colorectal CSCs and its underlying mechanisms of action in 5FU-resistant as opposed to 5FU-sensitive HCT116 cell lines *in vitro* and in xenograft mouse models.

We focused on 5FU-resistant colorectal cancer cells that are believed to be more relevant to the clinical setting as they mimic the residual cancer cells post chemotherapy. Our results showed that TQ exhibits strong inhibitory effect on the self-renewal potential of 5FU-resistant colorectal cancer stem/progenitor cells by inducing apoptosis and DNA damage. Furthermore, our data established TQ’s effect as a radiosensitizer on 2D and 3D cultured colorectal cancer cells. Lastly, we showed that TQ targets an enriched population of chemo-resistant colorectal CSCs *in vivo* by reducing proliferation, inducing apoptosis and inhibiting NF-κB expression in treated xenografts.

Since its discovery 50 years ago, 5FU has been the backbone of treatments for CRC, but with poor success rate of less than 30% [181]. The ineffectiveness of 5FU has been mainly limited by drug resistance [182-184]. Our first aim was to demonstrate the

effect of TQ on 5FU-resistant colorectal cancer cells in 2D before moving into the 3D culture system. Our results showed that TQ exhibited antitumor effects on 5FU-resistant HCT116 cells. In line with previously published data [116, 120], we showed that TQ reduced the viability of 5FU-sensitive HCT116 cells in a time- and dose-dependent manner.

Our major focus was to test the effect of TQ on colorectal CSCs. A major problem with the isolation of CSCs is that most techniques are cumbersome and expensive making them unideal for drug testing. In addition, cancer stem cell markers are expressed in a complex pattern; neither single marker expression nor simple combinations can be universally used for the isolation and enrichment of colorectal CSC [5, 59]. Consequently, we employed a 3D sphere formation assay to enrich for colorectal cancer stem/progenitor cells from 5FU-sensitive and resistant HCT116 cells and investigate the efficacy of TQ on targeting these cells. Sphere cultures represent a major 3D *in vitro* model in cancer stem cell research [66] and provide a means to evaluate the self-renewal capacity and differentiation potential of CSCs [67]. Sphere cultures have been used to isolate and propagate colon CSCs from primary tumors but have been rarely used to enrich CSCs from colorectal cancer cell lines [85-87]. In this study, we demonstrated the ability to grow and maintain colonospheres in culture up to G5. Notably, G5 colonospheres showed an increased expression of the stem cell maker CD44 when compared to G1 colonospheres, suggesting an enrichment in CSCs upon propagation. CD44 is a transmembrane glycoprotein highly expressed in almost every cancer cell and is crucial in tumor initiation and colonosphere propagation *in vitro* [185]. CD44 is known to have a multifunctional role in many cellular processes, like

survival, growth, and differentiation, and may regulate stemness in CSCs [186]. Furthermore, our results showed that TQ exhibits a strong inhibitory effect on the sphere-forming and self-renewal potential of 5FU-resistant colorectal cancer stem/progenitor cells demonstrating that CSCs, which are resistant to chemotherapy compared to the bulk of the tumor cells, are selectively and effectively targeted by TQ. We further confirmed this by the observed decrease in the sphere forming ability of the side population cells sorted from 5FU-resistant cells upon TQ treatment. Side population cells are characterized by high expression of ATP-binding cassette transporters (ABCG2) which can exclude Hoechst 33,342 nuclear dye and often represent cancer stem-like and/or drug resistant cancer cells [175]. Our results showed that 5FU-resistant cells demonstrate cancer stem-like features evident by the increased expression of side-population cells when compared to 5FU-sensitive cells.

To understand the underlying mechanism of the observed reduction in sphere-formation, we investigated apoptosis induction and activation of DNA damage as possible mechanisms of cell death. TQ has been shown to induce apoptosis by modulating several types of players including generation of reactive oxygen species [116], up-regulation of apoptotic mediators, interference with angiogenesis, metastasis and DNA damage markers [127, 156]. Indeed, TQ treatment led to increased TUNEL positivity and upregulation of p53 and p21 in colonospheres, indicating induction of apoptotic cell death.

H2AX is a member of the histone H2A family and is one of the first molecules to be phosphorylated at serine 139 (γ-H2AX) in response to double-strand DNA breaks. This phosphorylation mediates the recruitment of repair factors to the damaged DNA

sites [187]. H2AX has been proposed as a factor to assess response to treatment, and several agents and chemotherapeutic drugs used in colorectal cancer treatment have been shown to increase γ-H2AX, including oxaliplatin, sorafenib, valproic acid, and oncolytic adenovirus [188, 189]. The response to DNA damage results in either cell cycle arrest, to allow the lesions to be repaired, or in p53-dependent and independent apoptosis [190, 191]. Interestingly, our results showed opposite response to TQ treatment in terms of γ-H2AX expression between 5FU-sensitive and resistant colonospheres. TQ downregulated γ-H2AX in 5FU-sensitive cells, which could suggest that TQ has a low genotoxic potential in these cells since it induced p53 activation with minimal DNA damage response [192]. In addition, γ-H2AX plays an essential role in the process of DNA repair through the recruitment of DNA repair proteins such as 53BP1, RAD51, BRCA1, and MDC1 to the damage sites [193]. Therefore, this decrease in γ-H2AX could indicate reduced DNA repair in malignant cells, which enhances their sensitivity to TQ. In contrast, γ-H2AX was remarkably upregulated by TQ in 5FU-resistant cells, indicating activation of DNA damage response, which may generate a positive feedback loop that enhances p53 activity. DNA damage can cause various post-translational modifications on p53 that can enhance its ability to activate target genes and promote apoptosis [192] thus increasing the susceptibility of the chemo-resistant malignant cells to apoptosis by TQ. Further analysis is essential to understand the involved mechanism of action such as evaluating the expression of upstream and downstream effectors including p-ATM, CHEK2, DNA-PKc, MDM2.

Recent evidence showed that CSCs can resist ionizing radiation treatment. This has been explained by a metabolic status that is associated with: a) high free radical

scavenger levels e.g., glutathione, thioredoxin, and enzymatic proteins peroxidase and catalase, which might shield the cells against radiation-induced oxidative stress [194, 195], b) activated DNA checkpoints [196], which arrest cell cycle progression in the presence of DNA damage and allow cells to repair DNA and c) sustained hypoxic microenvironment, which trigger mechanisms important for the maintenance of CSCs such as hypoxia-inducible factor (HIF) signaling, autophagy, and EMT contributing to radio-resistance [197]. Therefore, new therapeutic radiosensitizers are required to overcome tumor radio-resistance and improve radiotherapy outcome. Various strategies have been proposed including synthetic inhibitors of particular constituent of radio-resistance pathways, in addition to natural radiosensitizers such as curcumin that can compensate for synthetic inhibitors limitations [198]. Studies on the function of TQ as a radiosensitizer are limited. The observed effect of TQ on γ-H2AX expression led us to examine the effect of TQ and radiation combination on colorectal cancer stem/progenitor cells. TQ was found to exert supra-additive cytotoxic and apoptotic effects on MCF7 and T47D breast cancer cells when combined with a single dose of ionizing radiation (2.5 Gy) [138]. Radio-resistance has been reported to be correlated to several signaling pathways involving NF-κB as the key molecule [199]. The NF-κB signaling pathway is activated in several types of cancer, and its activation contributes to the malignant characteristics of cancer cells [127]. Irradiation activates the NF-κβ signaling pathway, leading to the transcription of downstream effector proteins such as cyclin D1, BCL2, TNF-α, VEGF, XIAP and COX2 and the development of radio-resistance [200, 201]. NF-κB and its effector proteins have been shown to be correlated with poor radiotherapy response [201]. The therapeutic efficacy of radiotherapy can be

enhanced by inhibiting the NF-κB signaling pathway. In this study we showed that TQ reduced the expression of NF-κB indicating that TQ may have the potential to sensitize colorectal cancer cells to radiation. Indeed, TQ and radiation combination maintained a relatively high number of residual γ-H2AX foci 24hrs post irradiation in both cell lines suggesting decreased repair in these cells and increased sensitivity to apoptosis.

Exposure to ionizing radiation triggers activation of specific DNA damage signaling and repair mechanisms including the phosphorylation of H2AX in the vicinity of a double strand break (DSB) [187]. The formation and loss of γ-H2AX foci is measured following exposure to radiation doses. γ-H2AX kinetic studies have shown that maximum foci levels can be observed as early as 3-10 minutes. With increasing post-exposure time, the number of γ-H2AX foci decreases rapidly to about 50% of the initial level within 1hr followed by a slower loss of the residual foci present a few hours and up to 24hrs post exposure. γ-H2AX foci disappearance over time follows DSB rejoining in repair-competent cells [202]. Furthermore, our results showed that TQ sensitized colorectal CSCs to radiation as evident by reduced sphere forming ability and upregulation of γ-H2AX upon TQ and radiation combination. Further studies on the effect of TQ and radiation on NF-κB pathway and its downstream targets would help in understanding TQ's effect as a radiosensitizer and provide a potentially more effective treatment strategy to colorectal cancer.

Despite the advantages of 3D tumorosphere culture systems for studying CSC properties, they do not fully replicate the 3D structure and environment of an *in vivo* tumor [73] and/or mimic cancer tissues. Therefore, colorectal CSCs need to be further characterized through functional features in an *in vivo* setting. To experimentally prove

that the derived spheres are enriched with cells having stem-like properties, we injected a group of mice with HCT116 cells cultured in 2D monolayers and another group of mice with spheres. The validity of our model will be confirmed if the injected spheres showed a higher tumor initiation capacity than 2D monolayer cells. Indeed, the injection of spheres derived from 5FU- sensitive HCT116 cell line and not the 2D equivalent cell density into NOD-SCID immunocompromised mice resulted in tumor development, suggesting that spheres are rich in cells with stem-like properties.

Our next aim was to test the effect of TQ on targeting an enriched population of cells with stem-like properties *in vivo*. For this purpose, NOD-SCID and NOG mice were injected with spheres derived from 5FU-sensitive and resistant cell lines, respectively. Our results showed that treatment with 20 mg/kg body weight of TQ was able to significantly inhibit tumor growth in these mice when compared to control group. Remarkably, tumor volume in TQ-treated group remained significantly lower than that of control after stopping treatment for two weeks, indicating a relatively potent inhibitory effect of TQ on tumor growth. The most interesting finding was that TQ's effect on 5FU-resistant induced tumors was irreversible when compared to 5FU-sensitive tumors since the significant inhibition of tumor volume was maintained even after stopping TQ treatment for two weeks, suggesting a promising effect of TQ on the enriched population of chemo-resistant colorectal CSCs that is majorly responsible for tumor recurrence. This effect could be further enhanced with long-term exposure to TQ.

It is important to note that the oral administration of TQ was found to be safe in several animal models [203] and the effective anticancer dose used in this study (20 mg/kg) is non-toxic and much lower than reported doses. In fact, the LD50 of TQ in

mice and rats ranged between 57 and 104 mg/kg when injected intraperitoneally and reached 870 mg/kg when given orally (reviewed in Ref. [130]). Studies on the anticancer therapeutic potential of TQ and its safety profiles in humans are very limited and its pharmacologically relevant doses in animal or human blood have not been determined. In a Phase I clinical trial, TQ was found to be well tolerated at doses up to 10 mg/kg/day but no significant anticancer activity was observed at this dose [204]. A recent Phase II clinical study evaluating the effect of 100 mg and 200 mg TQ on oral potential malignant lesions is currently registered; however, it is still not open for participant recruitment (https://clinicaltrials.gov/ct2/show/NCT03208790?term=thymoquinone&rank=1). Nevertheless, several clinical trials testing the effect of *Nigella sativa* on various diseases including beta thalassemia major in children, dyslipidemia and arsenical keratosis have shown that it is not toxic in patients at doses up to 300 mg/day. (https://clinicaltrials.gov/ct2/results?cond=&term=nigella+sativa&type=&rslt=&age_v=&gndr=&intr=&titles=&outc=&spons=&lead=&id=&cntry=&state=&city=&dist=&locn=&strd_s=&strd_e=&prcd_s=&prcd_e=&sfpd_s=&sfpd_e=&lupd_s=&lupd_e=&sort=).

The exact mechanism(s) by which TQ exerts its antitumor activity *in vivo* is not well understood, since few data is available on the molecular mechanisms of TQ effects. In this study we showed that tumor growth inhibition by TQ in HCT116 xenograft mouse models may be attributed to its potent anti-proliferative effects, in addition to the induction of apoptosis as indicated by TUNEL and upregulated p53 and p21 expression. NF-κB is a crucial factor involved in the pathogenesis of cancer

through activation of genes and cytokines required for the induction of cellular proliferation [127] and has been shown to be regulated by TQ [205, 206]. In addition, MAPK signaling pathway is dysregulated in colorectal cancer, and various approaches for blocking signaling through this pathway have been studied [207]. We have previously shown that the inhibition of ERK pathway by MEK inhibitor PD98059 potentiated apoptosis induction by TQ [116]. We also documented that TQ directly binds to PAK1/ERK kinase complex, induces considerable conformational changes of PAK1 and interrupts its function as a scaffold for ERK1/2/MEK to recruit MEK to RAF at the membrane [115]. Importantly, MEK kinase was shown to induce NF-κB activation through the degradation of IκB-α, a major inhibitor of NF-κB [208]. Interestingly, our results showed that TQ treatment reduced NF-κB (p65) and p-MEK and upregulated Iκβ-α expression in xenograft mouse tissues, suggesting a role for MEK as a signal mediator involved in Iκβ-α-induced NF-κB inhibition and further supporting TQ's antitumor effects.

In summary, we showed that TQ has several activities that make it desirable as a therapeutic agent. First, TQ showed a significant potential in targeting chemo-resistant colorectal CSCs both *in vitro* and *in vivo*. Second, TQ exhibited anti-proliferative and anti-inflammatory effects and induced apoptosis and DNA damage in these cells. Lastly, TQ sensitized colorectal cells to radiation. These data together suggest that TQ could be used as an effective agent either alone or in combination with radiation and/or chemotherapeutic drugs to enhance the therapeutic efficacy and indicate that this relatively non-toxic and inexpensive compound merits further clinical investigation.

Of course, there is a need to consider how TQ could be administered given its low bioavailability. One mode of delivery could be an intravenous route of administration, which could have efficacy in therapeutic paradigms. In this regard, a recent study demonstrated that a biodegradable polymeric polyaprolactone (PCL) TQ encapsulating nanoparticles can be administered intravenously for the effective treatment of colorectal tumors in murine model [209]. More importantly, this method was found to be effective, stable and safe, suggesting that nanoparticles are promising carrier systems for the utilization of TQ for various therapeutic purposes against colorectal cancer.

BIBLIOGRAPHY

[1] A. Humphries, N.A. Wright, Colonic crypt organization and tumorigenesis, Nature Reviews Cancer, 8 (2008) 415-424.
[2] M.P. Kahai P, Lobo S. , Anatomy, Abdomen and Pelvis, Large Intestine., Treasure Island (FL): StatPearls Publishing, (2019).
[3] D.J. Huels, O.J. Sansom, Stem vs non-stem cell origin of colorectal cancer, Br J Cancer, 113 (2015) 1-5.
[4] S. Basu, G. Haase, A. Ben-Ze'ev, Wnt signaling in cancer stem cells and colon cancer metastasis, F1000Res, 5 (2016) F1000 Faculty Rev-1699.
[5] M. Todaro, M.G. Francipane, J.P. Medema, G. Stassi, Colon cancer stem cells: promise of targeted therapy, Gastroenterology, 138 (2010) 2151-2162.
[6] C. Lopez-Garcia, A.M. Klein, B.D. Simons, D.J. Winton, Intestinal Stem Cell Replacement Follows a Pattern of Neutral Drift, Science, 330 (2010) 822.
[7] H. Tian, B. Biehs, S. Warming, K.G. Leong, L. Rangell, O.D. Klein, F.J. de Sauvage, A reserve stem cell population in small intestine renders Lgr5-positive cells dispensable, Nature, 478 (2011) 255-259.
[8] C.S. Potten, R. Gandara, Y.R. Mahida, M. Loeffler, N.A. Wright, The stem cells of small intestinal crypts: where are they?, Cell proliferation, 42 (2009) 731-750.
[9] J.P. Medema, L. Vermeulen, Microenvironmental regulation of stem cells in intestinal homeostasis and cancer, Nature, 474 (2011) 318-326.
[10] F.J. Abdul Khalek, G.I. Gallicano, L. Mishra, Colon cancer stem cells, Gastrointest Cancer Res, (2010) S16-S23.
[11] G. Vaiopoulos, D. Kostakis, Koutsilieris, G. Papavassiliou, Concise Review: Colorectal Cancer Stem Cells, STEM CELLS 30 (2012) 363–371.
[12] R.L. Siegel, K.D. Miller, A. Jemal, Cancer statistics, 2020, CA: A Cancer Journal for Clinicians, 70 (2020) 7-30.
[13] M. Arnold, M.S. Sierra, M. Laversanne, I. Soerjomataram, A. Jemal, F. Bray, Global patterns and trends in colorectal cancer incidence and mortality, Gut, 66 (2017) 683.
[14] M.J. Munro, S.K. Wickremesekera, L. Peng, S.T. Tan, T. Itinteang, Cancer stem cells in colorectal cancer: a review, Journal of Clinical Pathology, 71 (2018) 110.
[15] K. Tariq, K. Ghias, Colorectal cancer carcinogenesis: a review of mechanisms, Cancer Biol Med, 13 (2016) 120-135.
[16] M.S. Pino, D.C. Chung, The chromosomal instability pathway in colon cancer, Gastroenterology, 138 (2010) 2059-2072.
[17] S.T. Bak, D. Sakellariou, J. Pena-Diaz, The dual nature of mismatch repair as antimutator and mutator: for better or for worse, Front Genet, 5 (2014) 287-287.
[18] D.J. Weisenberger, K.D. Siegmund, M. Campan, J. Young, T.I. Long, M.A. Faasse, G.H. Kang, M. Widschwendter, D. Weener, D. Buchanan, H. Koh, L. Simms, M. Barker, B. Leggett, J. Levine, M. Kim, A.J. French, S.N. Thibodeau, J. Jass, R. Haile, P.W. Laird, CpG island methylator phenotype underlies sporadic microsatellite

instability and is tightly associated with BRAF mutation in colorectal cancer, Nature genetics, 38 (2006) 787-793.
[19] E.J. Kuipers, W.M. Grady, D. Lieberman, T. Seufferlein, J.J. Sung, P.G. Boelens, C.J.H. van de Velde, T. Watanabe, Colorectal cancer, Nature Reviews Disease Primers, 1 (2015) 15065.
[20] A. Deverakonda, Diagnosis and Treatment of Colorectal Cancer: A Review, Research & Reviews: Journal of Medical and Health Sciences, 5 (2016).
[21] N. Zhang, Y. Yin, S.-J. Xu, W.-S. Chen, 5-Fluorouracil: mechanisms of resistance and reversal strategies, Molecules (Basel, Switzerland), 13 (2008) 1551-1569.
[22] D. Thomas, J. Zalcberg, 5-FLUOROURACIL: A PHARMACOLOGICAL PARADIGM IN THE USE OF CYTOTOXICS, Clinical and Experimental Pharmacology and Physiology $V 25, (1998) 887-895.
[23] B. van Triest, H.M. Pinedo, Y. van Hensbergen, K. Smid, F. Telleman, P.S. Schoenmakers, C.L. van der Wilt, J.A.M. van Laar, P. Noordhuis, G. Jansen, G.J. Peters, Thymidylate Synthase Level as the Main Predictive Parameter for Sensitivity to 5-Fluorouracil, but not for Folate-based Thymidylate Synthase Inhibitors, in 13 Nonselected Colon Cancer Cell Lines, Clinical Cancer Research, 5 (1999) 643.
[24] J.L. Grem, Screening for Dihydropyrimidine Dehydrogenase Deficiency, Clinical Cancer Research, 11 (2005) 5067.
[25] C.N. Arnold, A. Goel, C.R. Boland, Role of hMLH1 promoter hypermethylation in drug resistance to 5-fluorouracil in colorectal cancer cell lines, International journal of cancer, 106 (2003) 66-73.
[26] S. Violette, L. Poulain, E. Dussaulx, D. Pepin, A.M. Faussat, J. Chambaz, J.M. Lacorte, C. Staedel, T. Lesuffleur, Resistance of colon cancer cells to long-term 5-fluorouracil exposure is correlated to the relative level of Bcl-2 and Bcl-X(L) in addition to Bax and p53 status, International journal of cancer, 98 (2002) 498-504.
[27] X.F. Guo, E. Goessl, G. Jin, E.S. Collie-Duguid, J. Cassidy, W. Wang, V. O'Brien, Cell cycle perturbation and acquired 5-fluorouracil chemoresistance., Anticancer Res. , 28 (2008) 9-14
[28] Y.-K. Shin, B.C. Yoo, H.J. Chang, E. Jeon, S.-H. Hong, M.-S. Jung, S.-J. Lim, J.-G. Park, Down-regulation of Mitochondrial F₁F₀-ATP Synthase in Human Colon Cancer Cells with Induced 5-Fluorouracil Resistance, Cancer Research, 65 (2005) 3162.
[29] B.C. Yoo, E. Jeon, S.H. Hong, Y.K. Shin, H.J. Chang, J.G. Park, Metabotropic glutamate receptor 4-mediated 5-Fluorouracil resistance in a human colon cancer cell line, Clinical cancer research : an official journal of the American Association for Cancer Research, 10 (2004) 4176-4184.
[30] K. Katakura, H. Fujise, K. Takeda, O. Kaneko, M. Torii, M. Suzuki, K.P. Chang, Y. Hashiguchi, Overexpression of LaMDR2, a novel multidrug resistance ATP-binding cassette transporter, causes 5-fluorouracil resistance in Leishmania amazonensis11The sequence data reported in this paper have been submitted to the DDBJ database under the accession number AB008469, FEBS Letters, 561 (2004) 207-212.
[31] N.Y. Frank, T. Schatton, M.H. Frank, The therapeutic promise of the cancer stem cell concept, J Clin Invest, 120 (2010) 41-50.

[32] A. Lugli, G. Iezzi, I. Hostettler, M.G. Muraro, V. Mele, L. Tornillo, V. Carafa, G. Spagnoli, L. Terracciano, I. Zlobec, Prognostic impact of the expression of putative cancer stem cell markers CD133, CD166, CD44s, EpCAM, and ALDH1 in colorectal cancer, Br J Cancer, 103 (2010) 382-390.
[33] S. Babashah, Cancer Stem Cells: Emerging Concepts and Future Perspectives in Translational Oncology, Springer, (2015).
[34] T. Lapidot, C. Sirard, J. Vormoor, B. Murdoch, T. Hoang, J. Caceres-Cortes, M. Minden, B. Paterson, M.A. Caligiuri, J.E. Dick, A cell initiating human acute myeloid leukaemia after transplantation into SCID mice, Nature, 367 (1994) 645-648.
[35] M. Al-Hajj, M.S. Wicha, A. Benito-Hernandez, S.J. Morrison, M.F. Clarke, Prospective identification of tumorigenic breast cancer cells, Proceedings of the National Academy of Sciences of the United States of America, 100 (2003) 3983-3988.
[36] C.A. O'Brien, A. Pollett, S. Gallinger, J.E. Dick, A human colon cancer cell capable of initiating tumour growth in immunodeficient mice, Nature, 445 (2007) 106-110.
[37] S.K. Singh, C. Hawkins, I.D. Clarke, J.A. Squire, J. Bayani, T. Hide, R.M. Henkelman, M.D. Cusimano, P.B. Dirks, Identification of human brain tumour initiating cells, Nature, 432 (2004) 396-401.
[38] C. Li, D.G. Heidt, P. Dalerba, C.F. Burant, L. Zhang, V. Adsay, M. Wicha, M.F. Clarke, D.M. Simeone, Identification of Pancreatic Cancer Stem Cells, Cancer Research, 67 (2007) 1030.
[39] P.C. Hermann, S.L. Huber, T. Herrler, A. Aicher, J.W. Ellwart, M. Guba, C.J. Bruns, C. Heeschen, Distinct populations of cancer stem cells determine tumor growth and metastatic activity in human pancreatic cancer, Cell stem cell, 1 (2007) 313-323.
[40] L. Patrawala, T. Calhoun, R. Schneider-Broussard, H. Li, B. Bhatia, S. Tang, J.G. Reilly, D. Chandra, J. Zhou, K. Claypool, L. Coghlan, D.G. Tang, Highly purified CD44+ prostate cancer cells from xenograft human tumors are enriched in tumorigenic and metastatic progenitor cells, Oncogene, 25 (2006) 1696-1708.
[41] A.T. Collins, P.A. Berry, C. Hyde, M.J. Stower, N.J. Maitland, Prospective identification of tumorigenic prostate cancer stem cells, Cancer Res, 65 (2005) 10946-10951.
[42] C.B. Westphalen, S. Asfaha, Y. Hayakawa, Y. Takemoto, D.J. Lukin, A.H. Nuber, A. Brandtner, W. Setlik, H. Remotti, A. Muley, X. Chen, R. May, C.W. Houchen, J.G. Fox, M.D. Gershon, M. Quante, T.C. Wang, Long-lived intestinal tuft cells serve as colon cancer-initiating cells, J Clin Invest, 124 (2014) 1283-1295.
[43] F. Papaccio, F. Paino, T. Regad, G. Papaccio, V. Desiderio, V. Tirino, Concise Review: Cancer Cells, Cancer Stem Cells, and Mesenchymal Stem Cells: Influence in Cancer Development, Stem Cells Transl Med, 6 (2017) 2115-2125.
[44] M.L. Burness, D.A. Sipkins, The stem cell niche in health and malignancy, Seminars in Cancer Biology, 20 (2010) 107-115.
[45] J.E. Visvader, G.J. Lindeman, Cancer stem cells in solid tumours: accumulating evidence and unresolved questions, Nature reviews. Cancer, 8 (2008) 755-768.
[46] L. Vermeulen, F. De Sousa E Melo, M. van der Heijden, K. Cameron, J.H. de Jong, T. Borovski, J.B. Tuynman, M. Todaro, C. Merz, H. Rodermond, M.R. Sprick, K. Kemper, D.J. Richel, G. Stassi, J.P. Medema, Wnt activity defines colon cancer stem

cells and is regulated by the microenvironment, Nature Cell Biology, 12 (2010) 468-476.
[47] T. Reya, S.J. Morrison, M.F. Clarke, I.L. Weissman, Stem cells, cancer, and cancer stem cells, Nature, 414 (2001) 105-111.
[48] J. Taipale, P.A. Beachy, The Hedgehog and Wnt signalling pathways in cancer, Nature, 411 (2001) 349-354.
[49] G. Bhardwaj, B. Murdoch, D. Wu, D.P. Baker, K.P. Williams, K. Chadwick, L.E. Ling, F.N. Karanu, M. Bhatia, Sonic hedgehog induces the proliferation of primitive human hematopoietic cells via BMP regulation, Nature immunology, 2 (2001) 172-180.
[50] R.G.J. Vries, M. Huch, H. Clevers, Stem cells and cancer of the stomach and intestine, Molecular Oncology, 4 (2010) 373-384.
[51] A. Haegebarth, H. Clevers, Wnt signaling, lgr5, and stem cells in the intestine and skin, Am J Pathol, 174 (2009) 715-721.
[52] T. Fevr, S. Robine, D. Louvard, J. Huelsken, Wnt/beta-catenin is essential for intestinal homeostasis and maintenance of intestinal stem cells, Molecular and cellular biology, 27 (2007) 7551-7559.
[53] L. Ricci-Vitiani, A. Pagliuca, E. Palio, A. Zeuner, R. De Maria, Colon cancer stem cells, Gut, 57 (2008) 538.
[54] K. Ieta, F. Tanaka, N. Haraguchi, Y. Kita, H. Sakashita, K. Mimori, T. Matsumoto, H. Inoue, H. Kuwano, M. Mori, Biological and Genetic Characteristics of Tumor-Initiating Cells in Colon Cancer, Annals of Surgical Oncology, 15 (2008) 638-648.
[55] S.V. Shmelkov, J.M. Butler, A.T. Hooper, A. Hormigo, J. Kushner, T. Milde, R. St Clair, M. Baljevic, I. White, D.K. Jin, A. Chadburn, A.J. Murphy, D.M. Valenzuela, N.W. Gale, G. Thurston, G.D. Yancopoulos, M. D'Angelica, N. Kemeny, D. Lyden, S. Rafii, CD133 expression is not restricted to stem cells, and both CD133+ and CD133- metastatic colon cancer cells initiate tumors, J Clin Invest, 118 (2008) 2111-2120.
[56] C. Dittfeld, A. Dietrich, S. Peickert, S. Hering, M. Baumann, M. Grade, T. Ried, L.A. Kunz-Schughart, CD133 expression is not selective for tumor-initiating or radioresistant cell populations in the CRC cell lines HCT-116, Radiotherapy and Oncology, 92 (2009) 353-361.
[57] R.C. Langan, J.E. Mullinax, M.T. Raiji, T. Upham, T. Summers, A. Stojadinovic, I. Avital, Colorectal cancer biomarkers and the potential role of cancer stem cells, J Cancer, 4 (2013) 241-250.
[58] T. Pan, J. Xu, Y. Zhu, Self-renewal molecular mechanisms of colorectal cancer stem cells, International Journal of Molecular Medicine, 39 (2016).
[59] C.H. Stuelten, S.D. Mertins, J.I. Busch, M. Gowens, D.A. Scudiero, M.W. Burkett, K.M. Hite, M. Alley, M. Hollingshead, R.H. Shoemaker, J.E. Niederhuber, Complex display of putative tumor stem cell markers in the NCI60 tumor cell line panel, Stem Cells, 28 (2010) 649-660.
[60] A. Kreso, J.E. Dick, Evolution of the cancer stem cell model, Cell stem cell, 14 (2014) 275-291.
[61] Catherine A. O'Brien, A. Kreso, P. Ryan, Karin G. Hermans, L. Gibson, Y. Wang, A. Tsatsanis, S. Gallinger, John E. Dick, ID1 and ID3 Regulate the Self-Renewal Capacity of Human Colon Cancer-Initiating Cells through p21, Cancer Cell, 21 (2012) 777-792.

[62] A. Kreso, P. van Galen, N.M. Pedley, E. Lima-Fernandes, C. Frelin, T. Davis, L. Cao, R. Baiazitov, W. Du, N. Sydorenko, Y.C. Moon, L. Gibson, Y. Wang, C. Leung, N.N. Iscove, C.H. Arrowsmith, E. Szentgyorgyi, S. Gallinger, J.E. Dick, C.A. O'Brien, Self-renewal as a therapeutic target in human colorectal cancer, Nature medicine, 20 (2014) 29-36.
[63] A. Zeuner, M. Todaro, G. Stassi, R. De Maria, Colorectal cancer stem cells: from the crypt to the clinic, Cell stem cell, 15 (2014) 692-705.
[64] M. Almeqdadi, M.D. Mana, J. Roper, Ö.H. Yilmaz, Gut organoids: mini-tissues in culture to study intestinal physiology and disease, American Journal of Physiology-Cell Physiology, 317 (2019) C405-C419.
[65] H.F. Bahmad, K. Cheaito, R.M. Chalhoub, O. Hadadeh, A. Monzer, F. Ballout, A. El-Hajj, D. Mukherji, Y.N. Liu, G. Daoud, W. Abou-Kheir, Sphere-Formation Assay: Three-Dimensional in vitro Culturing of Prostate Cancer Stem/Progenitor Sphere-Forming Cells, Frontiers in oncology, 8 (2018) 347.
[66] L.-B. Weiswald, D. Bellet, V. Dangles-Marie, Spherical Cancer Models in Tumor Biology, Neoplasia, 17 (2015) 1-15.
[67] B. Bao, A. Ahmad, A.S. Azmi, S. Ali, F.H. Sarkar, Overview of cancer stem cells (CSCs) and mechanisms of their regulation: implications for cancer therapy, Curr Protoc Pharmacol, Chapter 14 (2013) Unit-14.25.
[68] C.A. Gilbert, A.H. Ross, Cancer stem cells: cell culture, markers, and targets for new therapies, J Cell Biochem, 108 (2009) 1031-1038.
[69] J.B. Kim, Three-dimensional tissue culture models in cancer biology, Seminars in Cancer Biology, 15 (2005) 365-377.
[70] D. Khaitan, S. Chandna, M.B. Arya, B.S. Dwarakanath, Establishment and characterization of multicellular spheroids from a human glioma cell line; Implications for tumor therapy, J Transl Med, 4 (2006) 12-12.
[71] G. Mehta, A.Y. Hsiao, M. Ingram, G.D. Luker, S. Takayama, Opportunities and challenges for use of tumor spheroids as models to test drug delivery and efficacy, J Control Release, 164 (2012) 192-204.
[72] L. Gurski, N. Petrelli, X. Jia, M. Farach-Carson, 3D Matrices for Anti-Cancer Drug Testing and Development, Oncology Issues, 25 (2010) 20-25.
[73] P. Valent, D. Bonnet, R. De Maria, T. Lapidot, M. Copland, J.V. Melo, C. Chomienne, F. Ishikawa, J.J. Schuringa, G. Stassi, B. Huntly, H. Herrmann, J. Soulier, A. Roesch, G.J. Schuurhuis, S. Wöhrer, M. Arock, J. Zuber, S. Cerny-Reiterer, H.E. Johnsen, M. Andreeff, C. Eaves, Cancer stem cell definitions and terminology: the devil is in the details, Nature Reviews Cancer, 12 (2012) 767-775.
[74] D. Ponti, A. Costa, N. Zaffaroni, G. Pratesi, G. Petrangolini, D. Coradini, S. Pilotti, M.A. Pierotti, M.G. Daidone, Isolation and in vitro propagation of tumorigenic breast cancer cells with stem/progenitor cell properties, Cancer Res, 65 (2005) 5506-5511.
[75] H.Z. Li, T.B. Yi, Z.Y. Wu, Suspension culture combined with chemotherapeutic agents for sorting of breast cancer stem cells, BMC cancer, 8 (2008) 135.
[76] Y. Zhong, K. Guan, S. Guo, C. Zhou, D. Wang, W. Ma, Y. Zhang, C. Li, S. Zhang, Spheres derived from the human SK-RC-42 renal cell carcinoma cell line are enriched in cancer stem cells, Cancer letters, 299 (2010) 150-160.

[77] Y. Uchida, S. Tanaka, A. Aihara, R. Adikrisna, K. Yoshitake, S. Matsumura, Y. Mitsunori, A. Murakata, N. Noguchi, T. Irie, A. Kudo, N. Nakamura, P.B. Lai, S. Arii, Analogy between sphere forming ability and stemness of human hepatoma cells, Oncology reports, 24 (2010) 1147-1151.
[78] N. Guzman-Ramirez, M. Voller, A. Wetterwald, M. Germann, N.A. Cross, C.A. Rentsch, J. Schalken, G.N. Thalmann, M.G. Cecchini, In vitro propagation and characterization of neoplastic stem/progenitor-like cells from human prostate cancer tissue, The Prostate, 69 (2009) 1683-1693.
[79] H.F. Bahmad, H. Samman, A. Monzer, O. Hadadeh, K. Cheaito, R. Abdel-Samad, B. Hayar, C. Pisano, H. Msheik, Y.N. Liu, N. Darwiche, W. Abou-Kheir, The synthetic retinoid ST1926 attenuates prostate cancer growth and potentially targets prostate cancer stem-like cells, Molecular carcinogenesis, 58 (2019) 1208-1220.
[80] R. El-Merahbi, Y.N. Liu, A. Eid, G. Daoud, L. Hosry, A. Monzer, T.H. Mouhieddine, A. Hamade, F. Najjar, W. Abou-Kheir, Berberis libanotica Ehrenb extract shows anti-neoplastic effects on prostate cancer stem/progenitor cells, PLoS One, 9 (2014) e112453.
[81] M. Gaviraghi, P. Tunici, S. Valensin, M. Rossi, C. Giordano, L. Magnoni, M. Dandrea, L. Montagna, R. Ritelli, A. Scarpa, A. Bakker, Pancreatic cancer spheres are more than just aggregates of stem marker-positive cells, Bioscience reports, 31 (2011) 45-55.
[82] A.J. Ghods, D. Irvin, G. Liu, X. Yuan, I.R. Abdulkadir, P. Tunici, B. Konda, S. Wachsmann-Hogiu, K.L. Black, J.S. Yu, Spheres isolated from 9L gliosarcoma rat cell line possess chemoresistant and aggressive cancer stem-like cells, Stem Cells, 25 (2007) 1645-1653.
[83] H.F. Bahmad, F. Chamaa, S. Assi, R.M. Chalhoub, T. Abou-Antoun, W. Abou-Kheir, Cancer Stem Cells in Neuroblastoma: Expanding the Therapeutic Frontier, Front Mol Neurosci, 12 (2019) 131-131.
[84] T.H. Mouhieddine, A. Nokkari, M.M. Itani, F. Chamaa, H. Bahmad, A. Monzer, R. El-Merahbi, G. Daoud, A. Eid, F.H. Kobeissy, W. Abou-Kheir, Metformin and Ara-a Effectively Suppress Brain Cancer by Targeting Cancer Stem/Progenitor Cells, Frontiers in neuroscience, 9 (2015) 442.
[85] L. Ricci-Vitiani, D.G. Lombardi, E. Pilozzi, M. Biffoni, M. Todaro, C. Peschle, R. De Maria, Identification and expansion of human colon-cancer-initiating cells, Nature, 445 (2007) 111-115.
[86] D.D. Fang, Y.J. Kim, C.N. Lee, S. Aggarwal, K. McKinnon, D. Mesmer, J. Norton, C.E. Birse, T. He, S.M. Ruben, P.A. Moore, Expansion of CD133(+) colon cancer cultures retaining stem cell properties to enable cancer stem cell target discovery, Br J Cancer, 102 (2010) 1265-1275.
[87] S. Wang, D. Kanojia, P.-K. Lo, V. Chandrashekaran, X. Duan, F. Berger, Q. Wang, H. Chen, Enrichment and Selective Targeting of Cancer Stem Cells in Colorectal Cancer Cell Lines, Human Genetics & Embryology, 01 (2012).
[88] C.E. Smart, B.J. Morrison, J.M. Saunus, A.C. Vargas, P. Keith, L. Reid, L. Wockner, M. Askarian-Amiri, D. Sarkar, P.T. Simpson, C. Clarke, C.W. Schmidt, B.A. Reynolds, S.R. Lakhani, J.A. Lopez, In vitro analysis of breast cancer cell line

tumourspheres and primary human breast epithelia mammospheres demonstrates inter- and intrasphere heterogeneity, PLoS One, 8 (2013) e64388-e64388.
[89] C.Y. Calvet, F.M. André, L.M. Mir, The Culture of Cancer Cell Lines as Tumorspheres Does Not Systematically Result in Cancer Stem Cell Enrichment, PLoS One, 9 (2014) e89644.
[90] D.E. Discher, D.J. Mooney, P.W. Zandstra, Growth Factors, Matrices, and Forces Combine and Control Stem Cells, Science, 324 (2009) 1673.
[91] M. Riihimäki, A. Hemminki, J. Sundquist, K. Hemminki, Patterns of metastasis in colon and rectal cancer, Scientific Reports, 6 (2016) 29765.
[92] N. Takebe, P.J. Harris, R.Q. Warren, S.P. Ivy, Targeting cancer stem cells by inhibiting Wnt, Notch, and Hedgehog pathways, Nature Reviews Clinical Oncology, 8 (2010) 97.
[93] E. Paldino, V. Tesori, P. Casalbore, A. Gasbarrini, M.A. Puglisi, Tumor initiating cells and chemoresistance: which is the best strategy to target colon cancer stem cells?, BioMed research international, 2014 (2014) 859871.
[94] L. Han, S. Shi, T. Gong, Z. Zhang, X. Sun, Cancer stem cells: therapeutic implications and perspectives in cancer therapy, Acta Pharmaceutica Sinica B, 3 (2013) 65-75.
[95] L.M. Smith, A. Nesterova, M.C. Ryan, S. Duniho, M. Jonas, M. Anderson, R.F. Zabinski, M.K. Sutherland, H.P. Gerber, K.L. Van Orden, P.A. Moore, S.M. Ruben, P.J. Carter, CD133/prominin-1 is a potential therapeutic target for antibody-drug conjugates in hepatocellular and gastric cancers, Br J Cancer, 99 (2008) 100-109.
[96] Y. Lombardo, A. Scopelliti, P. Cammareri, M. Todaro, F. Iovino, L. Ricci–Vitiani, G. Gulotta, F. Dieli, R. de Maria, G. Stassi, Bone Morphogenetic Protein 4 Induces Differentiation of Colorectal Cancer Stem Cells and Increases Their Response to Chemotherapy in Mice, Gastroenterology, 140 (2011) 297-309.e296.
[97] M. Todaro, M.P. Alea, A.B. Di Stefano, P. Cammareri, L. Vermeulen, F. Iovino, C. Tripodo, A. Russo, G. Gulotta, J.P. Medema, G. Stassi, Colon cancer stem cells dictate tumor growth and resist cell death by production of interleukin-4, Cell stem cell, 1 (2007) 389-402.
[98] V.R. Sinha, Honey, Critical aspects in rationale design of fluorouracil-based adjuvant therapies for the management of colon cancer, Critical reviews in therapeutic drug carrier systems, 29 (2012) 89-148.
[99] K. Chen, Y.-H. Huang, J.-L. Chen, Chen K, Huang YH, Chen JL.Understanding and targeting cancer stem cells: therapeutic implications and challenges. Acta Pharmacol Sin 34:732-740, Acta pharmacologica Sinica, 34 (2013).
[100] A.F. Majdalawieh, M.W. Fayyad, G.K. Nasrallah, Anti-cancer properties and mechanisms of action of thymoquinone, the major active ingredient of Nigella sativa, Critical reviews in food science and nutrition, 57 (2017) 3911-3928.
[101] A. Ahmad, R.K. Mishra, A. Vyawahare, A. Kumar, M.U. Rehman, W. Qamar, A.Q. Khan, R. Khan, Thymoquinone (2-Isoprpyl-5-methyl-1, 4-benzoquinone) as a chemopreventive/anticancer agent: Chemistry and biological effects, Saudi Pharm J, 27 (2019) 1113-1126.
[102] S. Akyol, O. Akyol, The interaction of glutathione and thymoquinone and their antioxidant properties, Electronic Journal of General Medicine, 15 (2018).

[103] K.M. Fararh, Y. Atoji, Y. Shimizu, T. Shiina, H. Nikami, T. Takewaki, Mechanisms of the hypoglycaemic and immunopotentiating effects of Nigella sativa L. oil in streptozotocin-induced diabetic hamsters, Research in Veterinary Science, 77 (2004) 123-129.
[104] E. Taka, P. Mendonca, E.A. Mazzio, S.D. Reed, R. Reams, K.F. Soliman, Molecular Targets Underlying the Anti-inflammatory Effects of Thymoquinone in LPS activated BV-2 Cells, The FASEB Journal, 32 (2018) 40.42-40.42.
[105] M.K. Cobourne-Duval, E. Taka, P. Mendonca, K.F.A. Soliman, Thymoquinone increases the expression of neuroprotective proteins while decreasing the expression of pro-inflammatory cytokines and the gene expression NFκB pathway signaling targets in LPS/IFNγ -activated BV-2 microglia cells, Journal of Neuroimmunology, 320 (2018) 87-97.
[106] Y. Lu, Y. Feng, D. Liu, Z. Zhang, K. Gao, W. Zhang, H. Tang, Thymoquinone Attenuates Myocardial Ischemia/Reperfusion Injury Through Activation of SIRT1 Signaling, Cellular Physiology and Biochemistry, 47 (2018) 1193-1206.
[107] N.M. Elsherbiny, M. El-Sherbiny, Thymoquinone attenuates Doxorubicin-induced nephrotoxicity in rats: Role of Nrf2 and NOX4, Chemico-Biological Interactions, 223 (2014) 102-108.
[108] Y. Yang, T. Bai, Y.L. Yao, D.Q. Zhang, Y.L. Wu, L.H. Lian, J.X. Nan, Upregulation of SIRT1-AMPK by thymoquinone in hepatic stellate cells ameliorates liver injury, Toxicology Letters, 262 (2016) 80-91.
[109] M.K. Shanmugam, F. Arfuso, A.P. Kumar, L. Wang, B.C. Goh, K.S. Ahn, A. Bishayee, G. Sethi, Modulation of diverse oncogenic transcription factors by thymoquinone, an essential oil compound isolated from the seeds of Nigella sativa Linn, Pharmacological research, 129 (2018) 357-364.
[110] O.H. Alobaedi, W.H. Talib, I.A. Basheti, Antitumor effect of thymoquinone combined with resveratrol on mice transplanted with breast cancer, Asian Pacific Journal of Tropical Medicine, 10 (2017) 400-408.
[111] B. Kou, W. Liu, W. Zhao, P. Duan, Y. Yang, Q. Yi, F. Guo, J. Li, J. Zhou, Q. Kou, Thymoquinone inhibits epithelial-mesenchymal transition in prostate cancer cells by negatively regulating the TGF-β/Smad2/3 signaling pathway, Oncology reports, 38 (2017) 3592-3598.
[112] L.-M. Feng, X.-F. Wang, Q.-X. Huang, Thymoquinone induces cytotoxicity and reprogramming of EMT in gastric cancer cells by targeting PI3K/Akt/mTOR pathway, Journal of Biosciences, 42 (2017) 547-554.
[113] J. Yang, X.-r. Kuang, P.-t. Lv, X.-x. Yan, Thymoquinone inhibits proliferation and invasion of human nonsmall-cell lung cancer cells via ERK pathway, Tumor Biology, 36 (2015) 259-269.
[114] L. Zhang, Y. Bai, Y. Yang, Thymoquinone chemosensitizes colon cancer cells through inhibition of NF-κB, Oncology Letters, 12 (2016) 2840-2845.
[115] C. El-Baba, V. Mahadevan, F.B. Fahlbusch, S. Mohan S, T.T. Rau, H. Gali-Muhtasib, R. Schneider-Stock, Thymoquinone-induced conformational changes of PAK1 interrupt prosurvival MEK-ERK signaling in colorectal cancer, Mol Cancer, 13 (2014) 201-201.

[116] N. El-Najjar, M. Chatila, H. Moukadem, H. Vuorela, M. Ocker, M. Gandesiri, R. Schneider-Stock, H. Gali-Muhtasib, Reactive oxygen species mediate thymoquinone-induced apoptosis and activate ERK and JNK signaling, Apoptosis : an international journal on programmed cell death, 15 (2010) 183-195.
[117] H. Gali-Muhtasib, M. Ocker, D. Kuester, S. Krueger, Z. El-Hajj, A. Diestel, M. Evert, N. El-Najjar, B. Peters, A. Jurjus, A. Roessner, R. Schneider-Stock, Thymoquinone reduces mouse colon tumor cell invasion and inhibits tumor growth in murine colon cancer models, Journal of cellular and molecular medicine, 12 (2008) 330-342.
[118] M. Roepke, A. Diestel, K. Bajbouj, D. Walluscheck, P. Schonfeld, A. Roessner, R. Schneider-Stock, H. Gali-Muhtasib, Lack of p53 augments thymoquinone-induced apoptosis and caspase activation in human osteosarcoma cells, Cancer biology & therapy, 6 (2007) 160-169.
[119] M. Zhang, H. Du, Z. Huang, P. Zhang, Y. Yue, W. Wang, W. Liu, J. Zeng, J. Ma, G. Chen, X. Wang, J. Fan, Thymoquinone induces apoptosis in bladder cancer cell via endoplasmic reticulum stress-dependent mitochondrial pathway, Chemico-Biological Interactions, 292 (2018) 65-75.
[120] R. Schneider-Stock, I.H. Fakhoury, A.M. Zaki, C.O. El-Baba, H.U. Gali-Muhtasib, Thymoquinone: fifty years of success in the battle against cancer models, Drug discovery today, 19 (2014) 18-30.
[121] H. Mollazadeh, A.R. Afshari, H. Hosseinzadeh, Review on the Potential Therapeutic Roles of Nigella sativa in the Treatment of Patients with Cancer: Involvement of Apoptosis: - Black cumin and cancer, J Pharmacopuncture, 20 (2017) 158-172.
[122] A. Tavakkoli, V. Mahdian, B.M. Razavi, H. Hosseinzadeh, Review on Clinical Trials of Black Seed (Nigella sativa) and Its Active Constituent, Thymoquinone, J Pharmacopuncture, 20 (2017) 179-193.
[123] C.C. Woo, A. Hsu, A.P. Kumar, G. Sethi, K.H.B. Tan, Thymoquinone inhibits tumor growth and induces apoptosis in a breast cancer xenograft mouse model: the role of p38 MAPK and ROS, PLoS One, 8 (2013) e75356-e75356.
[124] R. Khalife, M.H. Hodroj, R. Fakhoury, S. Rizk, Thymoquinone from Nigella sativa Seeds Promotes the Antitumor Activity of Noncytotoxic Doses of Topotecan in Human Colorectal Cancer Cells in Vitro, Planta medica, 82 (2016) 312-321.
[125] W.Q. Zhu, J. Wang, X.F. Guo, Z. Liu, W.G. Dong, Thymoquinone inhibits proliferation in gastric cancer via the STAT3 pathway in vivo and in vitro, World journal of gastroenterology, 22 (2016) 4149-4159.
[126] M. Lang, M. Borgmann, G. Oberhuber, R. Evstatiev, K. Jimenez, K.W. Dammann, M. Jambrich, V. Khare, C. Campregher, R. Ristl, C. Gasche, Thymoquinone attenuates tumor growth in ApcMin mice by interference with Wnt-signaling, Mol Cancer, 12 (2013) 41-41.
[127] Y.K. Mahmoud, H.M.A. Abdelrazek, Cancer: Thymoquinone antioxidant/pro-oxidant effect as potential anticancer remedy, Biomedicine & pharmacotherapy = Biomedecine & pharmacotherapie, 115 (2019) 108783.
[128] B. Ndreshkjana, A. Capci, V. Klein, P. Chanvorachote, J.K. Muenzner, K. Huebner, S. Steinmann, K. Erlenbach-Wuensch, C.I. Geppert, A. Agaimy, F. Ballout,

C. El-Baba, H. Gali-Muhtasib, A.V. Roehe, A. Hartmann, S.B. Tsogoeva, R. Schneider-Stock, Combination of 5-fluorouracil and thymoquinone targets stem cell gene signature in colorectal cancer cells, Cell death & disease, 10 (2019) 379.
[129] S. Hemaiswarya, M. Doble, Potential synergism of natural products in the treatment of cancer, Phytotherapy research : PTR, 20 (2006) 239-249.
[130] M. Asaduzzaman Khan, M. Tania, S. Fu, J. Fu, Thymoquinone, as an anticancer molecule: from basic research to clinical investigation, Oncotarget, 8 (2017) 51907-51919.
[131] A.A. Norwood, M. Tucci, H. Benghuzzi, A comparison of 5-fluorouracil and natural chemotherapeutic agents, EGCG and thymoquinone, delivered by sustained drug delivery on colon cancer cells, Biomedical sciences instrumentation, 43 (2007) 272-277.
[132] X. Lei, X. Lv, M. Liu, Z. Yang, M. Ji, X. Guo, W. Dong, Thymoquinone inhibits growth and augments 5-fluorouracil-induced apoptosis in gastric cancer cells both in vitro and in vivo, Biochemical and Biophysical Research Communications, 417 (2012) 864-868.
[133] O.A. Kensara, A.G. El-Shemi, A.M. Mohamed, B. Refaat, S. Idris, J. Ahmad, Thymoquinone subdues tumor growth and potentiates the chemopreventive effect of 5-fluorouracil on the early stages of colorectal carcinogenesis in rats, Drug Des Devel Ther, 10 (2016) 2239-2253.
[134] S.H. Jafri, J. Glass, R. Shi, S. Zhang, M. Prince, H. Kleiner-Hancock, Thymoquinone and cisplatin as a therapeutic combination in lung cancer: In vitro and in vivo, Journal of experimental & clinical cancer research : CR, 29 (2010) 87.
[135] A.J. Wilson, J. Saskowski, W. Barham, F. Yull, D. Khabele, Thymoquinone enhances cisplatin-response through direct tumor effects in a syngeneic mouse model of ovarian cancer, Journal of ovarian research, 8 (2015) 46.
[136] C. Sakalar, K. Izgi, B. Iskender, S. Sezen, H. Aksu, M. Cakir, B. Kurt, A. Turan, H. Canatan, The combination of thymoquinone and paclitaxel shows anti-tumor activity through the interplay with apoptosis network in triple-negative breast cancer, Tumour biology : the journal of the International Society for Oncodevelopmental Biology and Medicine, 37 (2016) 4467-4477.
[137] A. Dirican, H. Atmaca, E. Bozkurt, C. Erten, B. Karaca, R. Uslu, Novel combination of docetaxel and thymoquinone induces synergistic cytotoxicity and apoptosis in DU-145 human prostate cancer cells by modulating PI3K-AKT pathway, Clinical & translational oncology : official publication of the Federation of Spanish Oncology Societies and of the National Cancer Institute of Mexico, 17 (2015) 145-151.
[138] R. Velho-Pereira, A. Kumar, B.N. Pandey, A.G. Jagtap, K.P. Mishra, Radiosensitization in human breast carcinoma cells by thymoquinone: role of cell cycle and apoptosis, Cell biology international, 35 (2011) 1025-1029.
[139] Q. Hou, L. Liu, Y. Dong, J. Wu, L. Du, H. Dong, D. Li, Effects of Thymoquinone on radiation enteritis in mice, Scientific reports, 8 (2018) 15122-15122.
[140] F. Ballout, Z. Habli, O.N. Rahal, M. Fatfat, H. Gali-Muhtasib, Thymoquinone-based nanotechnology for cancer therapy: promises and challenges, Drug discovery today, 23 (2018) 1089-1098.
[141] M.N. Nagi, M.A. Mansour, PROTECTIVE EFFECT OF THYMOQUINONE AGAINST DOXORUBICIN–INDUCED CARDIOTOXICITY IN RATS: A

POSSIBLE MECHANISM OF PROTECTION, Pharmacological research, 41 (2000) 283-289.
[142] S.A. Pathan, G.K. Jain, S.M.A. Zaidi, S. Akhter, D. Vohora, P. Chander, P.L. Kole, F.J. Ahmad, R.K. Khar, Stability-indicating ultra-performance liquid chromatography method for the estimation of thymoquinone and its application in biopharmaceutical studies, Biomedical Chromatography, 25 (2011) 613-620.
[143] K.M. Alkharfy, A. Ahmad, R.M. Khan, W.M. Al-Shagha, Pharmacokinetic plasma behaviors of intravenous and oral bioavailability of thymoquinone in a rabbit model, European journal of drug metabolism and pharmacokinetics, 40 (2015) 319-323.
[144] L.Z. Salim, S. Mohan, R. Othman, S.I. Abdelwahab, B. Kamalidehghan, B.Y. Sheikh, M.Y. Ibrahim, Thymoquinone induces mitochondria-mediated apoptosis in acute lymphoblastic leukaemia in vitro, Molecules, 18 (2013) 11219-11240.
[145] E.M. Dergarabetian, K.I. Ghattass, S.B. El-Sitt, R.M. Al-Mismar, C.O. El-Baba, W.S. Itani, N.M. Melhem, H.A. El-Hajj, A.A. Bazarbachi, R. Schneider-Stock, H.U. Gali-Muhtasib, Thymoquinone induces apoptosis in malignant T-cells via generation of ROS, Frontiers in bioscience (Elite edition), 5 (2013) 706-719.
[146] K. Effenberger-Neidnicht, R. Schobert, Combinatorial effects of thymoquinone on the anti-cancer activity of doxorubicin, Cancer chemotherapy and pharmacology, 67 (2011) 867-874.
[147] G. Sethi, K.S. Ahn, B.B. Aggarwal, Targeting nuclear factor-kappa B activation pathway by thymoquinone: role in suppression of antiapoptotic gene products and enhancement of apoptosis, Molecular cancer research : MCR, 6 (2008) 1059-1070.
[148] B. Iskender, K. Izgi, H. Canatan, Novel anti-cancer agent myrtucommulone-A and thymoquinone abrogate epithelial-mesenchymal transition in cancer cells mainly through the inhibition of PI3K/AKT signalling axis, Molecular and cellular biochemistry, 416 (2016) 71-84.
[149] E.S. Al-Sheddi, N.N. Farshori, M.M. Al-Oqail, J. Musarrat, A.A. Al-Khedhairy, M.A. Siddiqui, Cytotoxicity of Nigella sativa seed oil and extract against human lung cancer cell line, Asian Pacific journal of cancer prevention : APJCP, 15 (2014) 983-987.
[150] J. Yang, X.R. Kuang, P.T. Lv, X.X. Yan, Thymoquinone inhibits proliferation and invasion of human nonsmall-cell lung cancer cells via ERK pathway, Tumour biology : the journal of the International Society for Oncodevelopmental Biology and Medicine, 36 (2015) 259-269.
[151] S. Rajput, B.N. Kumar, K.K. Dey, I. Pal, A. Parekh, M. Mandal, Molecular targeting of Akt by thymoquinone promotes G(1) arrest through translation inhibition of cyclin D1 and induces apoptosis in breast cancer cells, Life sciences, 93 (2013) 783-790.
[152] M.N. Dastjerdi, E.M. Mehdiabady, F.G. Iranpour, H. Bahramian, Effect of Thymoquinone on P53 Gene Expression and Consequence Apoptosis in Breast Cancer Cell Line, International journal of preventive medicine, 7 (2016) 66.
[153] M.A. Khan, M. Tania, C. Wei, Z. Mei, S. Fu, J. Cheng, J. Xu, J. Fu, Thymoquinone inhibits cancer metastasis by downregulating TWIST1 expression to reduce epithelial to mesenchymal transition, Oncotarget, 6 (2015) 19580-19591.
[154] J. Kundu, B.Y. Choi, C.H. Jeong, J.K. Kundu, K.S. Chun, Thymoquinone induces apoptosis in human colon cancer HCT116 cells through inactivation of STAT3 by

blocking JAK2- and Srcmediated phosphorylation of EGF receptor tyrosine kinase, Oncology reports, 32 (2014) 821-828.
[155] H. Gali-Muhtasib, M. Diab-Assaf, C. Boltze, J. Al-Hmaira, R. Hartig, A. Roessner, R. Schneider-Stock, Thymoquinone extracted from black seed triggers apoptotic cell death in human colorectal cancer cells via a p53-dependent mechanism, International journal of oncology, 25 (2004) 857-866.
[156] H. Gali-Muhtasib, D. Kuester, C. Mawrin, K. Bajbouj, A. Diestel, M. Ocker, C. Habold, C. Foltzer-Jourdainne, P. Schoenfeld, B. Peters, M. Diab-Assaf, U. Pommrich, W. Itani, H. Lippert, A. Roessner, R. Schneider-Stock, Thymoquinone triggers inactivation of the stress response pathway sensor CHEK1 and contributes to apoptosis in colorectal cancer cells, Cancer Res, 68 (2008) 5609-5618.
[157] R.L. Gurung, S.N. Lim, A.K. Khaw, J.F. Soon, K. Shenoy, S. Mohamed Ali, M. Jayapal, S. Sethu, R. Baskar, M.P. Hande, Thymoquinone induces telomere shortening, DNA damage and apoptosis in human glioblastoma cells, PLoS One, 5 (2010) e12124.
[158] K. Kolli-Bouhafs, A. Boukhari, A. Abusnina, E. Velot, J.P. Gies, C. Lugnier, P. Ronde, Thymoquinone reduces migration and invasion of human glioblastoma cells associated with FAK, MMP-2 and MMP-9 down-regulation, Investigational new drugs, 30 (2012) 2121-2131.
[159] A.E. Ashour, A.R. Abd-Allah, H.M. Korashy, S.M. Attia, A.Z. Alzahrani, Q. Saquib, S.A. Bakheet, H.E. Abdel-Hamied, S. Jamal, A.K. Rishi, Thymoquinone suppression of the human hepatocellular carcinoma cell growth involves inhibition of IL-8 expression, elevated levels of TRAIL receptors, oxidative stress and apoptosis, Molecular and cellular biochemistry, 389 (2014) 85-98.
[160] L. Peng, A. Liu, Y. Shen, H.Z. Xu, S.Z. Yang, X.Z. Ying, W. Liao, H.X. Liu, Z.Q. Lin, Q.Y. Chen, S.W. Cheng, W.D. Shen, Antitumor and anti-angiogenesis effects of thymoquinone on osteosarcoma through the NF-kappaB pathway, Oncology reports, 29 (2013) 571-578.
[161] A.O. Kaseb, K. Chinnakannu, D. Chen, A. Sivanandam, S. Tejwani, M. Menon, Q.P. Dou, G.P. Reddy, Androgen receptor and E2F-1 targeted thymoquinone therapy for hormone-refractory prostate cancer, Cancer Res, 67 (2007) 7782-7788.
[162] T. Yi, S.G. Cho, Z. Yi, X. Pang, M. Rodriguez, Y. Wang, G. Sethi, B.B. Aggarwal, M. Liu, Thymoquinone inhibits tumor angiogenesis and tumor growth through suppressing AKT and extracellular signal-regulated kinase signaling pathways, Molecular cancer therapeutics, 7 (2008) 1789-1796.
[163] M.P. Torres, M.P. Ponnusamy, S. Chakraborty, L.M. Smith, S. Das, H.A. Arafat, S.K. Batra, Effects of thymoquinone in the expression of mucin 4 in pancreatic cancer cells: implications for the development of novel cancer therapies, Molecular cancer therapeutics, 9 (2010) 1419-1431.
[164] L. Connelly, W. Barham, H.M. Onishko, T. Sherrill, L.A. Chodosh, T.S. Blackwell, F.E. Yull, Inhibition of NF-kappa B activity in mammary epithelium increases tumor latency and decreases tumor burden, Oncogene, 30 (2011) 1402-1412.
[165] C.C. Woo, A. Hsu, A.P. Kumar, G. Sethi, K.H. Tan, Thymoquinone inhibits tumor growth and induces apoptosis in a breast cancer xenograft mouse model: the role of p38 MAPK and ROS, PLoS One, 8 (2013) e75356.

[166] M. Lang, M. Borgmann, G. Oberhuber, R. Evstatiev, K. Jimenez, K.W. Dammann, M. Jambrich, V. Khare, C. Campregher, R. Ristl, C. Gasche, Thymoquinone attenuates tumor growth in ApcMin mice by interference with Wnt-signaling, Mol Cancer, 12 (2013) 41.
[167] S. Raghunandhakumar, A. Paramasivam, S. Senthilraja, C. Naveenkumar, S. Asokkumar, J. Binuclara, S. Jagan, P. Anandakumar, T. Devaki, Thymoquinone inhibits cell proliferation through regulation of G1/S phase cell cycle transition in N-nitrosodiethylamine-induced experimental rat hepatocellular carcinoma, Toxicol Lett, 223 (2013) 60-72.
[168] Y.M. Wang, [Inhibitory effects of thymoquinone on human pancreatic carcinoma orthotopically implanted in nude mice], Zhonghua yi xue za zhi, 91 (2011) 3111-3114.
[169] S. Das, K.K. Dey, G. Dey, I. Pal, A. Majumder, S. MaitiChoudhury, S.C. kundu, M. Mandal, Antineoplastic and apoptotic potential of traditional medicines thymoquinone and diosgenin in squamous cell carcinoma, PLoS One, 7 (2012) e46641.
[170] S. Attoub, O. Sperandio, H. Raza, K. Arafat, S. Al-Salam, M.A. Al Sultan, M. Al Safi, T. Takahashi, A. Adem, Thymoquinone as an anticancer agent: evidence from inhibition of cancer cells viability and invasion in vitro and tumor growth in vivo, Fundamental & clinical pharmacology, 27 (2013) 557-569.
[171] M.G. Brattain, W.D. Fine, F.M. Khaled, J. Thompson, D.E. Brattain, Heterogeneity of malignant cells from a human colonic carcinoma, Cancer Res, 41 (1981) 1751-1756.
[172] D. Ahmed, P.W. Eide, I.A. Eilertsen, S.A. Danielsen, M. Eknæs, M. Hektoen, G.E. Lind, R.A. Lothe, Epigenetic and genetic features of 24 colon cancer cell lines, Oncogenesis, 2 (2013) e71-e71.
[173] T.M. Yeung, S.C. Gandhi, J.L. Wilding, R. Muschel, W.F. Bodmer, Cancer stem cells from colorectal cancer-derived cell lines, Proceedings of the National Academy of Sciences of the United States of America, 107 (2010) 3722-3727.
[174] R. Abdel-Samad, P. Aouad, H. Gali-Muhtasib, Z. Sweidan, R. Hmadi, H. Kadara, E.L. D'Andrea, A. Fucci, C. Pisano, N. Darwiche, Mechanism of action of the atypical retinoid ST1926 in colorectal cancer: DNA damage and DNA polymerase α, Am J Cancer Res, 8 (2018) 39-55.
[175] J. Petriz, Flow Cytometry of the Side Population (SP), Current protocols in cytometry / editorial board, J. Paul Robinson, managing editor ... [et al.], Chapter 9 (2007) Unit9.23.
[176] M. Ito, K. Kobayashi, T. Nakahata, NOD/Shi-scid IL2rγnull (NOG) Mice More Appropriate for Humanized Mouse Models, in: T. Nomura, T. Watanabe, S. Habu (Eds.) Humanized Mice, Springer Berlin Heidelberg, Berlin, Heidelberg, 2008, pp. 53-76.
[177] W.A. Hammond, A. Swaika, K. Mody, Pharmacologic resistance in colorectal cancer: a review, Ther Adv Med Oncol, 8 (2016) 57-84.
[178] E.N. Garza-Trevino, S.L. Said-Fernandez, H.G. Martinez-Rodriguez, Understanding the colon cancer stem cells and perspectives on treatment, Cancer cell international, 15 (2015) 2.

[179] Z.Y. Xu, J.N. Tang, H.X. Xie, Y.A. Du, L. Huang, P.F. Yu, X.D. Cheng, 5-Fluorouracil chemotherapy of gastric cancer generates residual cells with properties of cancer stem cells, International journal of biological sciences, 11 (2015) 284-294.
[180] C. Denise, P. Paoli, M. Calvani, M.L. Taddei, E. Giannoni, S. Kopetz, S.M. Kazmi, M.M. Pia, P. Pettazzoni, E. Sacco, A. Caselli, M. Vanoni, M. Landriscina, P. Cirri, P. Chiarugi, 5-fluorouracil resistant colon cancer cells are addicted to OXPHOS to survive and enhance stem-like traits, Oncotarget, 6 (2015) 41706-41721.
[181] B. Pardini, R. Kumar, A. Naccarati, J. Novotny, R.B. Prasad, A. Forsti, K. Hemminki, P. Vodicka, J. Lorenzo Bermejo, 5-Fluorouracil-based chemotherapy for colorectal cancer and MTHFR/MTRR genotypes, British journal of clinical pharmacology, 72 (2011) 162-163.
[182] P.R. Subbarayan, M. Sarkar, G. Nelson, E. Benitez, S. Singhal, B. Ardalan, Chronic exposure of colorectal cancer cells in culture to fluoropyrimidine analogs induces thymidylate synthase and suppresses p53. A molecular explanation for the mechanism of 5-FU resistance, Anticancer research, 30 (2010) 1149-1156.
[183] L.C. Phua, M. Mal, P.K. Koh, P.Y. Cheah, E.C. Chan, H.K. Ho, Investigating the role of nucleoside transporters in the resistance of colorectal cancer to 5-fluorouracil therapy, Cancer chemotherapy and pharmacology, 71 (2013) 817-823.
[184] L. He, H. Zhu, S. Zhou, T. Wu, H. Wu, H. Yang, H. Mao, C. SekharKathera, A. Janardhan, A.M. Edick, A. Zhang, Z. Hu, F. Pan, Z. Guo, Wnt pathway is involved in 5-FU drug resistance of colorectal cancer cells, Experimental & Molecular Medicine, 50 (2018) 101.
[185] L. Du, H. Wang, L. He, J. Zhang, B. Ni, X. Wang, H. Jin, N. Cahuzac, M. Mehrpour, Y. Lu, Q. Chen, CD44 is of Functional Importance for Colorectal Cancer Stem Cells, Clinical Cancer Research, 14 (2008) 6751.
[186] K. Kemper, C. Grandela, J.P. Medema, Molecular identification and targeting of colorectal cancer stem cells, Oncotarget, 1 (2010) 387-395.
[187] M. Mirza-Aghazadeh-Attari, S.G. Darband, M. Kaviani, A. Mihanfar, J. Aghazadeh Attari, B. Yousefi, M. Majidinia, DNA damage response and repair in colorectal cancer: Defects, regulation and therapeutic implications, DNA Repair, 69 (2018) 34-52.
[188] M.D. Bressy C, Raddi N, Jdey W, Cornilleau G, Zig L, Guirouilh-Barbat J, Lopez B, Bawa O, Opolon P, Grellier E and Benihoud K. , Combined therapy of colon carcinomas with an oncolytic adenovirus and valproic acid, Oncotarget, 8 (2017) 97344-97360.
[189] Y.B. Kim, H.-C. Jeung, I. Jeong, K. Lee, S.Y. Rha, H.C. Chung, G.E. Kim, Mechanism of enhancement of radiation-induced cytotoxicity by sorafenib in colorectal cancer, J Radiat Res, 54 (2013) 52-60.
[190] S.-J. Chiu, Y.-J. Lee, T.-S. Hsu, W.-S. Chen, Oxaliplatin-induced gamma-H2AX activation via both p53-dependent and -independent pathways but is not associated with cell cycle arrest in human colorectal cancer cells, Chemico-Biological Interactions, 182 (2009) 173-182.
[191] M. Fragkos, J. Jurvansuu, P. Beard, H2AX is required for cell cycle arrest via the p53/p21 pathway, Molecular and cellular biology, 29 (2009) 2828-2840.

[192] R. Verma, M.J. Rigatti, G.S. Belinsky, C.A. Godman, C. Giardina, DNA damage response to the Mdm2 inhibitor nutlin-3, Biochem Pharmacol, 79 (2010) 565-574.
[193] T. Wang, P. Han, Y. He, C. Zhao, G. Wang, W. Yang, M. Shan, Y. Zhu, C. Yang, M. Weng, D. Wu, L. Gao, X. Jin, Y. Wei, B. Cui, G. Shen, X. Li, Lin28A enhances chemosensitivity of colon cancer cells to 5-FU by promoting apoptosis in a let-7 independent manner, Tumour biology : the journal of the International Society for Oncodevelopmental Biology and Medicine, 37 (2016) 7657-7665.
[194] T.M. Phillips, W.H. McBride, F. Pajonk, The response of CD24(-/low)/CD44+ breast cancer-initiating cells to radiation, Journal of the National Cancer Institute, 98 (2006) 1777-1785.
[195] M. Diehn, R.W. Cho, N.A. Lobo, T. Kalisky, M.J. Dorie, A.N. Kulp, D. Qian, J.S. Lam, L.E. Ailles, M. Wong, B. Joshua, M.J. Kaplan, I. Wapnir, F.M. Dirbas, G. Somlo, C. Garberoglio, B. Paz, J. Shen, S.K. Lau, S.R. Quake, J.M. Brown, I.L. Weissman, M.F. Clarke, Association of reactive oxygen species levels and radioresistance in cancer stem cells, Nature, 458 (2009) 780-783.
[196] S. Bao, Q. Wu, R.E. McLendon, Y. Hao, Q. Shi, A.B. Hjelmeland, M.W. Dewhirst, D.D. Bigner, J.N. Rich, Glioma stem cells promote radioresistance by preferential activation of the DNA damage response, Nature, 444 (2006) 756-760.
[197] A. Schulz, F. Meyer, A. Dubrovska, K. Borgmann, Cancer Stem Cells and Radioresistance: DNA Repair and Beyond, Cancers (Basel), 11 (2019) 862.
[198] A. Malik, M. Sultana, A. Qazi, M.H. Qazi, G. Parveen, S. Waquar, A.B. Ashraf, M. Rasool, Role of Natural Radiosensitizers and Cancer Cell Radioresistance: An Update, Anal Cell Pathol (Amst), 2016 (2016) 6146595-6146595.
[199] I.T. Chiang, Y.-C. Liu, F.-T. Hsu, Y.-C. Chien, C.-H. Kao, W.-J. Lin, J.-G. Chung, J.-J. Hwang, Curcumin synergistically enhances the radiosensitivity of human oral squamous cell carcinoma via suppression of radiation-induced NF-κB activity, Oncology reports, 31 (2014).
[200] A.B. Kunnumakkara, Diagaradjane, P., Guha, S., Deorukhkar, A., Shentu, S., Aggarwal, B.B. and Krishnan, S. , Curcumin sensitizes human colorectal cancer xenografts in nude mice to gamma-radiation by targeting nuclear factor-kappaB-regulated gene products., Clinical Cancer Research, 14 (2008) 2128-2136.
[201] T. Tamatani, M. Azuma, Y. Ashida, K. Motegi, R. Takashima, K. Harada, S.-i. Kawaguchi, M. Sato, Enhanced radiosensitization and chemosensitization in NF-κB-suppressed human oral cancer cells via the inhibition of γ-irradiation- and 5-FU-induced production of IL-6 and IL-8, International journal of cancer, 108 (2004) 912-921.
[202] K. Rothkamm, S. Horn, γ-H2AX as protein biomarker for radiation exposure, Ann. Ist. Super. Sanita, 45 (2009).
[203] M.M. Abukhader, The effect of route of administration in thymoquinone toxicity in male and female rats, Indian journal of pharmaceutical sciences, 74 (2012) 195-200.
[204] A. Al-Amri, A. Bamosa, Phase I safety and clinical activity study of thymoquinone in patients with advanced refractory malignant disease, Shiraz E-Med J, 10 (2009) 107-111.
[205] M.-C. Chen, N.-H. Lee, H.-H. Hsu, T.-J. Ho, C.-C. Tu, R.-J. Chen, Y.-M. Lin, V.P. Viswanadha, W.-W. Kuo, C.-Y. Huang, Inhibition of NF-κB and metastasis in

irinotecan (CPT-11)-resistant LoVo colon cancer cells by thymoquinone via JNK and p38, Environmental Toxicology, 32 (2017) 669-678.
[206] K.S. Siveen, N. Mustafa, F. Li, R. Kannaiyan, K.S. Ahn, A.P. Kumar, W.-J. Chng, G. Sethi, Thymoquinone overcomes chemoresistance and enhances the anticancer effects of bortezomib through abrogation of NF-κB regulated gene products in multiple myeloma xenograft mouse model, Oncotarget, 5 (2014) 634-648.
[207] L. Lin, D. Ding, Y. Jiang, Y. Li, S. Li, MEK inhibitors induce apoptosis via FoxO3a-dependent PUMA induction in colorectal cancer cells, Oncogenesis, 7 (2018) 67.
[208] M.M. Kloster, E.H. Naderi, H. Carlsen, H.K. Blomhoff, S. Naderi, Hyperactivation of NF-κB via the MEK signaling is indispensable for the inhibitory effect of cAMP on DNA damage-induced cell death, Mol Cancer, 10 (2011) 45.
[209] M.M.A. Abdel-Mottaleb, Biodegradable Thymoquinone Nanoparticles for Higher Therapeutic Efficiency in Murine Colorectal Cancer IJPPR Human, 7 (2016) 436-450.